12-2010

Characterization of anti-proteolytic and anti-proliferative activities of pentagalloylglucose; its potential application as a therapeutic agent in vascular diseases

Chaitra Cheluvaraju
Clemson University, chaitra.cheluvaraju@gmail.com

CHARACTERIZATION OF ANTI-PROTEOLYTIC AND ANTI-PROLIFERATIVE ACTIVITIES OF PENTAGALLOYLGLUCOSE; ITS POTENTIAL APPLICATION AS A THERAPEUTIC AGENT IN VASCULAR DISEASES

A Dissertation
Presented to
the Graduate School of
Clemson University

In Partial Fulfillment
of the Requirements for the Degree
Doctor of Philosophy
Bioengineering

---

by
Chaitra Cheluvaraju
December 2010

Accepted by:
Dr. Narendra Vyavahare, Committee Chair
Dr. Sarah Harcum
Dr. Martine LaBerge
Dr. Anand Ramamurthi
Dr. Ken Webb

ABSTRACT

Cardiovascular diseases are the leading causes of mortality in the United States and will cost around $500 billion this year alone. Elevated proteolytic activity, increased proliferation and migration of vascular smooth muscle cells are hallmarks of atherosclerosis, stenosis and aortic aneurysms. These diseases often manifest the transdifferentiation of vascular smooth muscle cells into osteoblast-like cells followed by deposition of hydroxyapatite-like mineral in the arterial walls.

Currently, there are no standard treatments available for vascular calcification or aneurysms. Atherosclerosis treatment options are limited to statins while balloon angioplasty and stenting – surgical procedures for stenosis, often end in restenosis. Therefore, we investigated pentagalloylglucose (PGG), a polyphenolic compound, as a therapeutic agent that can inhibit excess proteolytic activity, mitigate proliferation and disrupt the transformation of vascular smooth muscle cells into osteoblast-like cells. Previous experiments conducted in our lab have shown that PGG has elastoprotective properties in a rat aneurismal model. Studies conducted by other researchers have shown that PGG also has anti-cancer and anti-inflammatory properties.

Our results show that PGG effectively decreased the level of cathepsins K, L and S, and the activity of MMP-2 in tumor necrosis factor activated rat aortic smooth muscle cells (RASMCs) *in vitro*. Transcription levels of cathepsins K and S were dramatically decreased by PGG. Scratch test assay showed that PGG treatment resulted in visibly reduced migration and proliferation. PGG treatment also reduced the expression of

osteogenic markers in activated RASMCs. Gene expressions of CBFA-1 and MSX-2 were downregulated. Alkaline phosphatase activity was significantly reduced at days 1, 3 and 6. Addition of PGG 3 days past activation of RASMCs also resulted in decreased alkaline phosphatase activity, signifying that PGG could potentially reverse osteogenic differentiation of RASMCs.

We also conducted studies to verify if PGG could possibly increase elastin production in primary RASMCs by potentially inhibiting proteolytic activity. We found that levels of both tropoelastin and insoluble elastin were significantly increased in cells treated with PGG.

In order to deliver PGG locally to a diseased vascular site, we investigated the possibility of using nanoparticles. Poly(lactic-co-glycolic acid) nanoparticles encapsulated with PGG were prepared and their *in vitro* release profiles were studied. Sonication times during emulsion steps were varied and resulting encapsulation efficiencies were studied.

We conclude that PGG could potentially be a valuable therapeutic agent in vascular pathologies. Excess proteolytic activity, migration and proliferation of RASMCs were effectively controlled by PGG. PGG also inhibited the osteogenic signaling in smooth muscle cells through potentially affecting cell cycle progression by down regulating the gene expression of c-Fos. PGG could be used alone or with other existing treatments to control or reverse vascular diseases discussed above. Further optimization needs to be performed in order to determine the dose and mode of PGG delivery *in vivo*.

ACKNOWLEDGMENTS

I would like acknowledge my advisor Dr. Narendra Vyavahare for giving me an opportunity to work in his lab. I would also like to acknowledge the help of Dr. Martine LaBerge who has always been immensely supportive and encouraging throughout my time at Clemson. I would like to thank Dr. Anand Ramamurthi for his helpful insights and encouragement. I would like to thank Dr. Sarah Harcum for being a wonderful mentor, giving me extremely valuable advice and being so easy to talk to. Being a teaching assistant in her class was enjoyable and a great learning experience. Attending Dr. Webb's class has been the source for my love of molecular biology. I thank him for being so helpful about molecular biology techniques and analyses. I would also like to acknowledge the help of Cassie Gregory on numerous occasions and being such a good friend. Linda Jenkins has been so helpful in teaching me histological techniques. I would also like to thank Maria Martin, Leigh Humphries, Sherri Morrison, Dida Weeks and Maranda Arnold for their help in administrative matters. The staff at Godley Snell including Diane, Travis and Dr. Parrish has been extremely helpful during my animal experiments. Thanks to Brad Winn, Lavanya Venkataraman, Partha Deb and Laura Datko for providing me with cells for my experiments. Dr. Sherin Jacob's help has been indispensable for my studies involving PLGA films and nanoparticles. I would also like to acknowledge the financial support provided by National Institutes of Health (grant # HL61652 awarded to Dr. Narendra Vyavahare) and the Department of Bioengineering for providing me with teaching assistantship.

TABLE OF CONTENTS

Page

TABLE OF CONTENTS (CONTINUED)

Page

TABLE OF CONTENTS (CONTINUED)

Page

LIST OF TABLES

Table Page

LIST OF FIGURES

Figure Page

LIST OF FIGURES (CONTINUED)

Figure Page

LIST OF FIGURES (CONTINUED)

Figure Page

CHAPTER 1

INTRODUCTION

Cardiovascular diseases are the leading cause of mortality in many developed countries including the United States. In 2006 alone, cardiovascular diseases accounted for 34.3% of all deaths in the United States. The total cost of cardiovascular disease and stroke in the United States for 2010 is estimated to be $503.2 billion.[1] Hypercholesterolemia, hypertension, smoking, aging, genetic predisposition and diabetes mellitus are considered risk factors for atherosclerosis.[2] Cardiovascular diseases include atherosclerosis – deposition of fatty acids, stenosis – blockage of the arterial lumen, aneurysm – dilation of the aortic vessel and vascular calcification – ectopic mineralization of arterial tissue. All these pathological conditions involve a number of proteins, transcription factors and multiple cellular pathways. Controlling these diseases is important to prevent cardiac infarction, stroke or even death. Inhibitors of proteolytic enzymes are currently being studied extensively as potential therapeutic agents in many diseases.

Polyphenols are plant derived metabolites that contain multiple phenol groups. Polyphenols derived from tea and spices have shown to be effective at inhibiting proteolytic enzymes *in vitro*.[83] Pentagalloylglucose (PGG) is a polyphenol with a structure very similar to that of tannic acid. Previously in our lab, studies have shown that PGG successfully inhibited the degradation of elastin in a rat aneurysm model.

This research is focused on three pathological processes namely extracellular matrix degradation, calcification and smooth muscle cell proliferation. We hypothesize that all these three events are interrelated and PGG can arrest all these pathological processes.

1.1. AIM 1

Characterization of the anti-proteolytic and anti-proliferative activities of pentagalloylglucose in tumor necrosis factor activated rat aortic smooth muscle cells

Hypothesis

Primary rat aortic smooth muscle cells activated with tumor necrosis factor alpha produce excess proteolytic enzymes and undergo excess proliferation. This process is similar to pathological conditions observed in inflammatory clinical conditions. Pentagalloylglucose inhibits the activity of proteolytic enzymes and decreases proliferation of the activated cells.

1.2. AIM 2

Characterization of elastic fiber assembly by primary smooth muscle cells treated with pentagalloylglucose.

Hypothesis

Pentagalloylglucose increases the level of released tropoelastin and deposited insoluble elastin by inhibiting their proteolytic degradation. Pentagalloylglucose could also bind to the hydrophobic domains in tropoelastin making it more resistant to

elastases. Both these effects lead to increased extracellular assembly of mature elastic fibers.

1.3. AIM 3

Characterization of pentagalloylglucose induced anti-osteogenic differentiation of tumor necrosis factor activated rat aortic smooth muscle cells

Hypothesis

Pentagalloylglucose inhibits the dedifferentiation of activated rat aortic smooth muscle cells and prevents them from transforming into osteoblast-like cells. In parallel, pentagalloylglucose increases the calcium deposition by osteoblasts

1.4. AIM 4

Preparation and characterization of poly-(lactic-co-glycolic) acid nanoparticles encapsulating pentagalloylglucose that could potentially be used for local delivery of pentagalloylglucose *in vivo*

Hypothesis

Pentagalloylglucose can be encapsulated in polymeric nanoparticles. These nanoparticles can potentially be delivered to the vascular site and inhibit proteolytic activity locally. This process may aid in reducing the degradation of existing elastin and allow the deposition of insoluble elastin in animal models of aortic aneurysms and medial calcification.

1.5. AIM 5

Implementation and preliminary characterization of a new *in vitro* model of medial vascular calcification using cryo-sectioned arterial scaffolds

Hypothesis

Arteries cryo-sectioned perpendicular to the cross section can be used to line the bottom of well plates and create a scaffold for cells that mimics extracellular matrix in the medial layer of the artery. Interactions between vascular smooth muscle cells and the extracellular matrix in the medial layer can be studied using this model.

CHAPTER 2

LITERATURE REVIEW

2.1. VASCULAR ARCHITECTURE

The heart and the elastic arteries transport blood from the heart to the whole body. The large/elastic arterial wall consists of three layers – inner ‘intima’, ‘media’ and outer ‘adventita’. Intima is made of a thin lining of endothelium, its basal lamina and an elastic layer called internal elastic membrane. Endothelium contains simple squamous epithelial cells oriented in the direction of blood flow. These epithelial cells are connected to one another by tight gap junctions. The endothelium and the basal lamina control diffusion of most substances to the arterial walls.

Media of the elastic arteries is relatively thicker and has a different composition. This layer has sheets (lamellae) of elastic material interspersed with smooth muscle cell layers. The concentric elastin lamellae have fenestrations which are believed to help in diffusion of substances through the arterial wall. The smooth muscle cells are arranged in a spiral and interconnected by gap junctions. They synthesize the connective tissue proteins – elastin and collagen. Adventitia mainly consists of connective tissue and is usually thinner than media. The main structural protein is collagen along with a loose mesh of elastic fibers. Fibroblasts and macrophages are present in this layer. Tiny blood vessels called ‘vasa vasorum’ supply blood to the adventitia and outer portions of the media. Inner layers of the arterial wall are vascularized with the lumen.

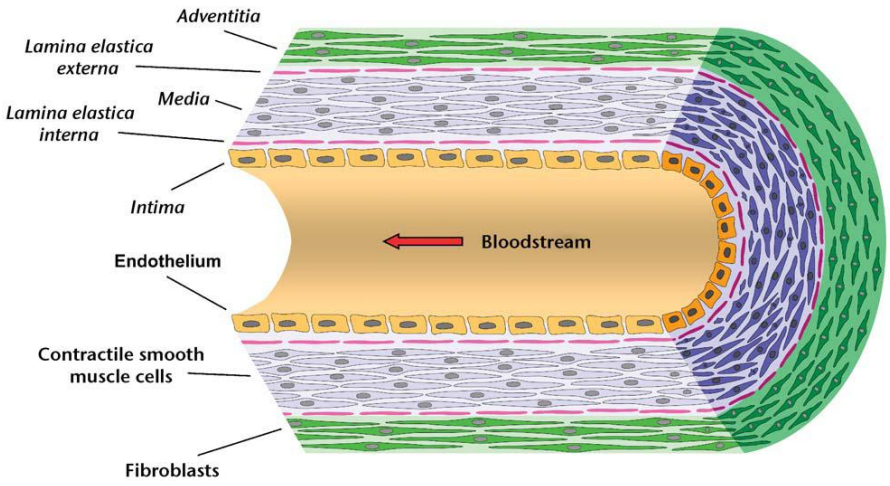

Figure 2.1: Morphology of a normal artery [3]

The large arteries, along with the heart, help maintain a pulsate flow of blood. During systole, the ventricles contract, causing the blood to flow through the elastic arteries. The pressure generated by the ventricles causes the distention of the elastic arteries which is opposed by the collagen fibers. The elastic tension built by the arteries is released and used to 'pump' the blood during diastole. This results in a synchronous pulsating of the arteries in response to the systole and diastole phases. This feature of the elastic arteries to behave as a supplementary pump is critical in maintaining blood pressure.[4]

2.2. VASCULAR PATHOLOGY

Cardiovascular disease is the leading cause of mortality in the United States. Mortality data for 2006 shows that cardiovascular disease caused for 34.3% of all deaths in 2006 in the United States. The total direct and indirect cost of cardiovascular disease and stroke in the United States for 2010 is estimated to be $503.2 billion.[1] Hypercholesterolemia, hypertension, smoking, aging, male gender and diabetes mellitus

are considered risk factors for atherosclerosis while a high ratio of high density lipoprotein (HDL) to low density lipoprotein (LDL) is considered beneficial for cardiovascular health.[2] Constant fluid flow causes shear stress and normal (perpendicular) stress results in cyclic strain of the arterial wall. With the progression of age, the constant stresses, combined with numerous factors such as inflammation and lipid deposition, results in many pathological conditions like hypertension, atherosclerosis, stenosis, medial calcification and aneurysm. These conditions are associated with several serious events like cardiac myofarction, thromboembolism and even death.[4]

2.3. ATHEROSCLEROSIS

Atherosclerosis is an inflammatory disease of the luminal surface of large and medium sized arteries. Aorta, carotid arteries, coronary arteries and the arteries of the lower extremities are affected by this disease.[5] Atherosclerotic lesions can begin to appear at childhood but can take decades before the pathological effects can be felt. The full-fledged atherosclerotic plaque is characterized by a large core made of necrotic fatty mass covered with a thin fibrous cap made of mostly collagen. Since atherosclerosis develops over a long period of time, initial cause for the development of plaque has been a subject of study. One of the most popular hypotheses is the 'response-to-injury model' which suggests that the endothelial layer is injured in some way leading to the advancement of atherosclerosis. Although it was first proposed in the mid nineteenth century, it is still widely accepted as a possible explanation. Chemical, mechanical or immunological insults that can cause endothelial dysfunction can lead to lipoproteins,

free radicals and toxic substances migrating to the sub-endothelial space.[3] Infectious agents including herpes virus and Chlamydia pneumonia are also considered possible causative agents.[6] Earlier sign of atherosclerosis is the appearance of yellowish, flat 'fatty streak' which is an accumulation of neointimal lipids, and is non-obstructive. 'Fibrous plaque' is found later in life, after the second or third decade, characterized by a more pronounced whitish lesion. At this stage, plaque contains infiltrating macrophages and other inflammatory cells, proliferating smooth muscle cells and deposited extracellular matrix proteins. On the interior of the fibrous plaque is a 'necrotic/lipid core' that contains foam cells, extracellular lipid, and cell debris. The fibrous plaques are capable of interrupting blood flow and can cause flow distortions in blood vessels. However, the surface of the plaque is stable and does not contain thrombotic material. It is unclear whether the fatty streak leads to the fibrous plaque or the latter can form de novo.[3] The plaque can lead to vascular remodeling, abnormalities in blood flow dynamics, partial or complete obstruction of blood flow many of which can lead to ischemia, decreased oxygen supply, to critical organs. These secondary conditions cause a positive feedback cycle leading to advancement of artery disease.[3]

2.4. VASCULAR CALCIFICATION

The presence of calcium deposits in the vessel wall is indicative of advanced atherosclerosis, and has been found to increase risk factors for coronary artery disease.[7, 8] With advanced age, vascular calcification causes a reduction in elasticity of the vessel wall. In high-risk asymptomatic adults the presence of calcification has been shown to increase the risk of a coronary death or nonfatal infarction.[9] Vascular calcification has been classified to be of four types based on the histological and anatomical perspectives by Vattikuti et al (2004) as (1) Atherosclerotic calcification (2) Medial calcification (3) Cardiac valve calcification and (4) Calciphylaxis.[10] Vascular calcification is present in 80% of advanced lesions and 90% of coronary artery disease.[11] Calcification in the plaque can complicate the situation due to risk of ulceration at the luminal surface, and hemorrhage from small vessels that grow into the lesion from the media of the blood vessel wall. Though advanced lesions can grow sufficiently large to block blood flow, the most important clinical complication is a severe occlusion due to the formation of a thrombus or blood clot, resulting in myocardial infarction or stroke. Furthermore, there is the risk of plaque rupture leading to thrombosis.[12] Considerable research in the past few years points to remarkable similarities between vascular calcification and bone ossification. This review will outline some of these similarities including the association of bone diseases like osteoporosis with pathological calcification of arteries. Recently, cells, proteins, and cytokines known to be involved in new bone formation have been observed atherosclerotic arteries. The increased expression of various bone-related proteins in atherosclerotic plaque, especially in areas of calcification has led to the

observation that arterial calcification is similar to the mechanism of new bone formation.[13-16] In order to highlight some of the parallels between arterial calcification and bone mineralization, we will review main aspects of bone physiology and then compare them to arterial calcification.

2.5. BONE PHYSIOLOGY – IMPORTANT MOLECULAR AND GENETIC ASPECTS

The skeletal system is a store for important minerals like calcium and magnesium. Thus, bone remodeling is a function of both mechanical stresses (Wolff's law) and the mineral ion requirements of the body. The homeostatic balance of the various mineral ions in the body is maintained by numerous hormones, genetic factors and environmental conditions. Osteoblasts are bone forming cells derived from mesenchymal progenitors. Osteoblasts lay down the mineralizable collagen matrix and are also involved in the ossification stage. Osteoclasts, derived from hematopoietic (mononuclear phagocyte) precursors, are responsible for degradation/resorption of bone and help maintain a homeostatic balance of mineral ions and aid in the repair and maintenance of skeletal structure. Both osteoblasts and osteoclasts are coupled in many ways and thus it is extremely difficult to alter one without affecting the other.

2.6. ROLE OF CYTOKINES AND GENETIC ASPECTS OF SKELETAL TISSUE

The structure of the skeleton in vertebrates is determined by complex signaling systems of various genes during and after embryogenesis. Most long bones develop by endochondral ossification that involves formation of a cartilage model, chondrocyte apoptosis and replacement of cartilage by mineralized bone. Flat bones, like the

craniofacial bones, are formed by intramembranous ossification in which bone is made directly by osteoblasts without a cartilaginous intermediate. During both types of ossification, there are a number of local growth factors, hormones, and genetic factors which influence and synchronize the events.[17] Pluripotent mesenchymal stem cells are capable of differentiation into adipocytes, myoblasts, chondrocytes, or osteoblasts. Commitment towards a particular lineage depends upon coordinated expression of sets of specific transcription factors and simultaneous suppression of other genetic programs that specify alternative cellular fates. As seen from the diagram, the main transcription factors responsible for the differentiation of mesenchymal stem cells into osteoblasts are Runx2 (also called core binding factor alpha -1 or cbfa-1) and Osx (osterix). Mice with targeted deletion of the gene encoding Cbfa1/Runx2 exhibit a complete lack of osteoblasts and die soon after birth.[18, 19] Distal-less5 (Dlx5), CBFA-1, and osterix (Osx) are transcription factors that are believed to be absolutely essential for differentiation of pluripotent mesenchymal progenitors into terminally differentiated osteoblasts.[20] CBFA-1 (also called Runx2) plays an important role in the terminal differentiation as well as functioning of osteoblasts. CBFA-1 has been known to induce collagen I, osteocalcin, and alkaline phosphatase gene expressions in osteoblasts.[21, 22] Muscle segment homeobox 2 (Msx-2) is a homeodomain transcription factor important for osteoblast differentiation and a downstream target of BMP signaling.[23]

2.7. THEORIES OF VASCULAR CALCIFICATION

There are several models to explain the process of vascular calcification and although none of the models can fully explain the pathological conditions associated with the disease, the models can be classified under the following categories:

1. Passive physiochemical models
2. Active cell mediated models

Passive physicochemical models of vascular calcification

This model affirms that vascular calcification is mainly due to of acellular mechanisms, and is governed by biochemical relationships. A charge neutralization theory proposed by D. W. Urry et al in 1971 suggests that elastin and collagen contain 'neutral sites' which have affinity for calcium ions.[24] Molecules such as alpha 2-HS glycoproteins (AHSGs) are active inhibitors of calcification in serum. AHSGs are ubiquitous, highly abundant in serum and bind to calcium efficiently preventing calcinosis or blockage of small blood vessels. AHSG-deficient mice with normal calcium ion levels develop sporadic perivascular calcification while hypercalcemic mice (induced by dietary means or by hormone treatment) die of lethal calcinosis.[25] Disphosphonates, proteoglycans (found in cartilage), magnesium & aluminum ions, serum proteins, metal-citrate complexes, and acidic proline-rich phosphoproteins suppress the growth of hydroxyapatite in various tissues and act as crystallization inhibitors.[26] Other studies claim that the phosphate group is responsible for the nucleation of calcium phosphate by means of the phosphoprotein complex and collagen.[27] Matrix vesicles have also been found to initiate calcification in atherosclerotic arteries.[28,29, 30] Matrix vesicles can induce

mineralization by compartmentalizing mineral ions and cause selective enrichment of specific proteins, enzymes, lipids and electrolytes. Rapid uptake of mineral ions by matrix vesicles leads to the crystalline phase, octacalcium phosphate (OCP) which is later converted to hydroxyapatite. Initial uptake of Calcium and phosphate ions by the matrix vesicles is protease sensitive, and is stimulated by o-phenanthroline, a Zinc ion chelator.[31] It has been observed that lipid molecules have been strongly associated with the initiation of matrix vesicle calcification.[32] This is very relevant to arterial calcification during atherosclerosis. Furthermore, Even though matrix vesicles essentially bud off from cells, almost all studies consider these vesicles to be more biochemical than cell-mediated. Although passive models of atherosclerotic calcification emphasize on the biological molecules being the main molecules involved in the pathology, they do not mention the involvement or relative importance of cells which secrete these molecules.

2.8. ACTIVE, CELL-MEDIATED MODELS OF VASCULAR CALCIFICATION

Arterial calcification began to be considered as an active process involving many cell types after the observations by Bostrom et al (1993) in which a division of the cultured vascular cells calcified and were named ‘Calcifying vascular cells’ or CVCs. These CVCs were distinct from the other vascular cells as they localized along with the expression of bone related proteins like BMP-2.[33, 34] Later, it was noticed that cultured vascular smooth muscle cells could also undergo spontaneous calcification *in vitro* and form mineralized nodules under certain conditions and express matrix proteins typically found in bone.[35, 36] Moreover, bone matrix-associated proteins appears to be expressed in a number of cell types in arterial tissue sections and thus the precise identification of the

CVCs in arterial calcification *in vivo* remains uncertain.[37, 38] Human and animal studies of atherosclerosis have shown the existence of cells that are phenotypically similar to the major cell types found in bone remodeling – osteoblasts, osteoclasts and chondroblasts. Endochondral ossification has also been observed in diseased arteries with the process indistinguishable from that of bone tissue.[38-41] Additionally, signaling pathways corresponding to those in bone were found in these calcifying cells.[14, 42] Similar to bone mineralization, arterial tissues also undergo mineralization through matrix vesicles.[29] The mineral composition of bone is chemically very similar to that found in calcified atherosclerotic plaques.[43] Thus, arterial calcification resembles bone mineralization very closely.

In the active model, the emphasis is on the phenotypes or change in phenotypes of various cell types in atherosclerotic arteries while very little importance is given to the actual chemical environment. However vascular calcification *in vivo* can be a combination of both models in varying degrees.

2.9. BONE RELATED PROTEINS AND THEIR ROLE IN VASCULAR CALCIFICATION

Various bone matrix regulatory proteins have been upregulated in atherosclerotic aortas. Diseased aortas demonstrated calcification of the plaques and up-regulation of BMP-2, BMP-4, osteopontin, osteocalcin, matrix Gla protein and bone sialoprotein compared to the healthy aortas. All these are markers of osteoblast differentiation or, in other words, bone formation.[43]

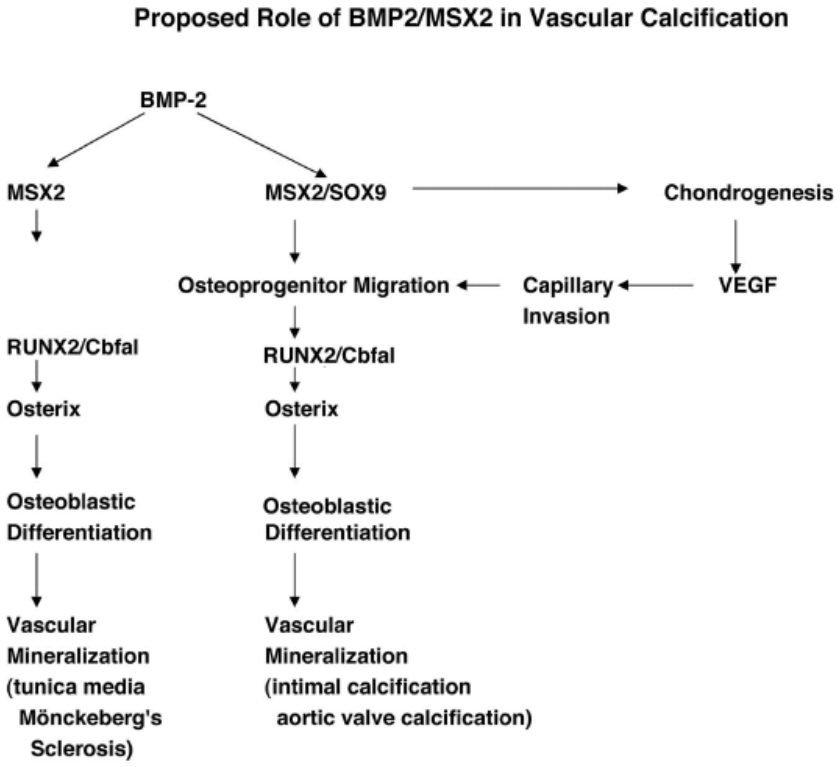

Figure 2.2: Proposed role of BMP2/MSX-2 in vascular calcification [44]

2.10. VASCULAR CALCIFICATION AND OSTEOPOROSIS

Presence of atherosclerosis and vascular calcification is often observed with osteoporosis and vice versa. It has been shown that women with vascular calcification have a higher risk of suffering fractures, a sign of osteoporosis. Indeed, the risk of fractures increased with the amount of vascular calcification.[44] Aging, estrogen deficiency, autoimmune disease, and lipid oxidation are some of the common risk factors for both diseases.[45, 46]

Interestingly, atherosclerotic calcification and bone loss in postmenopausal women happen almost concurrently leading to simultaneous deposition of calcium in vessels while loss of bone.[45, 46] Osteoprotegerin (OPG), receptor activator for nuclear factor κ β (RANK) and receptor activator for nuclear factor κ β ligand (RANKL) forma an important triad in the relationship between osteoblasts and osteoclasts in bone as shown in Figure 2.3. OPG has in fact hypothesized to be the key common factor between the two pathologies. Nevertheless, unlike the skeletal system, the exact mechanism of OPG/RANK/RANKL in vascular calcification has not been thoroughly analyzed yet. Therapies used for bone loss like bisphosphonates, OPG have also shown to prevent arterial calcification in animals.[47, 48]

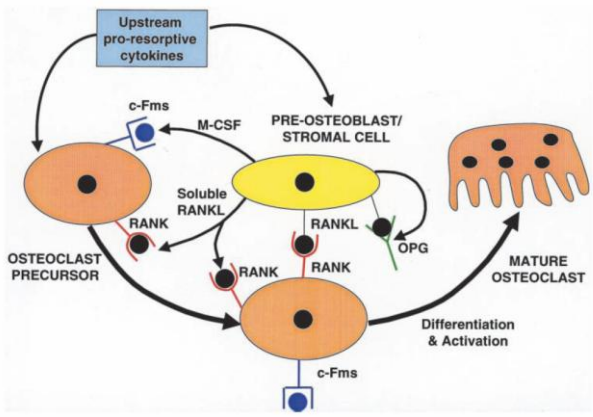

Figure 2.3: Relationship between OPG/RANK/RANKL in bone metabolism[49]

2.11. AORTIC ANEURYSMS

Abdominal aortic aneurysm (AAA) is often a fatal disease that largely affects older patients, accounting for at least 15,000 deaths in the year 2000. Aneurysm can be defined as a permanent local dilation of an artery to 150% of its normal diameter.[50] Progression of an aneurysm can lead to increased dilation, rupture and death. Aneurysms that occur in the cerebral arteries, called cerebral aneurysms, can cause stroke due to rupture, and even death. Most abdominal aortic aneurysms are asymptomatic and can thus go undetected. Early detection and monitoring are very important to implement changes in lifestyle and schedule surgery if necessary.

The main factor in the initiation and progression of AAA involves the proteolytic degradation of extracellular matrix proteins. Degradation of elastin and collagen, two main structural proteins of the artery, leads to weakening of the arterial wall, dilation and rupture. A range of proteolytic enzymes, including matrix metalloproteases (MMPs) play a very important role in degrading collagen and elastin and can lead to remodeling of the arterial wall, causing structural weakness. Factors such as cigarette smoking, increased oxidative stress and autoimmune conditions can increase risk factors for aneurysms. Increased stress on the arterial wall due to high blood pressure could also increase the risk of aneurysms, causing disordered flow.[51]

2.12. MATRIX METALLOPROTEINASES

MMPs are a family of about 25 endopeptidases that require zinc as co-factor. MMPs are secreted as inactive zymogens and are activated by cleavage of the pro domain. As the name suggests, MMPs degrade extracellular matrix proteins such as collagen and elastin. As shown in Table 2.1, members of the MMP family of proteases degrade various extracellular matrix proteins. In addition, MMPs play an important role in cell-cell and cell-matrix interactions. Several MT-MMPs (membrane type MMPs), MMP-2 among a few are expressed by healthy cells. Activated cells release more types and quantities of MMPs.[52]Similar to other proteases, MMPs are regulated at (1) Transcriptional level (2) Compartmentalization (3) Enzyme activation and (4) Enzyme inhibition. Tissue inhibitors of metalloproteinases are a group of four proteins that inhibit the activity of MMPs. TIMPs can bind to the active site of MMPs and inhibit their proteolytic activity. Some TIMPs are required for activation of some MMPs. Alpha-2macroglobulin is another MMP inhibitor that is found in the serum.[53]

Mammalian matrix metalloproteinases

Designation [a]	Common name	Other name(s)	Activation mechanism
1. MMP-1	Collagenase-1	Fibroblast collagenase,	Unknown
	Mcol-A, Mcol-B [b]	interstitial collagenase	Unknown
3. MMP-2	Gelatinase-A	72-kD gelatinase,	MT1-MMP/
		72-kD type IV collagenase	TIMP-2
4. MMP-3	Stromelysin-1	Transin-1	Unknown
5. MMP-7	Matrilysin	PUMP	Unknown
6. MMP-8	Collagenase-2	Neutrophil collagenase	Unknown
7. MMP-9	Gelatinase-B	92-kD gelatinase,	Unknown
		92-kD type IV collagenase	
8. MMP-10	Stromelysin-2	Transin-2	Unknown
9. MMP-11	Stromelysin-3		Furin
10. MMP-12	Metalloelastase		Unknown
11. MMP-13	Collagenase-3	Rat collagenase	MT1-MMP/
			TIMP-2
12. MMP-14	MT1-MMP	Membrane-type MMP	Furin
13. MMP-15	MT2-MMP		Furin
14. MMP-16	MT3-MMP		Furin
15. MMP-17	MT4-MMP		Furin
16. MMP-19	RASI-1		Unknown
17. MMP-20	Enamelysin		Unknown
18. MMP-21			Unknown
19. MMP-22			Unknown
20. MMP-23	CA-MMP		Furin
21. MMP-24	MT5-MMP		Furin
22. MMP-25	Leukolysin	MT6-MMP	Furin
23. MMP-26	Endometase	Matrilysin-2	Unknown
24. MMP-27 [c]			Unknown
25. MMP-28	Epilysin		Furin

Table 2.1: Mammalian matrix metalloproteinases [52]

MMPs are known to be expressed by atherosclerotic arteries while they are absent in healthy arteries.[54] Activated monocytes in an atherosclerotic plaque can release several cytokines and MMPs that degrade the extracellular matrix.[55] Calcification of elastin has also observed to be an important factor in atherosclerosis and is associated strongly with MMP activity.[56, 57]

2.13. CATHEPSINS

Cathepsins are lysosomal cysteine proteases that are mainly involved in intracellular protein turnover. There are 11 known cathepsins which are primarily involved in non-specific protein degradation within the lysosomes. Most cathepsins function in an acidic environment and exhibit reduced activity at higher pH with the exception of cathepsin S, which has optimal activity at pH 7.4. In pathological conditions, cathepsins are released into the extracellular space where they degrade extracellular matrix proteins.[58, 59] Cathepsin K was first isolated from rabbit osteoclasts. It is considered marker of osteoclasts since its proteolytic activity is critical for osteoclast bone resorption. Inactive cathepsin K results in a genetic bone disorder called pycnodysostosis characterized by abnormal bone resorption.[60-64] Cathepsin L is found in most mammalian cells. It mainly functions in normal protein turnover within lysosomes. Cathepsin L has also been implicated in pathological conditions such as excess bone resorption, tumor metastases and arthritis.[65-67] Cathepsin S is a lysosomal enzyme that is a highly potent elastase. It has been implicated in Alzheimer's disease and emphysema.[67] Spleen cells and antigen presenting cells such as B lymphocytes and macrophages express high levels of cathepsin S.[68-70]

2.14. ROLE OF TUMOR NECROSIS FACTOR-ALPHA IN ATHEROSCLEROSIS, VASCULAR CALCIFICATION AND ANEURYSMS

Atherosclerosis, intimal calcification and aneurysms are closely associated with inflammatory conditions. Inflammatory cells such as macrophages/

lymphocytes/neutrophils infiltrate into amounts of calcium and phosphorus in chronic kidney disease (CKD) patients compared to non-renal patients. In diabetic patients, glucose loading causes an increase in serum levels of TNFα.[71] Bone markers including bone morphogenetic protein -2 (BMP-2), bone sialo-protein, core binding factor alpha-1 (CBFA-1) were found in significantly higher amounts in CKD patients, even in non-calcified regions. Expression of TNFα and Msx-2 (muscle segment homeobox-2) were also upregulated along with increased osteoblastic differentiation of aortic smooth muscle cells in CKD patients.[72] Aortic calcification in diabetes and chronic kidney disease have common factors including low-grade arterial inflammation, and increased TNFα levels. Infliximab, a TNFα neutralizing antibody can diminish the aortic calcification through BMP-2-Msx-2-Wnt3a and Wnt7a signaling. In low density lipoprotein receptor knockout (LDLr-/-) mice (a model of hypercholesterolemia) fed with high fat diet, infliximab did not reduce obesity, hypercholesterolemia, or hyperglycemia but decreased BMP2, Msx-2, Wnt3a, and Wnt7a and decreased aortic calcium. Thus TNFα has an important role in diabetic and CKD related vascular calcification.[73, 74]

In vascular smooth muscle cells, TNFα increased the expression of CBFA-1, osterix, alkaline phosphatase, bone sialoprotein, all markers of osteogenic differentiation. Msx-2 expression was increased in these cells by TNFα through the nuclear factor kappa B (NF-κB), in a dose and time dependent manner. TNFα causes the osteogenic transdifferentiation through Msx-2 as demonstrated by increased alkaline phosphatase expression by over expression of Msx-2 and vice versa due to knockdown of Msx-2 by siRNA.[75] Vascular smooth muscle cells treated with TNFα and phosphate (Pi) showed

significant release of many pro-inflammatory cytokines, including tumor necrosis factor alpha (TNFα).[76] TNFα also causes the release of other cytokines and proteases. Vascular smooth muscle cells treated with TNFα showed enhance expression and activity of alkaline phosphatase, an osteoblast marker and increased calcium deposition. TNFα causes osteogenic differentiation through the cyclic adenosine monophosphate (cAMP) pathway as demonstrated by higher levels of intracellular cAMP and its inhibition by a protein kinase-A inhibitor.[77] Alpha-tocopherol (Vitamin E) has been evaluated for effectiveness against cardiovascular diseases in many studies. A novel tocopheryl phosphate mixture reduced pro-inflammatory markers in atherosclerosis including interleukin-1beta (IL-1beta), IL-8, TNFα and reduced lesion development.[78] In a study conducted with patients with aortic stiffness related to atherosclerosis, anti-TNF-alpha therapy improved aortic stiffness compared to untreated patients.[79] These studies confirm the importance of TNFα in vascular pathologies and the potential of inhibiting TNFα and its downstream effects.

2.15. POLYPHENOLS

Polyphenols are micronutrients found abundantly in plant food sources and have become the topic of research in the past 15 years, mainly due to the discovery of their antioxidant properties. Plants produce polyphenols as secondary metabolites as a defense mechanism against ultraviolet radiation or pathogens. Polyphenols can be classified based on the number of phenol rings and structural elements between the phenolic rings as: phenolic acids, flavonoids, stilbenes and lignans as shown in Figure 2.4.[80]

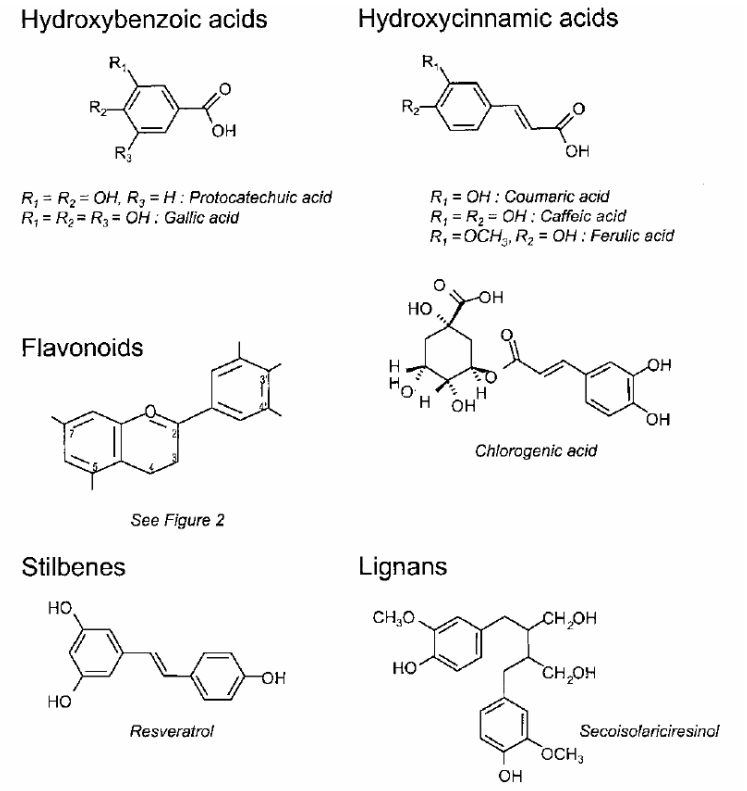

Figure 2.4: Types of polyphenols [80]

Phenolic acids are further classified as derivatives of benzoic acids or derivatives of cinnamic acids.[80] Structure of flavonoids consists of two aromatic rings (A and B) bound together by three carbon atoms that comprise an oxygenated heterocycle (ring C). Flavonoids are categorized into 6 subclasses based on type of heterocycle involved: flavones, isoflavones, flavanones, anthocyanidins, and flavanols (catechins and proanthocyanidins) as shown in Figure 2.5.[80]

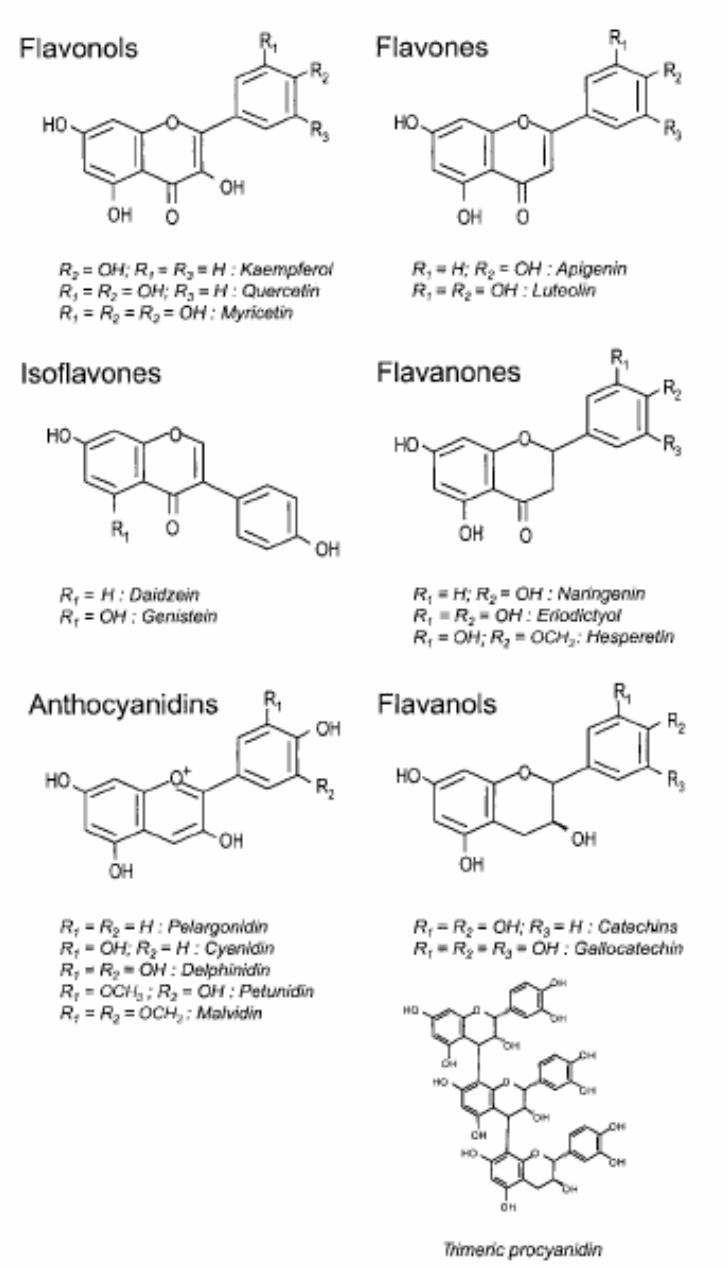

Figure 2.5: Types of flavonoids [80]

Polyphenols have been shown to have various beneficial effects on health as outline in many recent reviews. The benefits include anti-inflammatory, anti-cancer and antioxidant effects.[81-85] Polyphenols also known to down-regulate expression of pro-

inflammatory mediators, matrix metalloproteinases, and adhesion molecules.[86] Polyphenols affect multiple pathways in cells as shown in Figure 2.6.

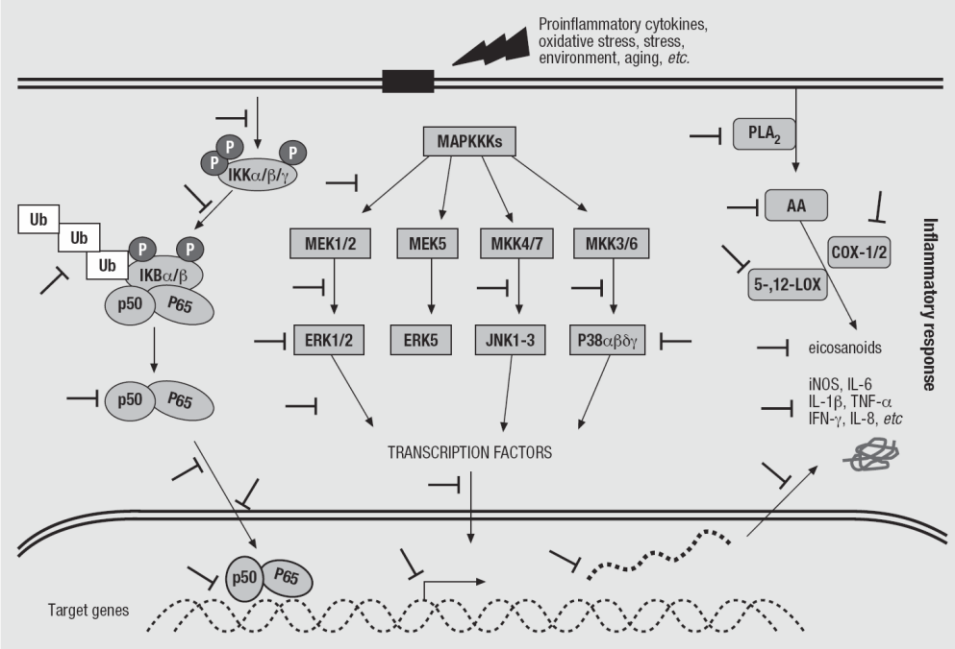

Figure 2.6: Polyphenol has various anti-inflammatory effects [87]

Polyphenols act as antioxidants *in vitro* by scavenge oxidative stress agents or additionally by inhibiting oxidative stress induced NF-κB, activator protein-1 (AP-1), oxidative stress inducing enzymes such as nitric oxide synthase, and xanthine oxidase. Antioxidant activities of polyphenols have been demonstrated more definitively *in vitro* than *in vivo*.[88] Turmeric contains a polyphenols called curcumin that can act as an antioxidant and modulate important signaling pathways mediated through NF-kappaB and mitogen-activated protein kinase pathways.[86] Epigallocatechin-3-O-gallate (EGCG) an anti-oxidant found in green tea is believed to have anti-inflammatory properties. In a

study conducted on EGCG treated human umbilical vein endothelial cells (HUVECs), the cells exhibited lower monocyte adhesion due to TNFα.[89] EGCG also inhibits ultraviolet B induced AP-1 and NF-κB-dependent transcriptional activation.[90] Pentagalloylglucose (PGG) is a polyphenol with a structure as shown in Figure 2.7. PGG has five gallic acid residues (structure shown in Figure 2.8) attached to a glucose core.[91] PGG has been investigated by various researchers to have anti-proteolytic, anti-cancer and antioxidant properties.

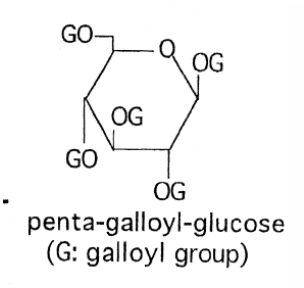

Figure 2.7: Structure of pentagalloylglucose [91]

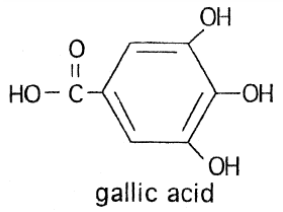

Figure 2.8: Gallic acid structure [91]

Pentagalloylglucose was effective in scavenging free radical 1,1-diphenyl-2-picrylhydrazyl (DPPH) and protect against lipid peroxidation in leukemia cell line treated with hydrogen peroxide. Gallic acid induced the expression of multiple antioxidant enzyme genes.[92] PGG has shown promise as an anti-cancer agent in many studies. PGG suppresses the growth of prostate cancer xenografts in nude mice and induces apoptosis in prostate cancer cell line and could be used as a potential cancer therapeutic drug.[93] PGG inhibits estrogen receptor function and suppressed the growth of estrogen-responsive human breast cancer cells. Estrogen receptor alpha levels were decreased by PGG through degradation in lysosomes.[94] PGG induces cell cycle arrest at G1 phase through downregulation of cyclin-dependent kinases 2 & 4, and upregulation of cyclin-dependent kinase inhibitors p27 & p21 in human breast cancer cells. In addition to inducing apoptosis in human leukemic cells, PGG also has inhibitory effects on 26s

proteasomes in Jurkat T cells. PGG affects cell cycles in human leukemic cells through its action as a proteasome inhibitor.[95]

CHAPTER 3

CHARACTERIZATION OF ANTI-PROTEOLYTIC AND ANTI-PROLIFERATIVE ACTIVITIES OF PENTAGALLOYLGLUCOSE IN TUMOR NECROSIS FACTOR ACTIVATED RAT AORTIC SMOOTH MUSCLE CELLS

3.1. INTRODUCTION

Mechanical strength and healthy function of the arteries depends on the integrity of elastin and collagen. Increased proteolytic activity is a hallmark of many diseases including atherosclerosis, aneurysms, stenosis and vascular calcification. Excess release of proteases results in indiscriminate degradation of extracellular matrix proteins particularly, elastin and collagen.[96-100] It is therefore important to inhibit excess proteolytic activity to control disease progression and preserve the mechanical properties of arteries.

Major classes of proteolytic enzymes that are shown to be activated in vascular diseases are matrix metalloproteinases (MMPs) and cathepsins. MMPs are a family of enzymes that participate in various cellular functions and degrade extracellular matrix proteins.[52] MMP-2 and MMP-9 are potent collagenases that are important in vascular diseases.[96-100]

Cathepsins are lysosomal cysteine proteases that can be released extracellularly during pathological conditions. Cathepsin K is a strong collagenase while cathepsin S is a potent elastase. Cathepsins K, L and S are upregulated in multiple vascular pathologies.

[101-103] Healthy medial vascular smooth muscle cells (VSMCs) are generally found in the media and exist in a contractile state. Changes that cause the phenotypic transition of VSMCs into a synthetic state occur concurrently with extracellular matrix degradation. Narrowing of the arterial lumen (stenosis) involves the migration of these synthetic VMSCs into the subendothelial layer. Subsequently, the VSMCs proliferate and deposit additional extracellular matrix causes the lumen to occlude, which results in stenosis. Surgical procedures such as balloon angioplasty or stenting can expand the luminal diameter but are usually followed by restenosis.[104,105] Polyphenolic compounds have shown to be beneficial in inhibiting the activity of proteolytic enzymes in multiple studies.[106-108] Pentagalloylglucose (PGG) has been used in previous studies in our lab and proven to be elastoprotective in a rat model of aneurysm.[109,110] In these studies, we studied the effects of PGG on the proteolytic activity, proliferation and migration of rat aortic smooth muscle cells when supplemented in cell culture media.

3.2. MATERIALS AND METHODS

3.2.a Cell Culture

Primary rat aortic smooth muscle cells (RASMCs) purchased from Cell Applications Inc, were seeded at passages 8-10 on well plates for all experiments. Cells were grown in DMEM with 10% fetal bovine serum and 1% penicillin-streptomycin. TNFα (rat recombinant, Peprotech Cat# 400-14) and PGG (kind gift from OmniChem, Belgium) were supplemented in cell culture media as described below.

In preliminary experiments (n=2 per group), cells were treated with 0 ng/ml, 10 ng/ml, 50 ng/ml, and 100 ng/ml of TNFα to determine the effect on MMP-2 and cathepsin L activity. A p value of equal to or less 0.05 was considered statistically significant; however more samples are necessary to obtain meaningful results.

From the results of the preliminary experiments, a concentration of 50 ng/ml of TNFα was determined to be optimal for our experiments (results described in section 3.4a). Further experiments were conducted as described in the following paragraphs.

3.2.b Experimental groups

TNFα and PGG were added simultaneously at day 0 and samples collected at days 1, 3 and 6. Delayed group (D6) consisted of cells supplemented with TNFα at day 0, PGG added at day 3, and samples were collected at day 6.

3.2.c Live/dead assay

RASMCs were grown with TNFα, PGG, or both added together. Cells grown in absence of either TNFα or PGG were considered as a control group. At the end of 6 days, cell viability was determined using a LIVE/DEAD Cell Viability assay (Molecular Probes L3224). Cells fluorescing green are considered alive while cells fluorescing red are considered dead.

3.2.d Proliferation assay

Proliferation of cells was estimated using the MTT (3-(4,5-Dimethyl-2-thiazolyl)-2,5-diphenyl-2H-tetrazolium bromide) assay. Equal number of cells were seeded and treated with TNFα, PGG, both added together. Cells grown in the control group were not

treated with either TNFα or PGG. Cell proliferation at day 0 (before any treatment) was also assessed to confirm that equal numbers of cells were seeded. Briefly, 5 mg of MTT (Sigma M2128) was dissolved in 10 ml of serum-free media and added to cells. After 4 hours, media was carefully aspirated and the insoluble formazan dye was collected with acidified isopropanol. Absorbance was read at 560 nm and normalized to control (no treatment) readings.

3.2.e Real-time PCR

RNA was isolated from cells using GE Illustra mini RNA isolation kit and quantified using the Agilent 2100 bioanalyzer. Equal amounts of RNA were reverse transcribed with the Applied Biosystems High Capacity reverse transcription kit. Real-time PCR was conducted using Qiagen SYBR green master mix on the Rotorgene PCR machine. Delta-delta Ct method was used to calculate relative gene expression with 18S rRNA as the housekeeping gene.[111]

3.2.f Gelatin zymography

Protein samples were normalized to total protein quantified using bicinchoninic acid assay (Pierce). Equal quantities of protein were loaded with non-denaturing buffer in wells of pre-cast gelatin zymogram gel (Biorad 161-1131) and run at 85V for 120 minutes. The gels were then washed in 2.5% Triton X-100 for 30 minutes and incubated overnight in activation buffer to detect MMP-2, -9 (50mmol/L Tris-base, 5mmol/L calcium chloride, 200mmol/L sodium chloride, 0.02% brij pH 7.5). The gels were then stained with commassie blue, destained and imaged. Densitometric analysis was

performed using ImageJ software.[112] Average densities of experimental groups were normalized to the control (no treatment) group and plotted as percentage of control.

3.2.g Western blot

Cells were grown as described earlier with some modifications to detect cathepsins in conditioned media. Twenty four hours before time of collection, media was replaced with serum-free media containing the corresponding supplements. Serum-free conditioned media was collected at days 2, 3 and 6 and concentrated 20-30X using Amicon 10 kDa molecular cut-off filters. Total protein was quantified with bicinchoninic acid assay (Pierce). Equal amounts of protein were boiled with denaturing buffer and loaded in pre-cast gels (Biorad 161-1102). Gels were run at 85V for 120 minutes and transferred to PVDF membrane (Millipore) at 50V for 120 minutes. The blots were blocked in 5% non-fat dry milk (LabScientific) overnight at 4 ^{o}C, incubated in primary antibodies against cathepsin S (SCBT sc-30057, rabbit anti-rat), cathepsin K (Biovision 3588-100, rabbit anti-rat) and cathepsin L (Abcam ab6314, mouse anti-rat). This was followed by incubation with secondary antibody (anti-mouse/rabbit) and detection (Roche BM Chemiluminescence kit, anti-mouse/rabbit). Bands were imaged with Alpha Innotech chemiluminescence detector.

3.2.h Migration assay

In vitro scratch test was conducted to study cell migration in response to injury. Previously published protocol for the scratch assay was followed.[113] Briefly, cells were seeded onto 6 well plates and grown until confluence. A ‘scratch’ was made with a sterile

pipette tip to simulate a wound. TNFα, PGG, or both together were added (0 hr). A control group cells were 'scratched' without any treatment. Images of the scratch area were taken at 0, 24 and 48 hours.

3.2.i Data analysis

Results are expressed as mean ± SEM with triplicates for all experimental groups. Statistical analysis of data was calculated using student's t-test and probability value (p) was calculated. A p-value equal to or less than 0.05 was considered statistically significant.

3.3. RESULTS

3.3.a Results of preliminary experiments

The activities of MMP-2, MMP-9 and cathepsin L were determined by gelatin zymography. RASMCs treated with various concentrations of TNFα and the cathepsin L activity levels from 3 day cell lysates are shown by zymography in Figure 3.1. TNFα increased the activity of cathepsin L at all the concentrations used as shown by densitometric analysis in a dose dependent manner (Figure 3.2).

MMP-2 activity in cells treated with various concentrations of TNFα was detected by zymography as shown in Figure 3.3. Densitometric analysis of MMP-2 zymogram is shown in Figure 3.4. Since the concentration of 50 ng/ml caused a noticeable increase in cathepsin L activity (1.5 fold) of 3 day cell lysates and 1.4 fold increase in MMP-2 activity, TNFα was used at this concentration for subsequent experiments.

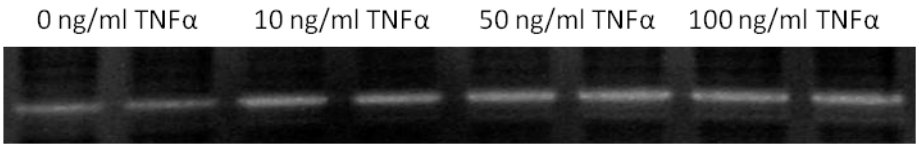

Figure 3.1: Gelatin zymography for cathepsin L activity in day 3 lysates

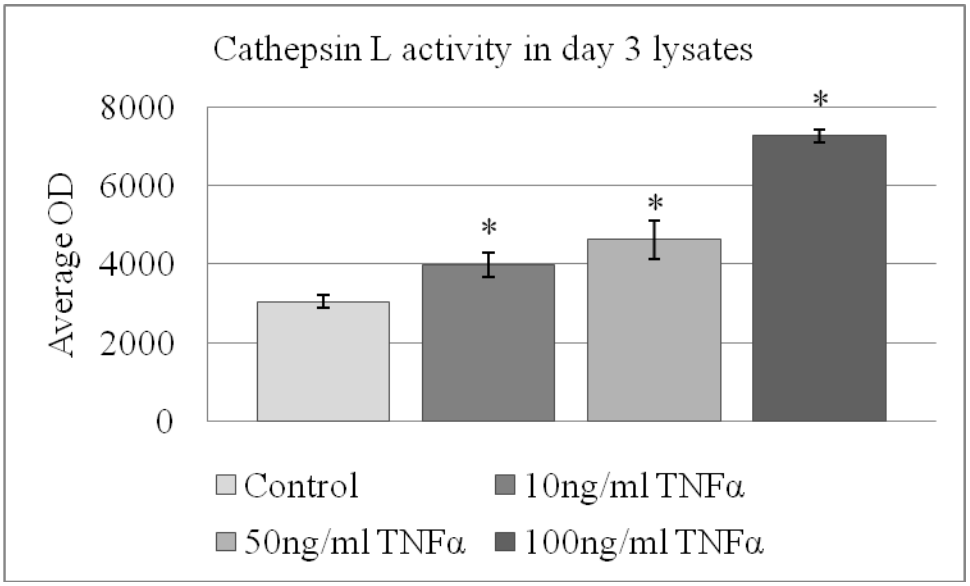

Figure 3.2: Densitometric analysis of cathepsin L zymogram in day 3 lysates. * indicates statistically significant with $p<0.05$ and $n=2$.

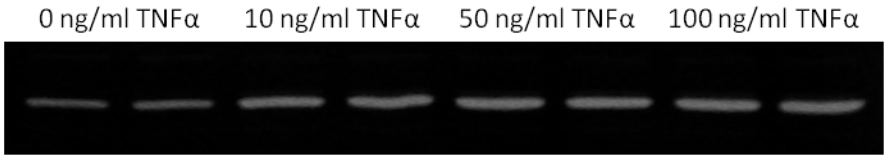

Figure 3.3: Gelatin zymography for MMP-2 in day 3 conditioned media

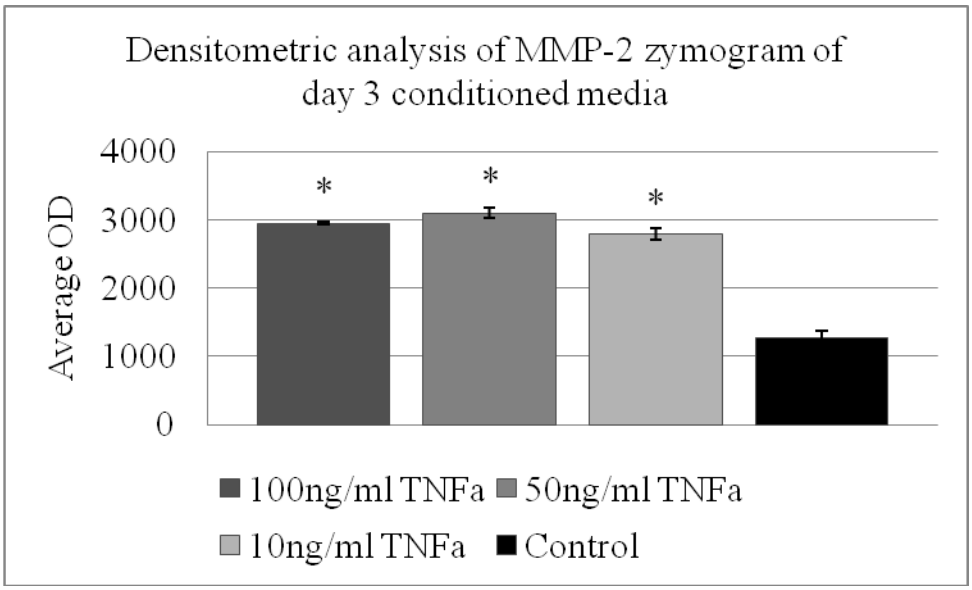

Figure 3.4: Densitometric analysis of MMP-2 zymogram of day 3 conditioned media. * indicates statistically significant with $p<0.05$ and $n=2$.

3.3.b PGG did not cause cytotoxicity in rat aortic smooth muscle cells

Live/dead assay was conducted to determine any cytotoxic effects of 50 ng/ml TNFα, 10 μmol/L PGG or their combination on RASMCs. The results of live/dead assay (Figure 3.5) showed similar numbers of dead cells in all groups. This demonstrates that 50 ng/ml TNFα, 10 μmol/L PGG, or their combined treatment have no significant cytotoxic effects the concentrations used in our experiments. Previously, PGG has been shown to induce minimal cytotoxic effects at concentrations of 0.03% - 0.3%.[109] As seen in Figure 3.5, images of the cells show minimal number of dead cells as denoted by red fluorescence. These images also showed that RASMCs treated with 50 ng/ml TNFα became more cuboidal in morphology suggesting a deviation from the usual spindle-shape of aortic smooth muscle cells. When PGG was combined with TNFα, more cells had spindle shaped morphology at the end of 6 days suggesting that PGG maintained smooth muscle cells in their native state. In order to determine if proliferation of these cells were affected by the treatments, MTT assay was performed as described in section 3.3.g.

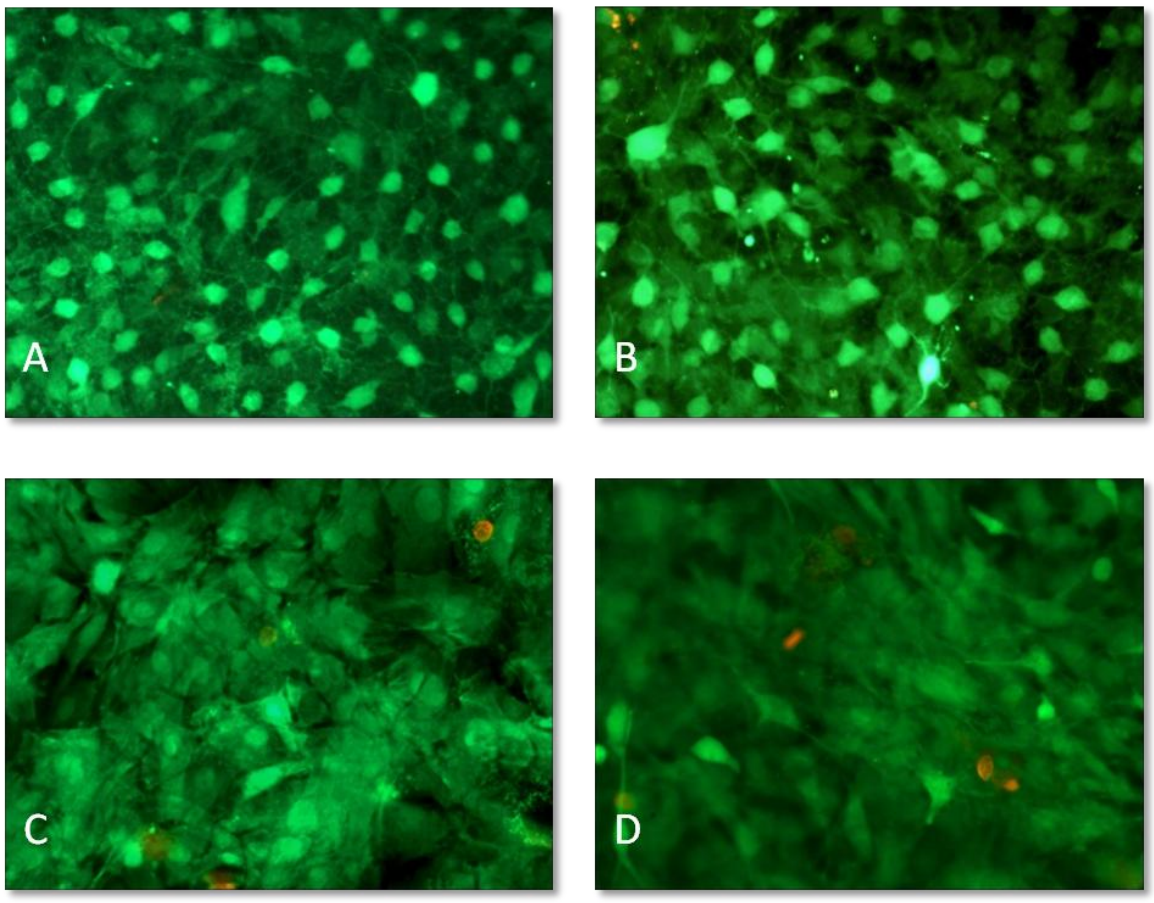

Figure 3.5: Live/dead assay of RASMCs treated with TNFα (A), TNFα+PGG (B), PGG (C) or no treatments (D) for 6 days. Green fluorescence shows live cells while red fluorescence denotes dead cells.

3.3.c PGG significantly decreased transcription of proteolytic enzymes

The effect of TNFα and PGG on the gene expressions of proteolytic enzymes was examined. Real-time PCR results demonstrated that PGG significantly affected the gene expression levels of cathepsins at day 3 as shown in Figures 3.6. Cathepsins K (CTSK) gene expression was increased more than 7-fold by TNFα. When PGG was added along with TNFα, gene expression of cathepsin K in RASMCs was decreased to 3-fold. Cathepsin S (CTSS) gene expression was dramatically increased by TNFα (160-fold) compared to the control cells. PGG down regulated the mRNA levels of cathepsin S by more than 60%. Cathepsin L (CTSL) and cystatin C (Cys C) gene levels were not significantly affected due to the treatments.

Expression levels of cathepsins at day 6 are shown in Figure 3.7. At day 6, TNFα increased the gene expression of cathepsin K. PGG, when added together with TNFα, decreased the expression of cathepsin K but not significantly. Cathepsin S gene expression due to TNFα treatment showed 80-fold increase which is 50% of the expression at day 3. However, adding PGG along with TNFα did not decrease the expression of cathepsin S gene at day 6. Cathepsin L and cystatin C gene expression did not differ considerably due to treatments.

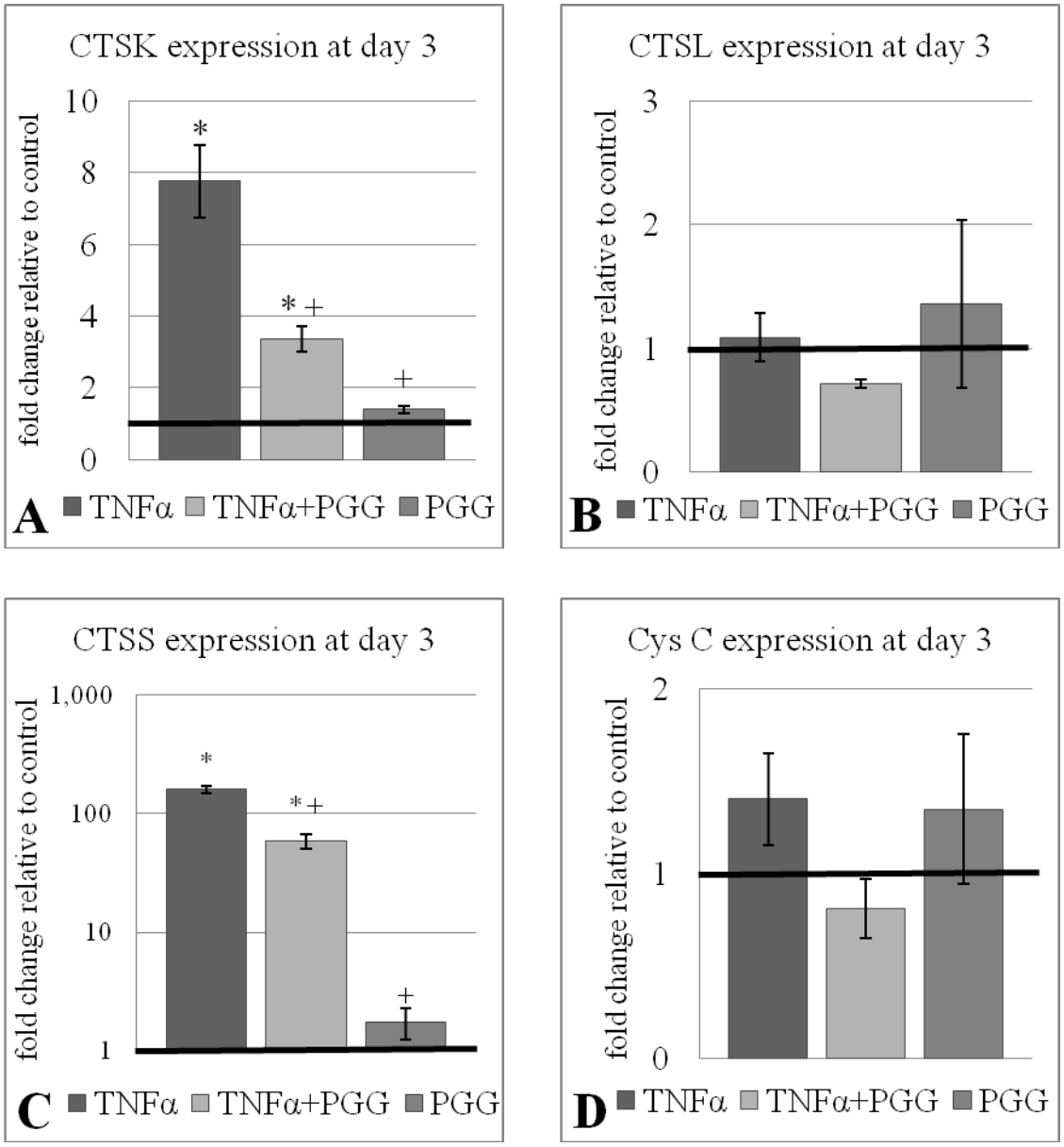

Figure 3.6: Real-time PCR of proteolytic enzymes in day 3 RASMCs. * indicates significantly different from the control group and + indicates significantly different from the TNFα group ($p<0.05$).

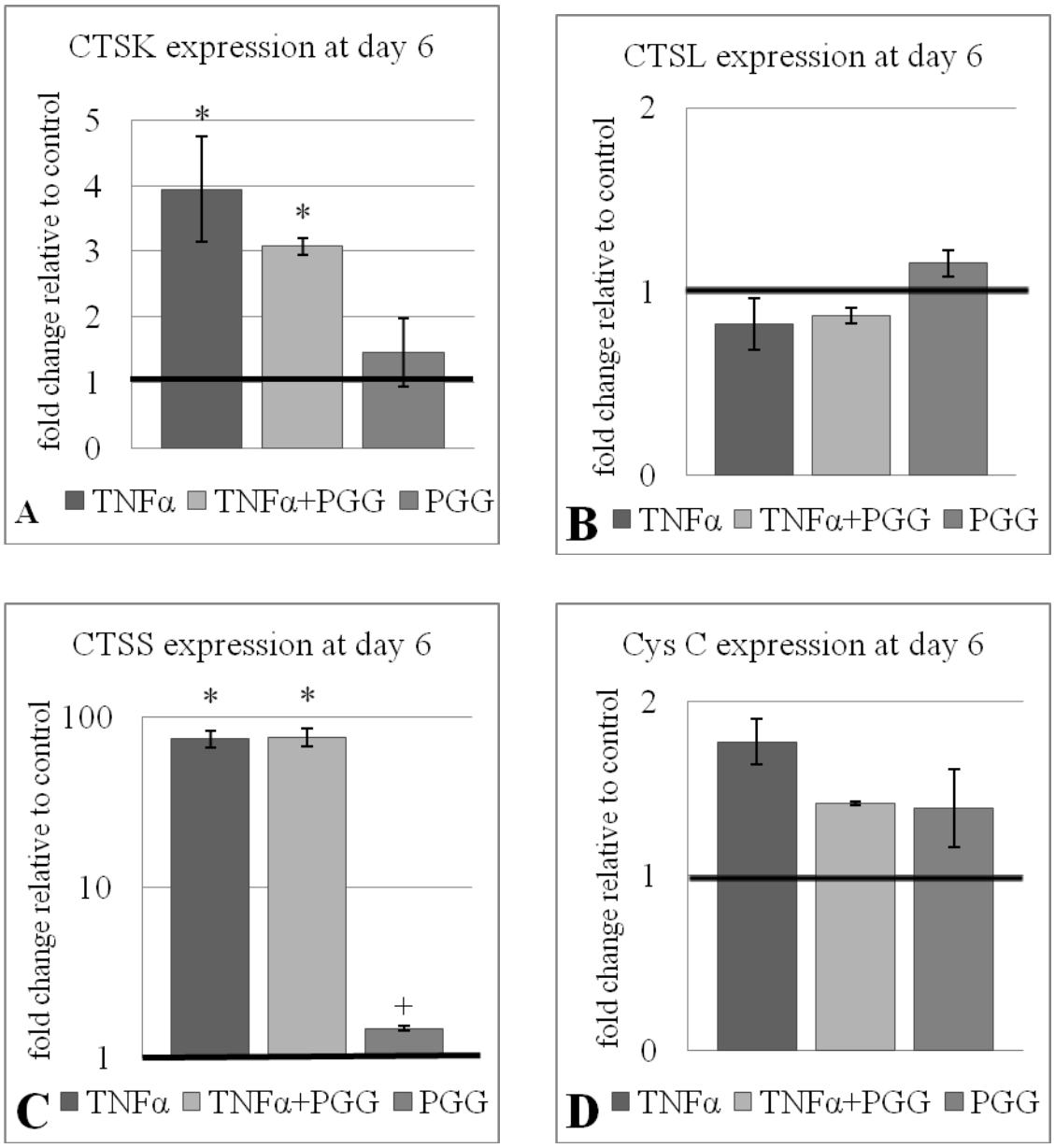

Figure 3.7: Real time PCR of proteolytic enzymes in day 6 RASMCs. * indicates significantly different from the control group and + indicates significantly different from the TNFα group ($p<0.05$).

3.3.d PGG significantly inhibits MMP-2 activity in conditioned media

Zymography was conducted on conditioned media samples in order to assess the activity of MMP-2 and MMP-9 enzymes that were released into the extracellular milieu. Gelatin zymography results showed that MMP-2 activity was significantly increased with TNFα treatment. Cells grown with TNFα showed increased activity of both pro-MMP-2 (72 kDa) and active MMP-2 (68 kDa). At days 1 and 3, PGG significantly reduced the activity of pro MMP-2 and at days 3 and 6, PGG inhibited active MMP-2 significantly. In contrast, the addition of PGG to cultures (without TNFα) decreased the activity of pro-MMP-2.

When PGG was added 3 days post addition of TNFα, MMP-2 activity was not significantly inhibited by PGG. PGG may not thus be effective at reversing the increase in activity of MMP-2 due to treatment with TNFα.

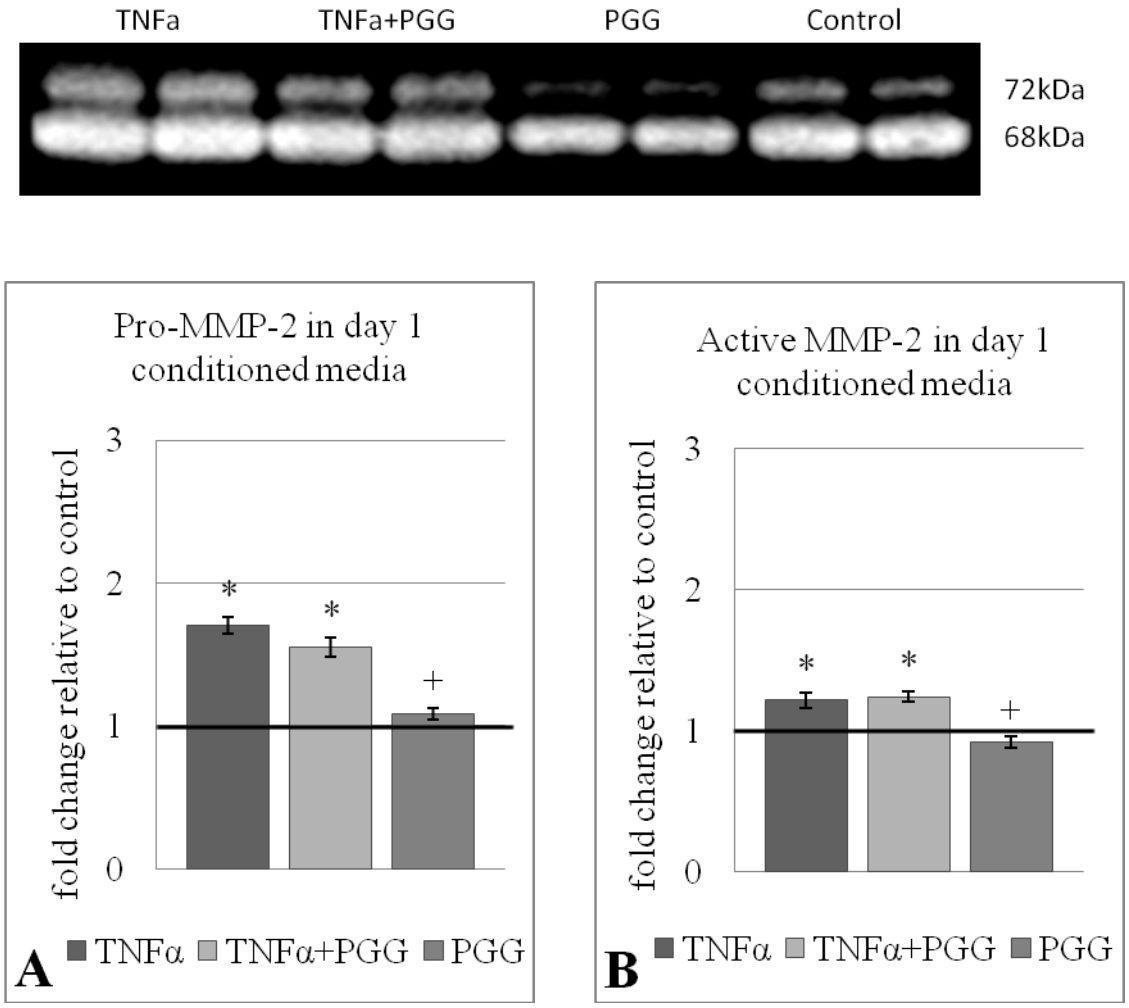

Figure 3.8: MMP-2 zymogram and densitometric analysis of day 1 conditioned media. * indicates significantly different from the control group and + indicates significantly different from the TNFα group ($p<0.05$).

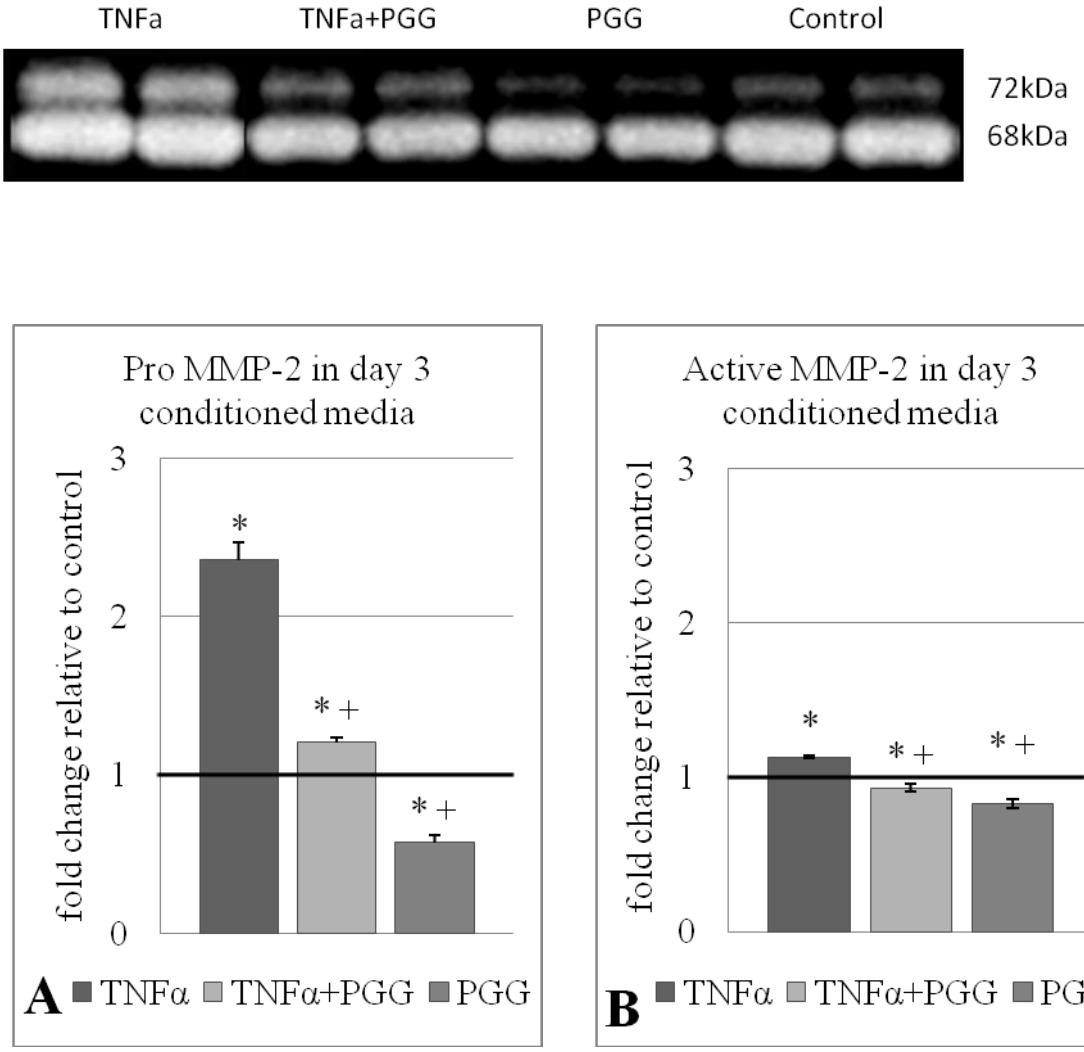

Figure 3.9: MMP-2 zymogram and densitometric analysis of day 3 conditioned media. * indicates significantly different from the control group and + indicates significantly different from the TNFα group ($p<0.05$).

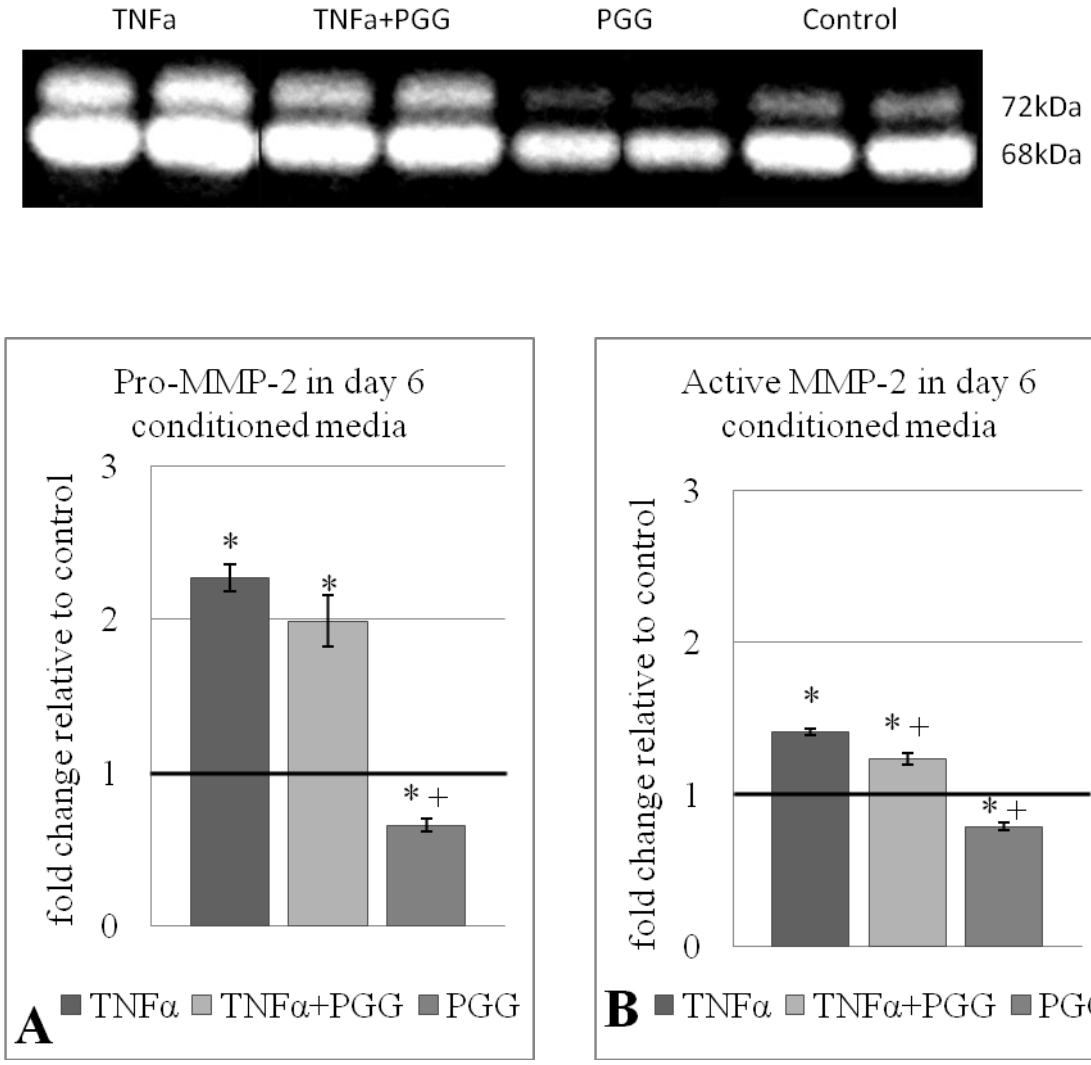

Figure 3.10: MMP-2 zymogram and densitometric analysis of day 6 conditioned media. * indicates significantly different from the control group and + indicates significantly different from the TNFα group ($p<0.05$).

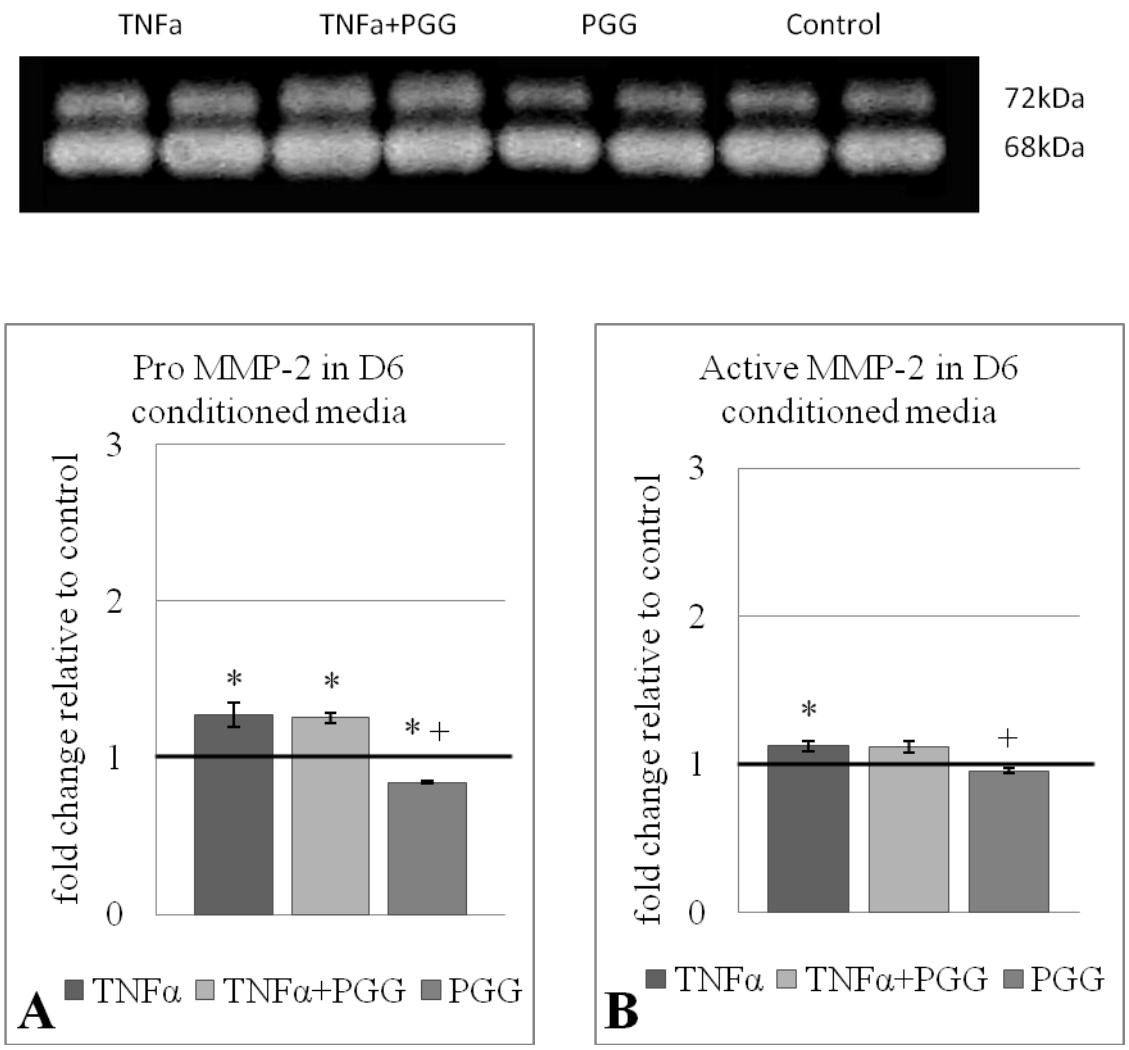

Figure 3.11: MMP-2 zymogram and densitometric analysis of D6 conditioned media. * indicates significantly different from the control and + indicates significantly different from the TNFα group ($p<0.05$).

3.3.e TNFα and PGG regulate MMP-9 activity

Gelatin zymography was conducted to estimate MMP-9 activity in conditioned media of RAMSCs. Pro-MMP-9 activity in the TNFα group was decreased or not significantly different from the control group at all time points (Figures 3.12, 3.13, 3.14, and 3.15). Active MMP-9 was regulated differently than pro-MMP-9. All experimental groups showed active MMP-9 levels not very different from control group (less than 5% difference) at day 1 and day 3. At day 6, active MMP-9 levels were significantly higher in all experimental groups compared to the control group. At day 6, group with PGG and TNFα showed significantly higher pro-MMP-9 activity than both control group and TNFα groups. MMP-9 activity was regulated differently than MMP-2 in our experiments. The increase in MMP-9 activities in groups treated with PGG could be a compensatory mechanism for the decrease in MMP-2 activities. However, the differential regulation of MMP-9 could have other implications both *in vitro* and *in vivo*.

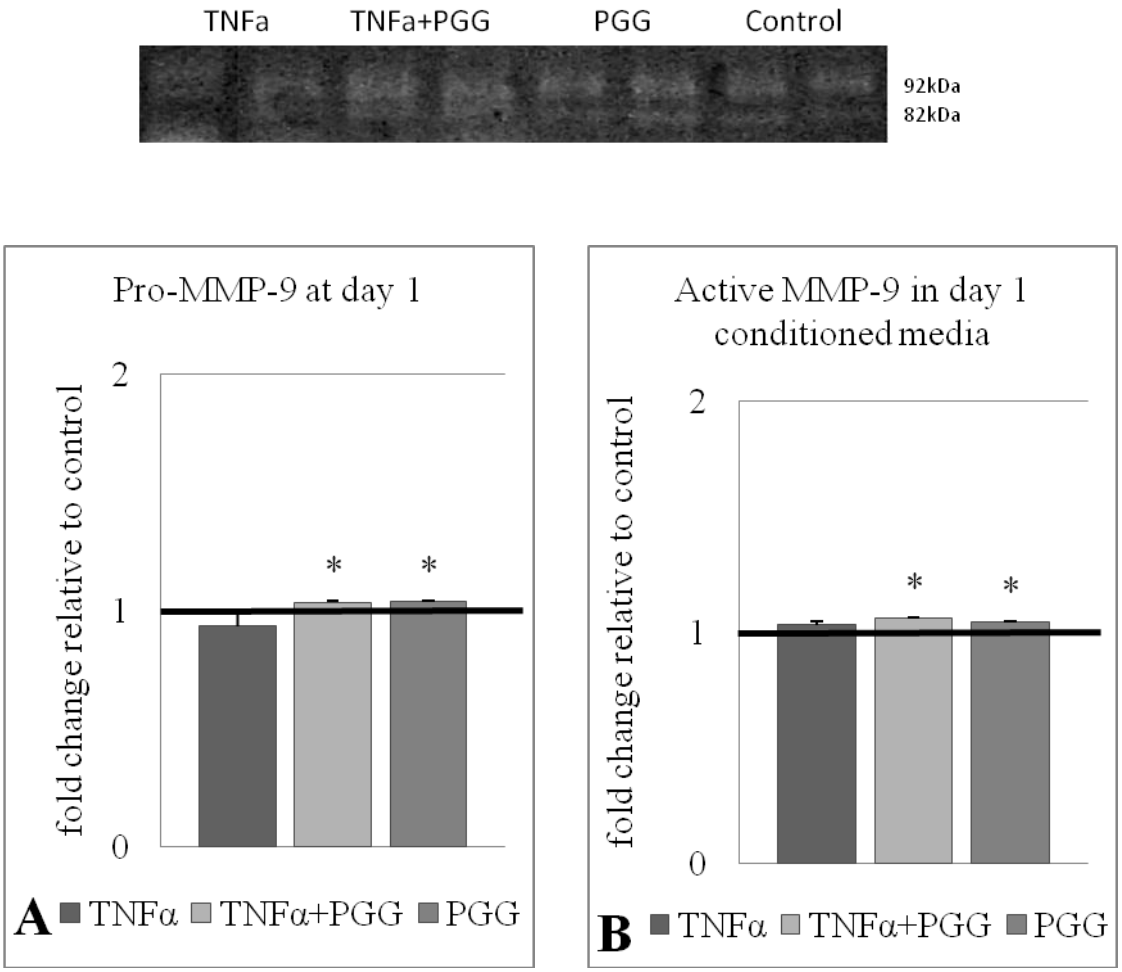

Figure 3.12 MMP-9 zymogram and densitometric analysis of day 1 conditioned media. * indicates significantly different from the control group ($p<0.05$).

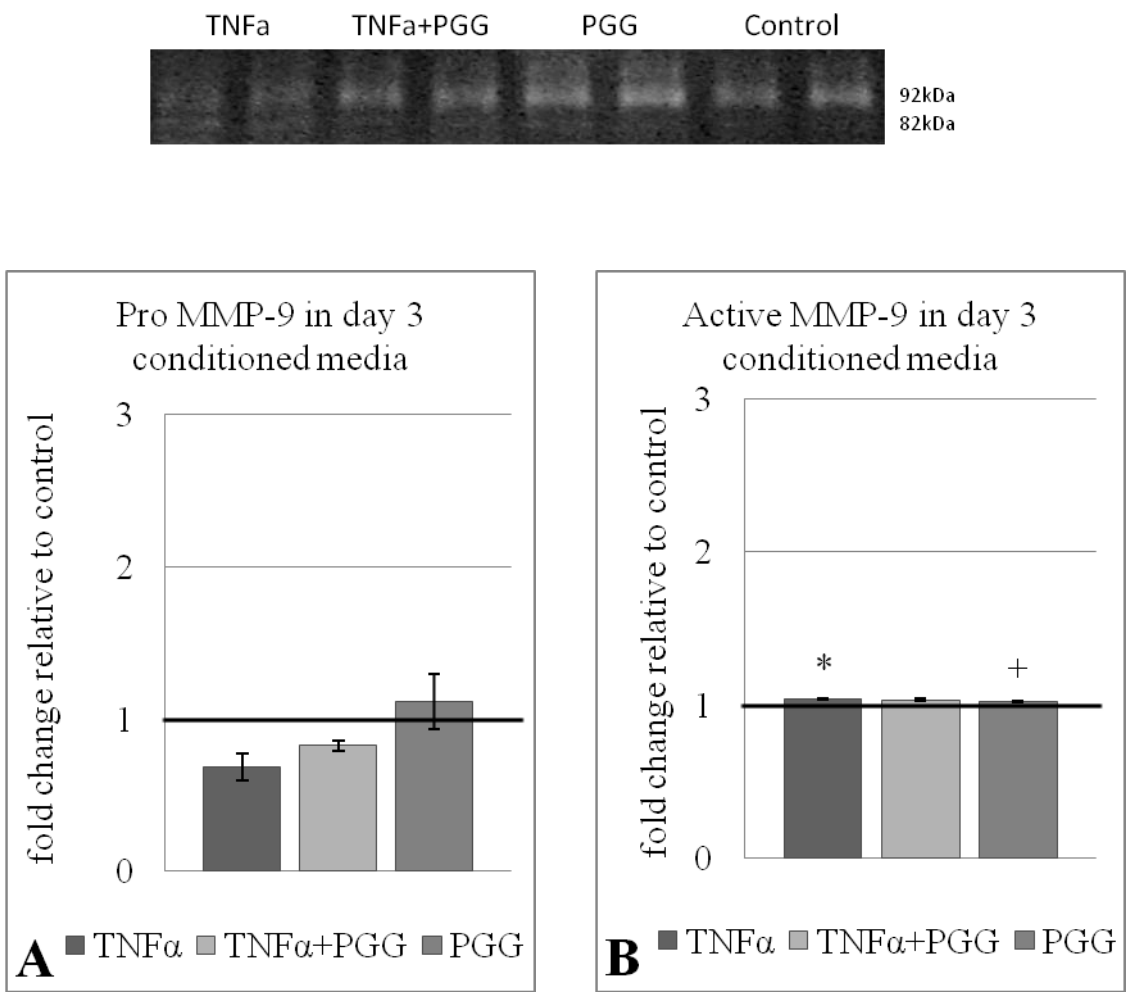

Figure 3.13 MMP-9 zymogram and densitometric analysis of day 3 conditioned media. * indicates significantly different from the control group and + indicates significantly different from the TNFα group ($p<0.05$).

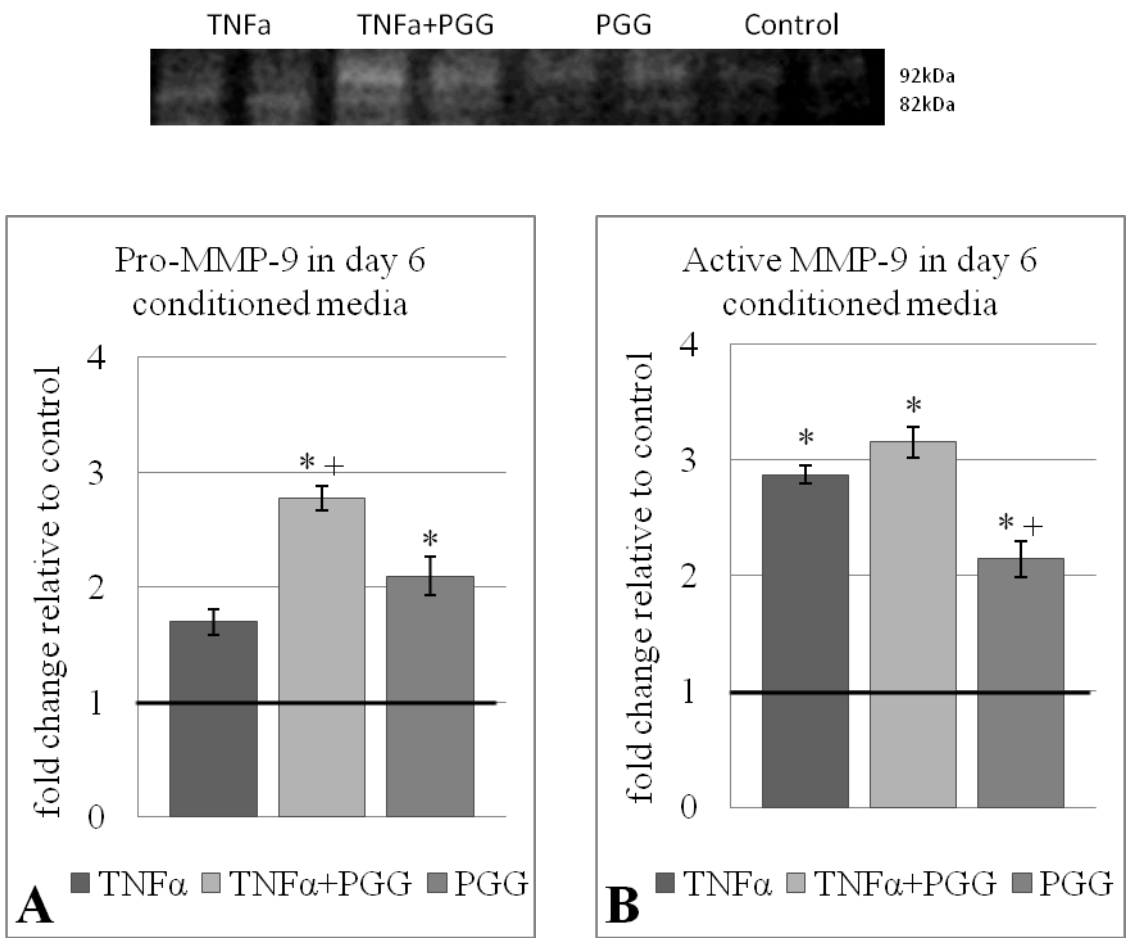

Figure 3.14 MMP-9 zymogram and densitometric analysis of day 6 conditioned media. * indicates significantly different from the control group and + indicates significantly different from the TNFα group ($p<0.05$).

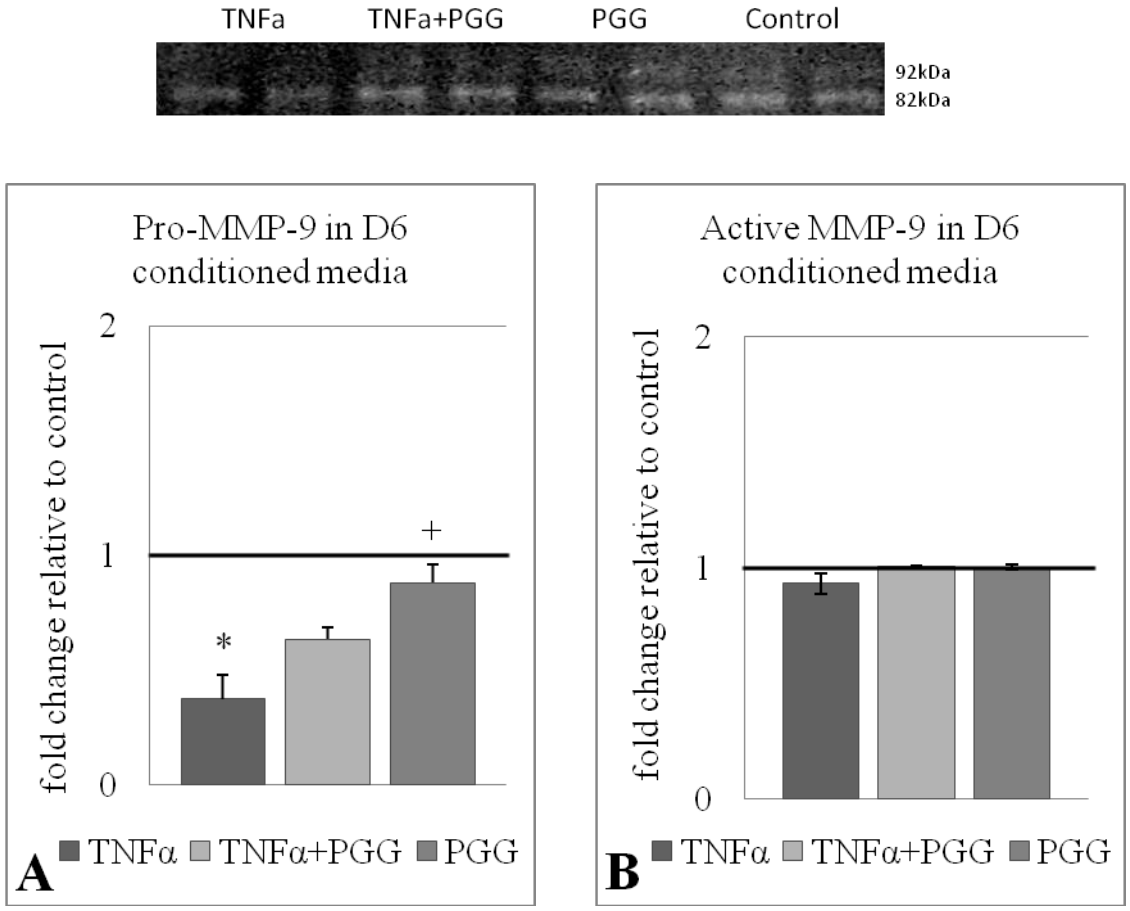

Figure 3.15: MMP-9 zymogram and densitometric analysis of D6 conditioned media. * indicates significantly different from the control group and + indicates significantly different from the TNFα group ($p<0.05$).

3.3.f PGG causes a decrease in extracellular levels of cathepsins K, L and S

Western blot analysis of potent proteolytic cathepsins K, L and S was conducted to determine amounts of cathepsins K, L and S. Cathepsin K levels in conditioned media at different time points are shown in Figure 3.16. TNFα increased the level of extracellular cathepsin K at all time points. At day 2 and day 6, PGG reduced the levels of cathepsin K when added together with TNFα. At day 3, cathepsin K inhibition due to PGG was not noticeable. PGG treatment alone showed reduced the amount of cathepsin K at day 1 and day 6 compared to the control group. PGG, when added 3 days past TNFα treatment did not show any noticeable difference in cathepsin K level.

Cathepsin L levels in the conditioned media detected by Western blotting is shown in Figure 3.17. Western blot of conditioned media in the PGG (without TNFα) group showed no detectable cathepsin L levels at all time points, including the D6 group. Control group conditioned media also showed barely detectable levels of cathepsin L at day 3 and no detectable cathepsin L at day 2, day 6 and D6. The addition of TNFα increased amount of cathepsin L while the combination of TNFα and PGG treatments showed decreased levels of cathepsin L. PGG was able to reverse the increase in cathepsin L induced by TNFα in the D6 experimental group.

Cathepsin S was detected using Western blotting at specified time points as shown in Figure 3.18. PGG dramatically inhibited the amount of cathepsin S at all time points, even when added after 3 days post treatment with TNFα. PGG treatment alone showed very low levels of cathepsin S at all time points.

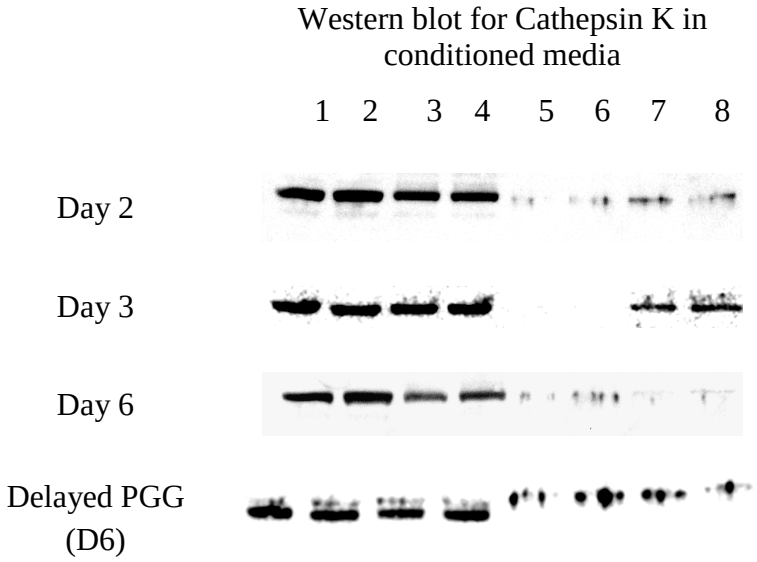

Figure 3.16: Western blotting for cathepsin K in conditioned media. Lanes 1-2: 50 ng/ml TNFα, 3-4: 50 ng/ml TNFα + 10 µmol/L PGG, 5-6:10 µmol/L PGG, 7-8: Control (no treatment).

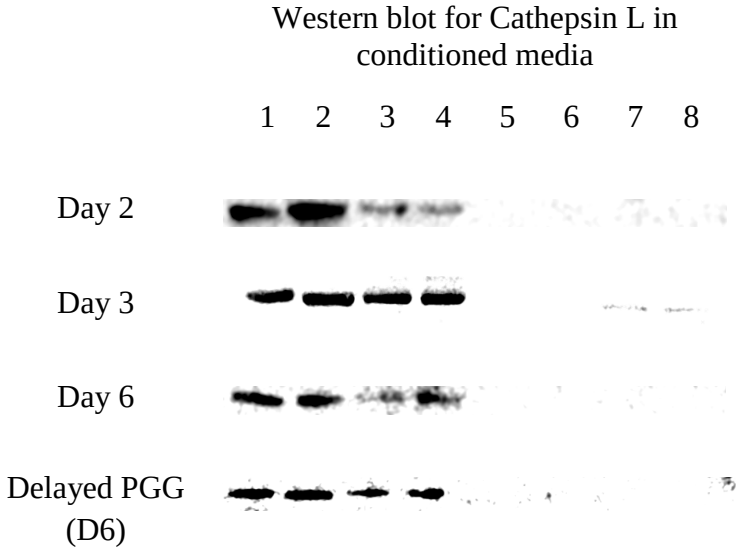

Figure 3.17: Western blotting for cathepsin L in conditioned media. Lanes 1-2: 50 ng/ml TNFα, 3-4: 50 ng/ml TNFα + 10 µmol/L PGG, 5-6: 10 µmol/L PGG, 7-8: Control (no treatment).

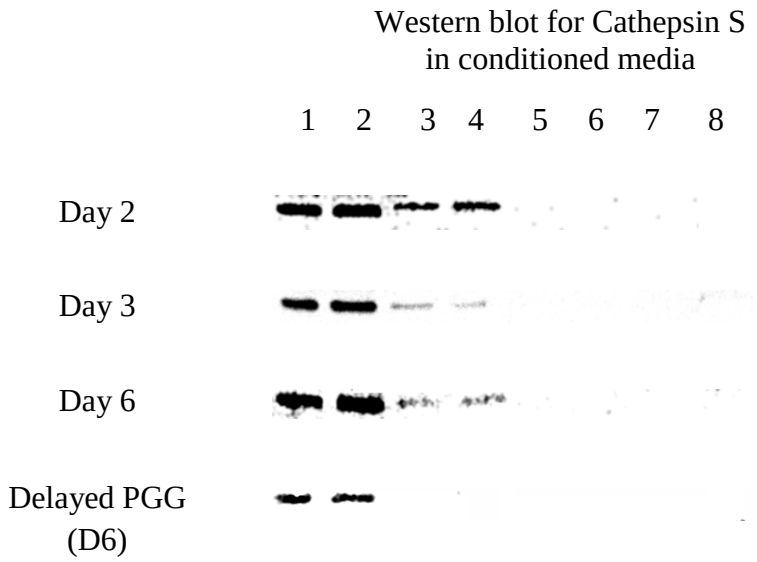

Figure 3.18: Western blotting for cathepsin S in conditioned media. Lanes 1-2: 50 ng/ml TNFα, 3-4: 50 ng/ml TNFα + 10 µmol/L PGG, 5-6: 10 µmol/L PGG, 7-8: Control (no treatment).

3.3.g Rat aortic smooth muscle cell proliferation is inhibited by PGG

MTT assay was conducted to estimate the effect of PGG treatments on cell proliferation at different time points. Average absorbances of the experimental groups were plotted as percentages of control were (Figure 3.19). TNFα caused significant increase in proliferation of RASMCs at day 6. PGG reduced this increase in proliferation significantly at day 6. PGG treatment also decreased proliferation significantly at day 6. As demonstrated by the live/dead assay in Figure 3.5, PGG does not exert cytotoxic effects. Thus, PGG inhibits proliferation by preventing cell division and not by causing cell death.

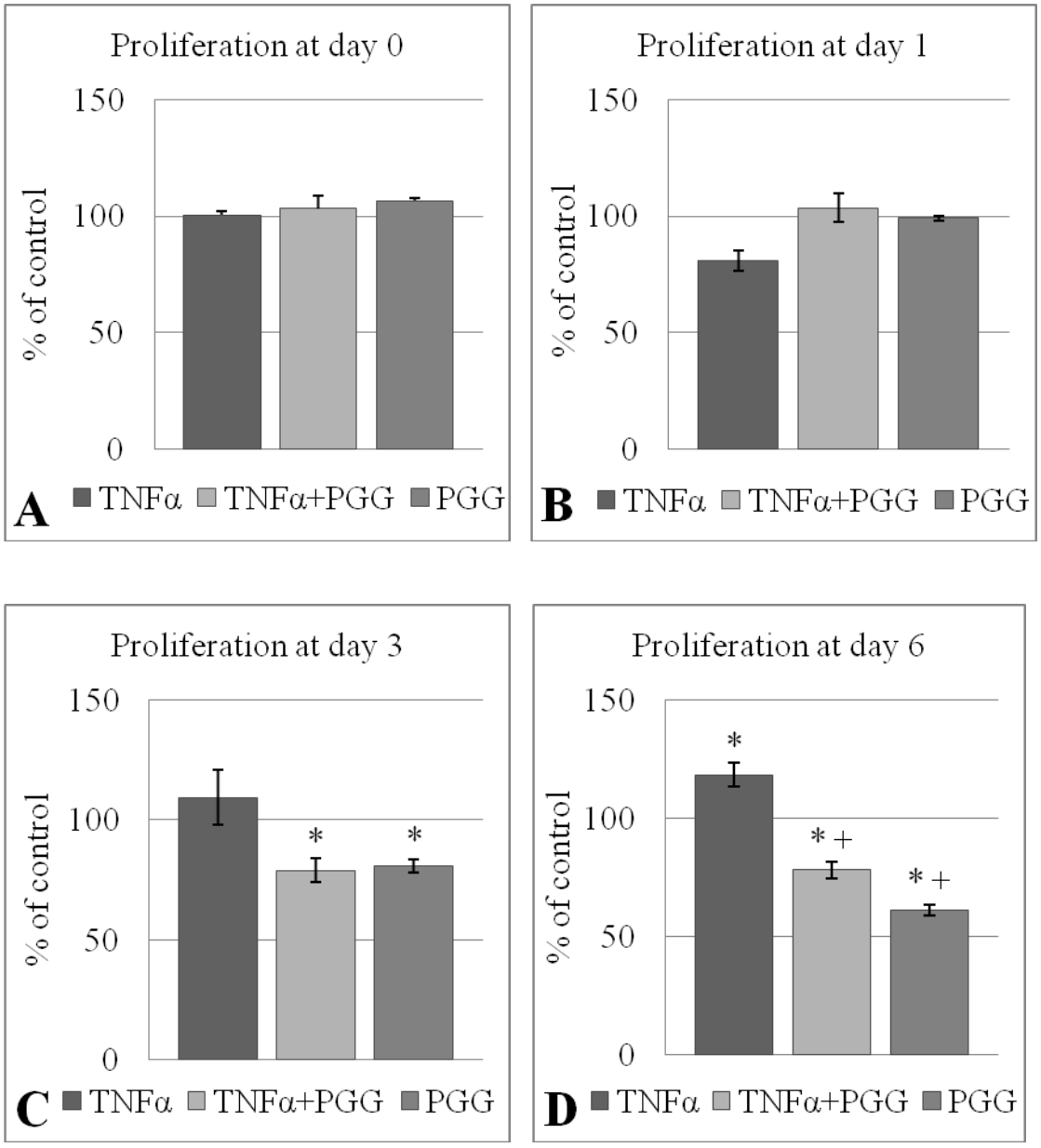

Figure 3.19: Proliferation of RASMCs as measured by the MTT assay. * indicates significantly higher than the control group and + significantly lower than the TNFα group ($p<0.05$).

3.3.h PGG reduces cell migration induced by injury

The *in vitro* scratch assay was conducted to assess cell migration. This assay is helpful in determining the speed with which the cells will migrate to fill an artificially induced 'wound'. Images from the scratch assay are shown in Figure 3.20. Cells treated with TNFα proliferate and migrate towards the gap more rapidly than the control group. PGG when added simultaneously with TNFα decreased the migration and appeared to have a more flattened morphology. PGG treatment alone shows very limited migration and proliferation compared to control. Outline of the scratch is still detectable in the PGG group after 48 hours of the scratch.

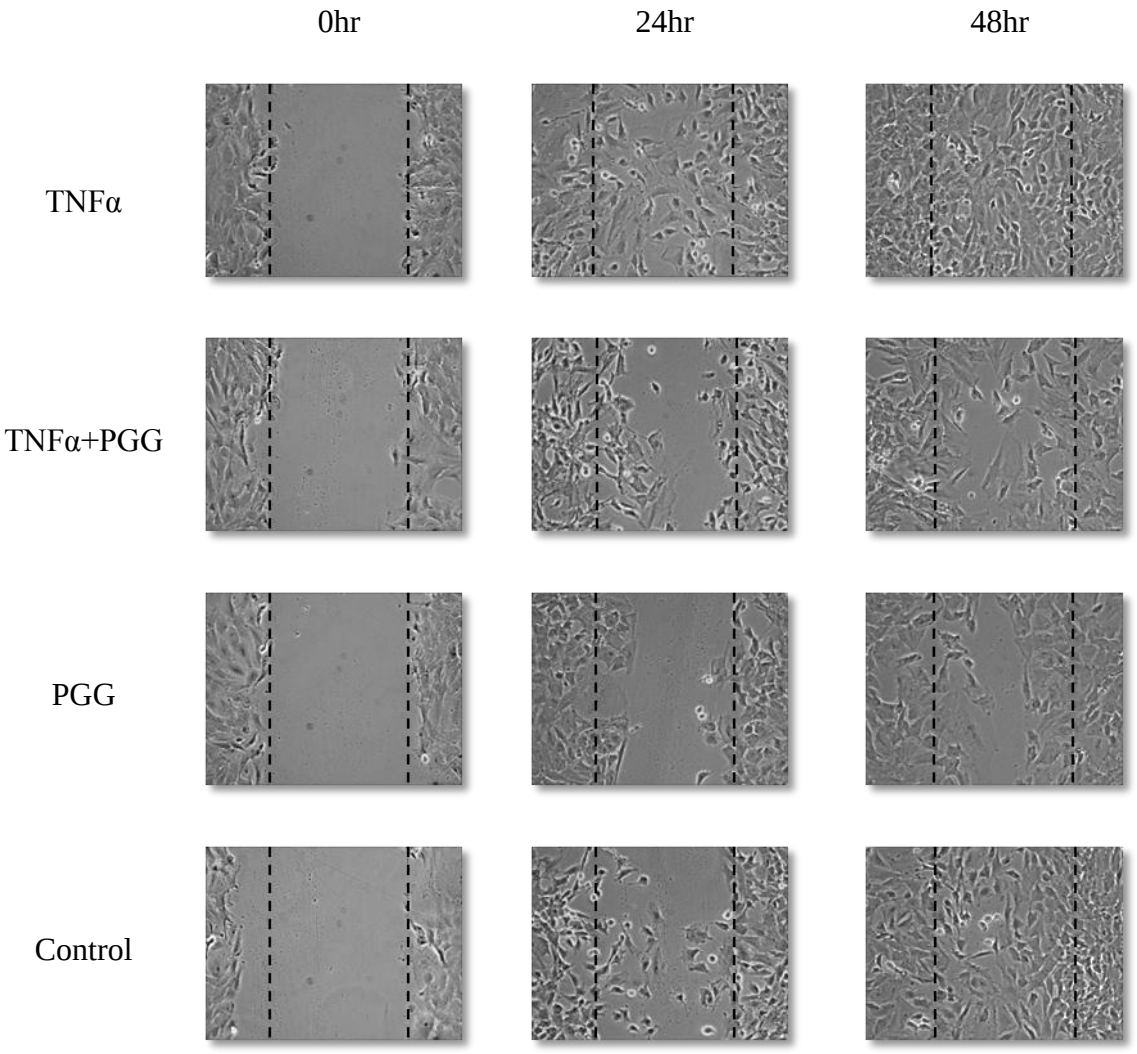

Figure 3.20: RASMC migration assessed using the scratch test. Dotted lines indicate the approximate boundaries of scratch.

3.4. DISCUSSION

In this study, we supplemented media of RASMCs with TNFα to simulate a condition that mimics inflammatory conditions associated with atherosclerosis, aneurysms and restenosis *in vivo*. Although this is not a complete representation of *in vivo* conditions, TNFα has been shown to induce increased expression and activities of several proteolytic enzymes *in vitro*. We studied the activities of MMP-2 and MMP-9 using gelatin zymography. We also assessed the amounts of cathepsins K, L and S in the conditioned media. Cell migration and proliferation were also assessed using scratch test and MTT assay respectively.

Cathepsins and matrix metalloproteases are important mediators in various pathological conditions.[114] Atherosclerosis and restenosis often involve excess proliferation of vascular smooth muscle cells (VSMCs) in response to injury.[115,116] Atherosclerosis, initiated by deposition of fatty acids, involves release of inflammatory factors such as tumor necrosis factor and interleukins.[117-120] These cytokines are linked to increased proliferation of various types of cells including VSMCs. VSMCs respond to injury by increased proliferation and deposition of extracellular matrix, mainly collagen in the surrounding area. In cases of minor injury, the process continues towards healing the injury and repairing any damage. However, atherosclerosis and restenosis are chronic conditions leading to a vicious cycle that sustain inflammatory conditions. VSMCs in chronic inflammatory conditions release extracellular matrix proteases that degrade collagen and elastin.[121-123] The release of extracellular matrix fragments interact with

cellular receptors and induce further release of inflammatory cytokines from newly formed VSMCs as well as macrophages in the area.[124,124-127] This vicious cycle persists until the lumen is occluded and surgical or pharmaceutical measures are taken. A similar process takes place in case of aneurysms. Initial injury is brought on by atherosclerosis, genetic predisposition or lifestyle factors such as smoking. VSMCs and macrophages secrete elastases and collagenases causing the local arterial wall to weaken. The VSMCs then produce excess collagen to compensate for reduced mechanical strength associated with degraded elastin. Freshly synthesized collagen is more easily degraded by the released proteases resulting in a vicious cycle of collagen deposition and degradation. Pro-inflammatory cytokines such as TNFα have been strongly associated with aneurysms.[128-131] Using zymography, a technique that can demonstrate proteolytic activity, we confirmed that TNFα induces increased activities of extracellular MMP-2 and intracellular cathepsin L. Western blot analysis shows that cathepsin S, K and L release into the extracellular milieu is also augmented by TNFα. This simulates pathological conditions associated with atherosclerosis, restenosis and aortic aneurysms that lead to degradation of elastic fibers and collagen within the arterial wall. Inhibition of MMPs and cathepsins has shown to be beneficial in multiple diseases including vascular pathologies. Other dietary polyphenols have shown that some dietary polyphenols can have inhibitory activity against some proteolytic enzymes.[106, 132] In our studies, we have looked at the effect of PGG on cathepsins, which has not been established previously. We showed that PGG can be used as an inhibitor of MMP-2, cathepsins K, L & S and it can potentially protect elastin in the arterial walls from

degradation. Cathepsins K, L and S have been shown to play an important role in vascular pathology including atherosclerosis, plaque stability, and arterial calcification.[133-136] TNFα is known to induce the expression of proteolytic enzymes by various types of cells.[137-140,116,137] PGG inhibits the amount of cathepsins K, L & S released by VSMCs into the extracellular space as shown by Western blot analysis. Increased gene expression of cathepsins K & S induced by TNFα was also markedly decreased by PGG as shown by PCR analysis of 3 day samples. Initially, we had hypothesized that PGG cross-links elastin and thus increases its resistance to proteolytic enzymes. While this has been shown both *in vitro* and *in vivo*, PGG was used in high concentrations to effectively cross-link elastin (0.06%) and collagen (0.3%).[109,110,141] In our studies, we have used relatively very low concentrations (10 μmol/L) of PGG. We believe that at these low concentrations, PGG has intracellular effects that were not studied or observed in previous studies. PGG inhibited the activity of pro-MMP-2 in the earlier time points and reduced the activity of active MMP-2 in the later time points. MMP-9 activity of the RASMCs was upregulated by PGG. Studies on various human cells have shown that TNFα increases MMP-9 activity.[142-144] However, the zymography results from our experiments suggest that rat derived cells may respond differently than human cells in their MMP-9 activity in response to TNFα. It is not clear if PGG directly affects the activity of MMP-9 or the increase in MMP-9 activity is due to RASMCs compensating for reduced MMP-2 activity.

Atherosclerosis and restenosis also involve the migration of VSMCs into the lumen, where the endothelial layer has been compromised due to fatty acid deposition or

surgical intervention (balloon angioplasty).[105,145] Increased proteolytic activity can reduce extracellular matrix composition thus making it easy for VSMCs to migrate towards the lumen. Some polyphenols have been shown to inhibit the proliferation of cancer cells and VSMCs through interference in cell cycle signaling.[146-149] Our studies have shown that PGG significantly inhibits proliferation of rat aortic smooth muscle cells without being cytotoxic. We hypothesize that PGG affects the cell cycle signaling and maintains the cells in a 'differentiated' state by preventing DNA synthesis and mitosis. More research needs to be done to confirm this hypothesis.

As discussed above, migration and proliferation occur frequently in vascular diseases. The scratch test results showed that PGG inhibits the migration of smooth muscle cells in the *in vitro* model of vascular injury. Migration is closely linked to the release of proteolytic enzymes since cells need to degrade extracellular matrix in order to migrate and inhibition of proteolytic enzymes could be a potential approach to controlling migration of cells. In our study, PGG inhibited proteolytic enzymes and migration effectively. We conclude that PGG not only stabilize extracellular matrix but can have intracellular effects through control of gene and protein expressions of proteolytic enzymes. More studies are needed to understand the potential therapeutic effects and any unexpected side effects of PGG.

CHAPTER 4

CHARACTERIZATION OF INCREASED TROPOELASTIN PRODUCTION AND INCREASED DEPOSITION OF INSOLUBLE ELASTIN BY PRIMARY RAT AORTIC SMOOTH MUSCLE CELLS TREATED WITH PENTAGALLOYLGLUCOSE

4.1. INTRODUCTION

Elastic fibers are an important part of the extracellular matrix in various tissues. They provide important mechanical properties like elasticity and resilience. Tropoelastin is the soluble elastin that is released by cells. It is assembled within microfibrillar glycoproteins present the matrix and then crosslinked by lysyl oxidase to form insoluble elastic fibers. Mature elastic fibers consist of elastin cores and microfibrils at the periphery.[80] Elastin is a major constituent of several tissues including aorta (57%), elastic ligaments (50%), lung (7%) and skin (5%).[81] Importance of elastin has been elucidated by knockout mice. Heterozygous mice (ELN+/-) had decreased arterial compliance with hypertension but had a normal life expectancy. The physical properties of the blood vessels can be explained by arterial remodeling due to reduced amount of elastin. These mice also displayed altered aging processes in the aorta which suggests the importance of elastin arrangement during early stages in the formation of the vessel.[82] Complete lack of the elastin gene ELN-/- results in early mortality of mice due to extensive, uncontrolled proliferation of smooth muscle cells and consequent vessel obstruction.[83] The amino acid sequence of tropoelastin has hydrophilic and hydrophobic domains alternating with each

other. The hydrophobic domains are rich in glycine, valine and proline, occurring in repeating motifs. Hydrophilic regions are rich in lysine and alanine which are involved in crosslinking of elastin.

Human tropoelastin is encoded by a single gene with multiple isoforms. Eleven forms of human tropoelastin splice forms have been characterized. The tropoelastin mRNA encodes a 72kDa protein and with the removal of signal peptide, resulting in a mature protein of 60kDa.[84] The C-terminus is one of the most important and well-conserved regions in tropoelastin. It contains the only two cysteine residues which form the disulfide bond. The protein terminates with a positively charged sequence RKRK. Any major disruption in the C-terminus like the disruption of the disulphide bond can drastically reduce the ability of tropoelastin to assemble and form elastic fibers.[85] The tertiary structure of the cross linked elastin has not been fully determined but significant research has characterized the secondary structure.[86] Tropoelastin secondary structure also includes poly-proline II, compact beta turns and disordered structure, which contribute to its highly flexible nature.[87] In vascular tissue, elastin synthesis occurs as shown in Figure 4.1. The cells secrete tropoelastin which is believed to be chaperoned by the 67kDa protein (elastin-laminin receptor or ELR) to the cell surface.[88] Tropoelastin, once released into the extracellular space, self assembles into globules of several microns. These globules remain attached to the cells surface in the early stages. The globules are cross-linked by copper dependent enzyme called lysyl oxidase and aligned along the microfibril scaffolds.[89] Once mature, cross-linked elastin is formed and deposited in the extracellular space, and tropoelastin production is reduced. Turnover of mature elastin is

very low, with most of elastin formation occurring in late fetal and early neonatal periods in mammals. By adulthood, elastin production is very low or non-existent.[90] Tropoelastin production can resume in case of injury and is affected by various factors like TNFα, IL-1, insulin-like growth factor-1 and especially transforming growth factor-beta (TGFβ).[91]

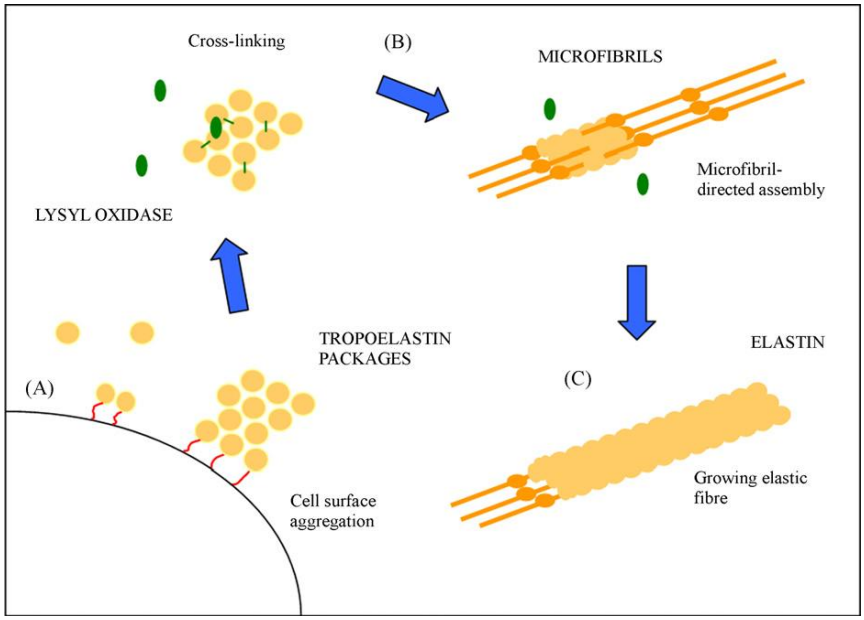

Figure 4.1: Elastin fiber synthesis from tropoelastin [89]

The human elastin gene has a functional promoter that exhibits upstream and downstream regulatory elements. Cyclic adenosine monophosphate (cAMP), glucocorticoid and insulin-like growth factor (IGF) responsive elements are present in this region indicating that tropoelastin production is influenced by growth factors.[91,92] Elastin mRNA production can be influenced by insulin-like growth factor and post-transcriptionally by TGFβ, which stabilizes the transcripts considerably.[93,94]

The complex process of elastogenesis begins with the formation of the tropoelastin molecule. A 67 kDa ELR (also referred to as the chaperone), a spliced

variant of the beta-galactosidase acts as a chaperone for tropoelastin as shown in Figure 4.2. The 67kDa ELR binds to the tropoelastin and this prevents premature aggregation of elastin in the intracellular space.[95] The complex is transported to the extracellular space where the chaperone molecule releases the tropoelastin molecule. The chaperone has a higher affinity for galactosugars than for tropoelastin resulting in release of tropoelastin. The 67 kDa ELR is recyclable and is internalized again after tropoelastin release.[96] The significance of the C-terminal domain of tropoelastin is evident as its interaction with the N-terminal of the microfibrillar associated glycoprotein is crucial for correct elastogenesis.[97] After the action of lysyl oxidase and coacervation of tropoelastin microspheres, alignment occurs on the microfibrils. Formation of cross links causes the elastin to become insoluble.[98] The 67kDa ELR that acts as the chaperone for tropoelastin is also referred to as the elastin binding protein (EBP). Multiple studies have shown the role of ELR in various cell responses. ELR is involved also in responding to products of elastin degradation.

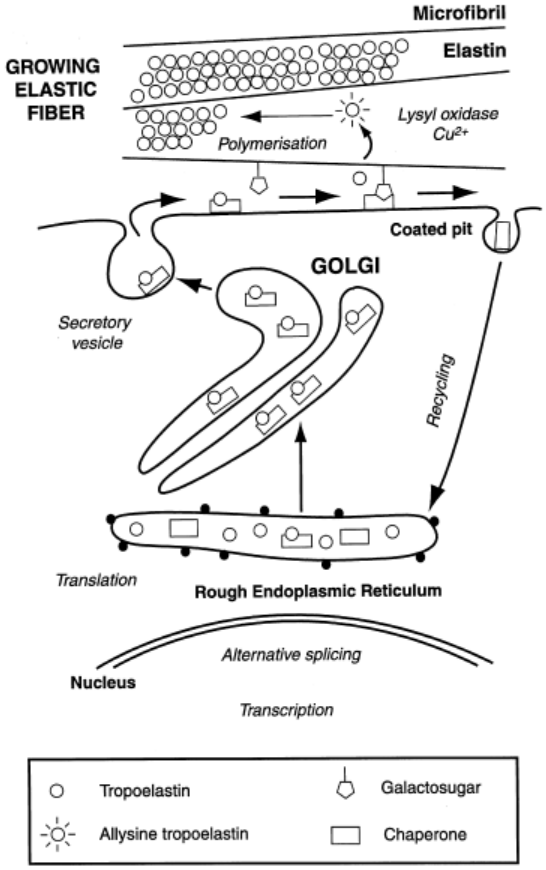

Figure 4.2: Elastin synthesis using the elastin binding protein (chaperone) [96]

Degradation of elastin is an important aspect of diseases such as aneurysms, atherosclerosis and vascular calcification. In earlier studies, pentagalloylglucose (PGG) has been used to preserve the morphology of elastin and prevent its degradation *in vivo*. We wanted to investigate the effects on the production of elastin in rat aortic smooth muscle cells. Our aim was to determine to what extent PGG behaved as a fixative *in vitro* for elastin, by preventing elastin degradation due to proteolytic enzymes. This study also observed that PGG had other effects on smooth muscle cells.

4.2. MATERIALS AND METHODS

4.2.a Cell culture

Primary rat aortic smooth muscle cells (RASMCs) were seeded on 12-well plates and grown in DMEM containing 20% fetal bovine serum and 1% penicillin-streptomycin. Media was supplemented with different concentrations of PGG, a kind gift from Omnichem (Belgium).

4.2.b Fastin colorimetric assay for elastin

Cell lysates were collected at set time points and tropoelastin was quantified using a colorimetric method (Fastin kit, Biocolor). Insoluble elastin was extracted with hot oxalic acid while soluble elastin (tropoelastin) was obtained from supernatant obtained by centrifugation of cell lysates.

4.2.c Western blot for tropoelastin

Cell lysates were collected with mammalian extraction buffer (Solulyze-M, Gelantis) and total protein quantified with bicinchoninic acid assay (Pierce). Equal amounts of protein were boiled in denaturing buffer and loaded in pre-cast gels (Biorad 161-1102). Gels were run at 85V for 120 minutes and transferred to PVDF membrane (Millipore) at 50V for 120 minutes. The blots were blocked in 5% non-fat dry milk (LabScientific) overnight at 4 C, and then incubated with the primary antibody (RDI# TP592 rabbit anti-elastin) against tropoelastin. This was followed by incubation with secondary antibody and detection (Roche BM Chemiluminescence kit anti-mouse/rabbit). Bands were imaged with Alpha Innotech chemiluminescence detector.

4.2.d Gelatin zymography for cathepsin L

Protein samples were normalized to total protein quantified using bicinchoninic acid assay (Pierce). Equal quantities of protein were loaded with non-denaturing buffer in wells of pre-cast gelatin zymogram gel (Biorad 161-1131) and run at 85V for 120 minutes. The gels were then washed in 2.5% Triton X-100 for 30 minutes and incubated overnight in activation buffer to detect cathepsin L (100mmol/L sodium acetate pH 4.8, 20mmol/L L-cysteine). The gels were then stained with commassie blue, destained and imaged. Image analysis was performed using ImageJ.

4.2.e Data analysis

Results are expressed as mean ± SEM for triplicates for all experimental groups. Statistical analysis of data was calculated using student's t-test and probability value (p) was calculated and $p<0.05$ was considered statistically significant.

4.3. RESULTS

We conducted experiments with RASMCs from different sources in order to determine if PGG affects elastin production due to source of RASMCs. Similar studies were conducted to compare elastin production by RASMCs derived from adult or neonatal rats, freshly isolated or previously frozen (in 10% dimethyl sulfoxide in liquid nitrogen).

In our pilot studies, we used 3 concentrations of PGG - 1µmol/L, 10µmol/L and 25µmol/L supplemented in media of freshly isolated primary adult RASMCs. Fastin assay was conducted on cell lysates to assess quantity of soluble tropoelastin and

insoluble elastin, and the values were plotted as percentages relative to the untreated control group (shown in Figure 4.3). At the end of 4 weeks, 25µmol/L PGG increased the amount of tropoelastin significantly compared to control as shown in Figure 4.4. Insoluble elastin was significantly higher in the cells treated with 10µmol/L PGG. Insoluble elastin in the cells treated with 25µmol/L PGG was too low to be detected using the Fastin kit and hence were not included in the figure. Furthermore, most cells died by the end of 4 weeks when treated with 25µmol/L PGG.

Next, we used a lower concentration of PGG so we can compare the effects of 3 PGG non-cytotoxic concentrations. We conducted a 4 week study with 100 nmol/L, 1 µmol/L, 10 µmol/L PGG, and without PGG (control). These concentrations were used on freshly isolated primary adult RASMCs, previously frozen adult primary RASMCs, and previously frozen neonatal primary RASMCs.

Freshly isolated primary adult RASMCs showed increased insoluble elastin deposition at the end of 4 weeks as shown in Figure 4.5. Previously frozen primary adult RASMCs and neonatal RASMCs did not show an increase in elastin production due to PGG treatment as shown in Figure 4.6 and Figure 4.7 respectively. Almost all the neonatal RASMCs died by the end of 4 weeks when treated with 10 µmol/L PGG and hence elastin was not detectable in that group. Neonatal RASMCs are potentially more sensitive than adult RASMCs to similar concentrations of PGG.

For further studies, only one concentration of PGG (10µmol/L) was used since this concentration provided increased production of insoluble elastin relative to control as shown in Figures 4.4, and 4.5. Freshly isolated primary adult RASMCs were treated with

either 10 µmol/L PGG or no treatment (control). Fastin colorimetric assay was used to quantify tropoelastin and insoluble elastin, both of which showed significant increase compared to control as shown in Figure 4.8. Western blotting confirmed the Fastin assay results as shown in Figure 4.9. Gelatin zymography to detect cathepsin L showed a dramatic decrease in the activity of the enzyme in the cells treated with PGG as seen in Figure 4.10.

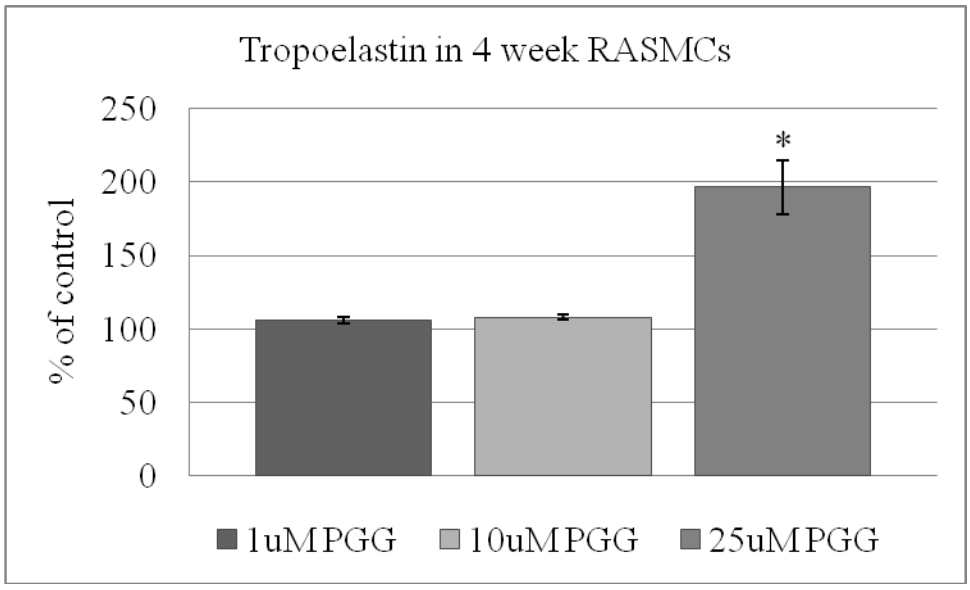

Figure 4.3: Tropoelastin in 4 week RASMC lysates. * indicates significantly higher than the control group

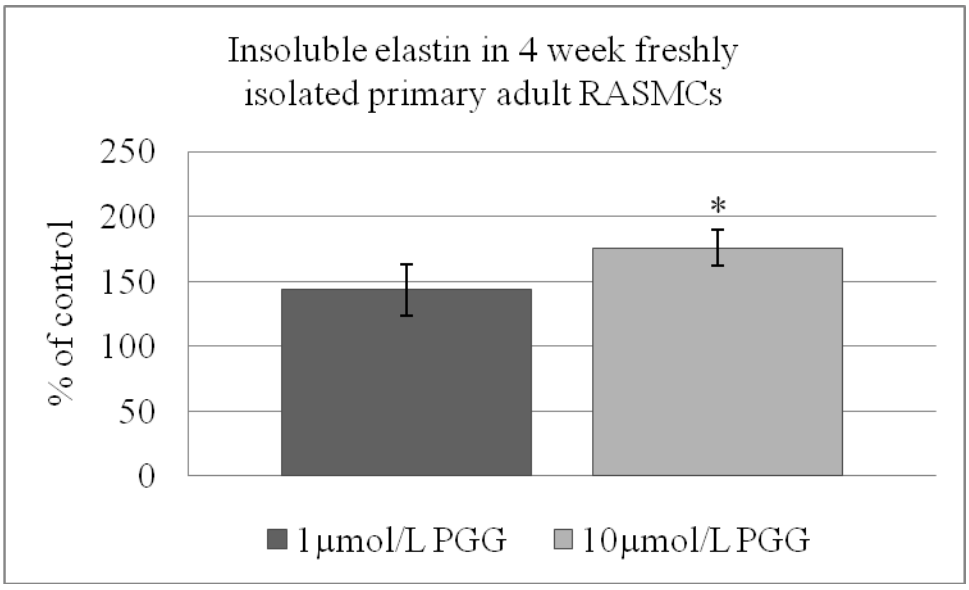

Figure 4.4: Insoluble elastin in 4 week RASMCs. * indicates significantly higher than the control group

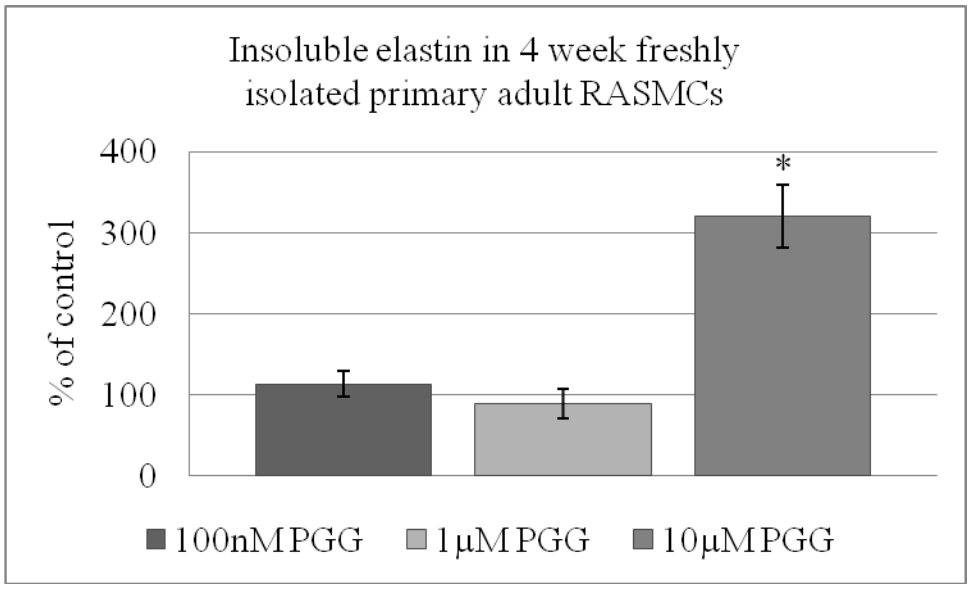

Figure 4.5: Insoluble elastin in 4 week freshly isolated primary adult RASMCs. * indicates significantly higher than the control group

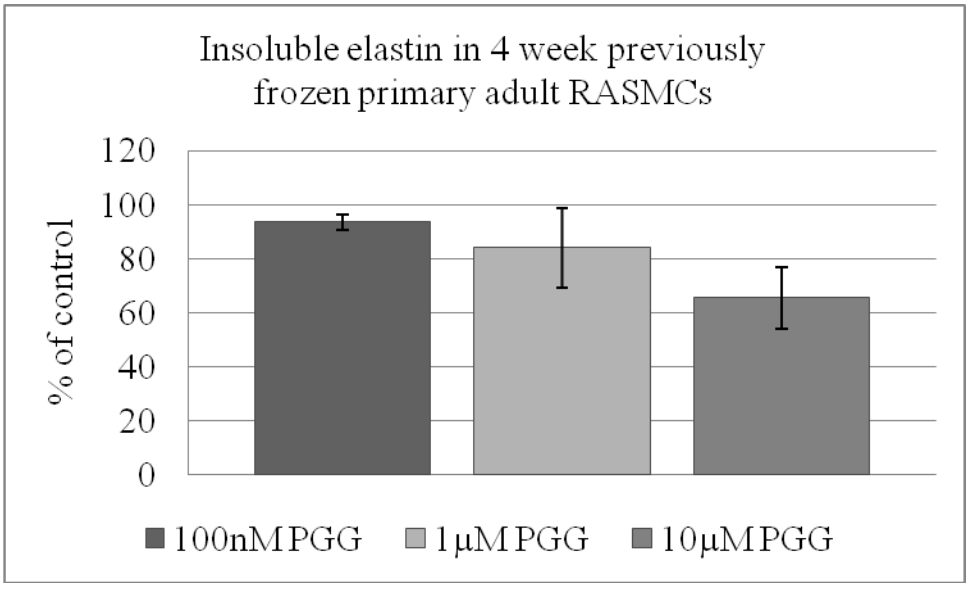

Figure 4.6: Insoluble elastin in 4 week primary adult RASMCs that were previously frozen

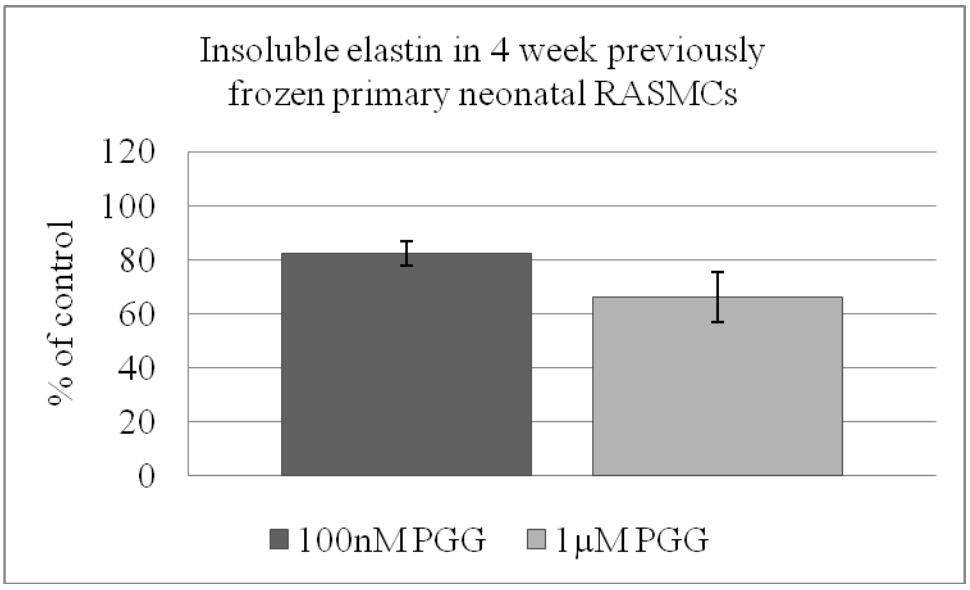

Figure 4.7: Insoluble elastin in 4 week neonatal primary RASMCs that were previously stored in liquid nitrogen.

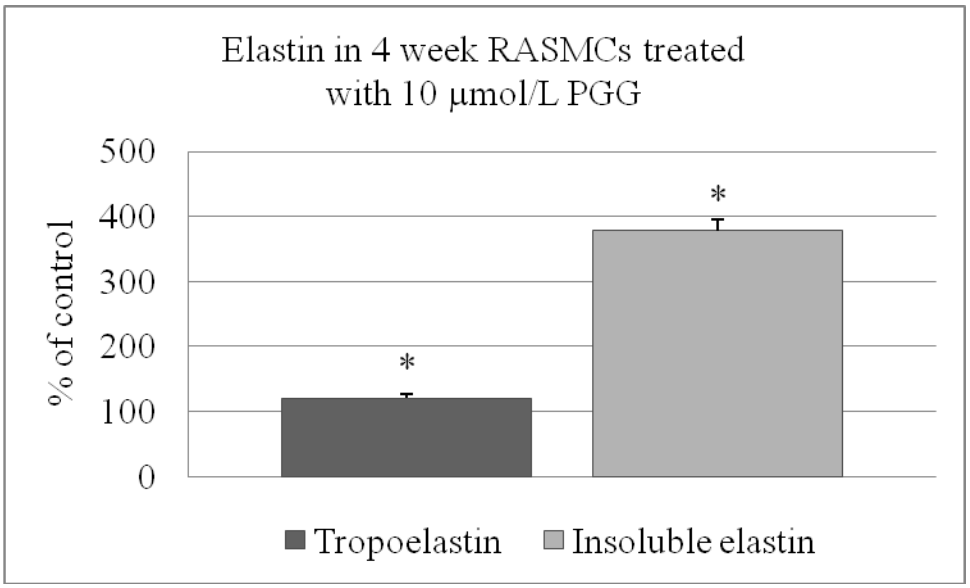

Figure 4.8: Elastin quantification in 4 week freshly isolated primary adult RASMCs. * indicates significantly higher than the control group ($p<0.05$)

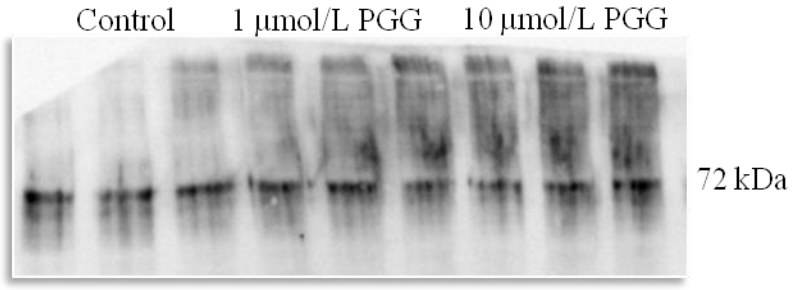

Figure 4.9: Western blotting for elastin from 4 week freshly isolated primary adult RASMC lysates

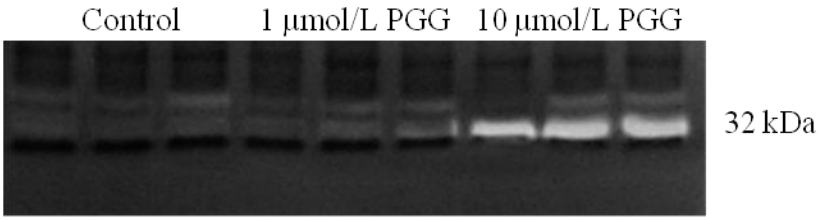

Figure 4.10: Gelatin zymography for cathepsin L in 4 week cell lysates

4.4. DISCUSSION

PGG increases the amount of tropoelastin and insoluble elastin produced by primary rat aortic smooth muscle cells that have not been previously frozen. We found that the optimal concentration of PGG for this purpose is 10µmol/L.

However, experiments with frozen RASMCs cultured with PGG showed no significant increase in elastin production due to PGG. These results suggests that freezing these cells caused some critical change in the of elastin production process and, this change altered the response of these cells to PGG.

PGG could potentially be used to increase the amount of cross-linked elastin in arterial tissue. Delivery of PGG to aneurysmal arteries can help to increase the production of elastin by the rat aortic smooth muscle cells. When used at higher concentrations, PGG was a fixative for native elastin in aorta and prevented elastases from degrading elastin.[109,110] However, the concentrations of PGG we have used in these *in vitro* studies are much lower and cause changes in proteolytic activity of the rat aortic smooth muscle cells. The delivery mode and optimal concentration of PGG to be delivered *in vivo* in to have increased elastogenesis have to be determined. Once these parameters have been

optimized, PGG could be a potential therapeutic agent that reverses the degradation of elastin and aids in deposition of newly formed insoluble elastin.

CHAPTER 5

CHARACTERIZATION OF PENTAGALLOYLGLUCOSE INDUCED ANTI-OSTEOGENIC DIFFERENTIATION OF TUMOR NECROSIS FACTOR-ALPHA ACTIVATED RASMCS

5.1. INTRODUCTION

Ectopic mineralization of arteries is associated with other diseases such as atherosclerosis, hypercholesterolemia, diabetes, and chronic kidney disease. Vascular calcification is an active, cell-mediated process that involves dedifferentiation of vascular smooth muscle cells into osteogenic cells and the deposition of calcium phosphate in arterial walls.[150,151] Healthy arterial smooth muscle cells are contractile, non-proliferative and exhibit markers such as smooth muscle actin and heavy chain myosin. Inflammatory conditions resulting from an initial injury, such as deposition of fatty acids or hypertension, causes the migration of monocytes from the bloodstream into the subendothelial layer. The monocytes differentiate into macrophages and release pro-inflammatory cytokines and proteolytic enzymes. The cytokines and proteases in the subendothelial and medial regions create a local inflammatory zone where the smooth muscle cells are induced to proliferate, migrate and dedifferentiate.[10,152,153] Migration of smooth muscle cells into the luminal area and their excess proliferation can cause stenosis (narrowing) of the arterial lumen. Balloon angioplasty can surgically increase the diameter of a stenotic artery but often this leads to a relapse with increased migration and proliferation of the smooth muscle cells called ‘restenosis’.[104,154,155] In case of vascular

calcification, markers of osteogenic differentiation such as increased alkaline phosphatase activity, increased core binding factor alpha-1 (CBFA-1), increased muscle segment homeobox -2 (MSX-2), and deposited of calcium phosphate can be observed in vascular smooth muscle cells.[156-158] Extensive meta-analyses have shown that osteoporosis and vascular calcification often occur simultaneously. Patients with osteoporosis also show increased incidences of vascular medial calcification. Osteoporosis is characterized by an imbalance between bone deposition (by osteoblasts) and bone resorption (by osteoclasts) leading to excess loss of mineralization. Vascular calcification, on the other hand is the ectopic mineralization of arterial tissue with increased osteoblastic activity.[159,160,161] Thus, any therapeutic agent for either diseases should not adversely affect the other.

Vascular smooth muscle cell (VMSC) calcification *in vitro* has been studied in the past by using various methods. Mimicking hyperphosphatemic and/or hypercalcemic conditions are common and convenient methods to simulate *in vitro*.[162] Adding beta glycerophosphate to the media is the most common method of inducing hyperphosphatemia cell culture.[163,164] Primary human vascular smooth muscle cells grown hypercalcemic and hyperphosphatemic media showed higher calcification.[165] However, this occurred only in the presence of cells and hence must involve cellular processes. In addition, osteogenic markers CBFA-1, alkaline phosphatase mRNA levels were also increased.[34]

Other methods of inducing osteogenic differentiation of vascular smooth muscle cells *in vitro* include addition of elastin peptides and addition of oxidative stress factors

such as hydrogen peroxide and oxidized-low density lipoproteins.[124,166]Addition of osteogenic proteins such as BMP-2 also induce osteoblast-like features in aortic smooth muscle cells.[167] In order to create an *in vitro* model that mimicked an inflammatory condition, we used TNFα. Earlier studies have shown that supplementing TNFα in the media of vascular smooth muscle cells causes an increase in osteogenic makers.[74,168] Combined with increased phosphate, TNFα increases mineralization in aortic smooth muscle cells. We used this *in vitro* system to test whether PGG treatment would prevent osteogenic differentiation of RASMCs.

Gene expression of several osteogenic markers, activity of alkaline phosphatase and proliferation of rat aortic smooth muscle cells were studied. In addition, we studied proliferation, alkaline phosphatase activity and calcification of osteoblasts treated with PGG. This was conducted in order to test the effects of PGG on osteoblasts and study any undesired effects on physiological bone formation. Ideally, any systemic delivery of a therapeutic agent to prevent arterial calcification should not affect bone physiology or cause extreme bone loss. Through a parallel study of aortic smooth muscle cells and osteoblasts, we studied the effect of PGG as a therapeutic agent for vascular calcification and osteoporosis. If PGG is delivered systemically, this study can give some insight into any potential side effects on osteoblast functioning.

5.2. MATERIALS AND METHODS

5.2.a Preliminary experiments

We conducted preliminary studies to assess the optimal concentration of TNFα to be used in our experiments. Primary RASMCs purchased from Cell Applications Inc were grown at passages 8 through 10. Cells were grown in DMEM containing 10% fetal bovine serum and 1% penicillin-streptomycin. Media was changed every 3 days. Rat recombinant tumor necrosis factor-alpha (Peprotech Cat#400-14) was added to the cell culture media at concentrations of 0 ng/ml, 10 ng/ml, 50 ng/ml and 100 ng/ml. At the end of 6 days, cell lysates were collected and alkaline phosphatase activity measured as described in section 5.3.f. Based on the results of the preliminary experiments as described in section 5.4.a, the concentration of 50 ng/ml of TNFα was chosen for all subsequent experiments. Cell culture experiments based on these preliminary results were conducted as described in the sections below.

5.2.b Cell Culture

Primary RASMCs purchased from Cell Applications Inc were grown at passages 8 through 10. Cells were grown in DMEM containing 10% fetal bovine serum and 1% penicillin-streptomycin. Media was changed every 3 days. TNFα was added to the cell culture media at a concentration of 50 ng/ml. PGG was added to cell culture media at a concentration of 10 µmol/L.

Osteoblast cells (7F2 osteoblast cell line) were grown in alpha-MEM with 10% fetal bovine serum, 1% penicillin-streptomycin and 50 µg/ml ascorbic acid-2-phosphate

(growth media). Once confluent, growth media supplemented with 10 mmol/L β-glycerophosphate was used to cause the osteoblasts to differentiate and deposit calcium phosphate.

5.2.c Experimental groups

TNFα and PGG were added simultaneously at day 0 and samples were collected at days 1, 3 and 6. The delayed group (D6) consisted of cells supplemented with TNFα at day 0 and PGG added at day 3 with samples collected at day 6.

5.2.d Proliferation

Methylthiazolyldiphenyl-tetrazolium bromide, MTT, 3-(4,5-Dimethyl-2-thiazolyl)-2,5-diphenyl-2H-tetrazolium bromide (Sigma) was used to determine the relative proliferation rates. 5 mg of MTT was dissolved in 1ml phosphate buffered saline and further diluted in 9ml of DMEM. Conditioned media of cells grown for 3 days or 6 days was aspirated and the cells rinsed carefully with phosphate buffered saline. 0.5 ml of the final MTT solution was added to each well and incubated at 37 C for 4 hours. At the end of four hours, the MTT solution was carefully aspirated and the insoluble purple formazan product was dissolved using 0.1% HCl in isopropanol. Absorbance was read at 560nm and plotted as percentages of control group.

5.2.e Real-time PCR

RNA was isolated from cells using the GE Illustra mini RNA isolation kit and quantified using the Agilent 2100 bioanalyzer. Equal amounts of RNA were reverse transcribed with the Applied Biosystems High Capacity reverse transcription kit. Real-time PCR was conducted using Qiagen SYBR green master mix on a Rotorgene 3000 PCR machine. The delta-delta Ct method was used to calculate relative gene expression with 18S rRNA as the housekeeping gene.

5.2.f Alkaline phosphatase activity

Alkaline phosphatase activity was measured using a colorimetric method that uses para-Nitrophenol phosphate (pNPP) as a substrate. Briefly, 5 mg of pNPP was dissolved in diethanolamine buffer (pH 10). Samples were combined with the pNPP solution and incubated at 37˚ C for 30 minutes. Alkaline phosphatase standards were also incubated with pNPP buffer to obtain a standard curve. The reaction caused the cleavage of phosphate group in pNPP and release para-Nitrophenol, a yellow soluble product. The absorbance for the product was measured at 405 nm and alkaline phosphatase activity was calculated (mU). The activities of the experimental groups were normalized to the control group and the percentage change was calculated.

5.2.g Histochemical staining for alkaline phosphatase

Visually, alkaline phosphatase activity was assessed using BCIP/NBT (5-bromo-4-chloro-3-indolyl phosphate/ nitro blue tetrazolium) substrate (Sigma). Conditioned media of cells at the indicated time points were aspirated and rinsed with PBS. Equal

volumes of BCIP/NBT were added to the cells and incubated in the dark for 6-8 hours at room temperature. The BCIP/NBT solution was aspirated and cells were washed in PBS followed by fixation in 4% formalin-PBS solution.

5.2.h Calcium quantification assay

At the time points mentioned, media was aspirated and cell layers were washed with phosphate buffered saline (PBS). 250ul of 2N hydrochloric acid was added to each well, shaken for overnight at room temperature and collected by scraping the cell layers. O-cresolphthalein complexone assay was performed to quantify calcium and normalized to total protein.

5.2.i von Kossa staining

At the time points indicated, media was aspirated and cell layers were washed with PBS. The cells were then fixed in 4% Formalin-PBS for 10 minutes at room temperature and washed with PBS. The cells were then incubated in freshly made 5% silver nitrate solution in the dark for 30 minutes, washed thoroughly with DDI water and incubated in UV light for 1 hour for color development.

5.2.j Alizarin red staining

At the time points indicated, media was aspirated and cell layers were washed with PBS. After fixation in 4% formalin-PBS, cells were stained with 2% Alizarin red solution for 1 minute and excess stain was washed thoroughly with distilled deionized water.

5.2.k Data analysis

Results are expressed as mean ± SEM with triplicates for all experimental groups. Statistical analysis of data was calculated using student's t-test and probability value (p) was calculated and $p<0.05$ was considered statistically significant.

5.3. RESULTS

5.3.a Results of preliminary study to determine the optimal concentration of TNFα

Increase in alkaline phosphatase (ALP) activity induced by TNFα was measured at day 6. As shown in Figure 5.1, 50 and 100 ng of TNFα caused similar increase in ALP, thus we chose to use a concentration of 50 ng/ml TNFα for our further experiments.

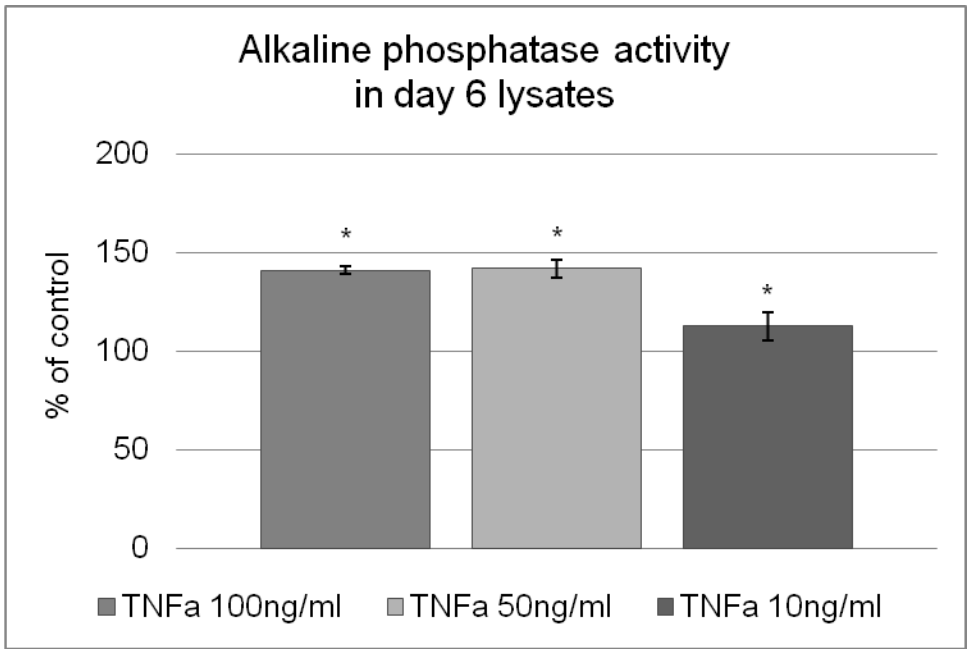

Figure 5.1: Alkaline phosphatase activity in day 6 RASMCs. * indicates significantly higher than the control group ($p<0.05$)

5.3.b PGG inhibits increased proliferation induced by TNFα

Cell proliferation was quantified using the MTT assay and results are shown in Figure 5.2. MTT assay showed increased proliferation in the TNFα groups (by almost 50%). The addition of PGG along with TNFα inhibited the increased proliferation significantly. PGG alone showed reduced proliferation compared to the control group (Fig 5.2). Cytotoxicity test (data not shown) demonstrated that PGG is not cytotoxic to these cells at the concentration used. Proliferation of osteoblasts was similarly affected by PGG. At days 1, 3 and 6 PGG showed significant reduction in proliferation of osteoblasts as shown in Figure 5.3.

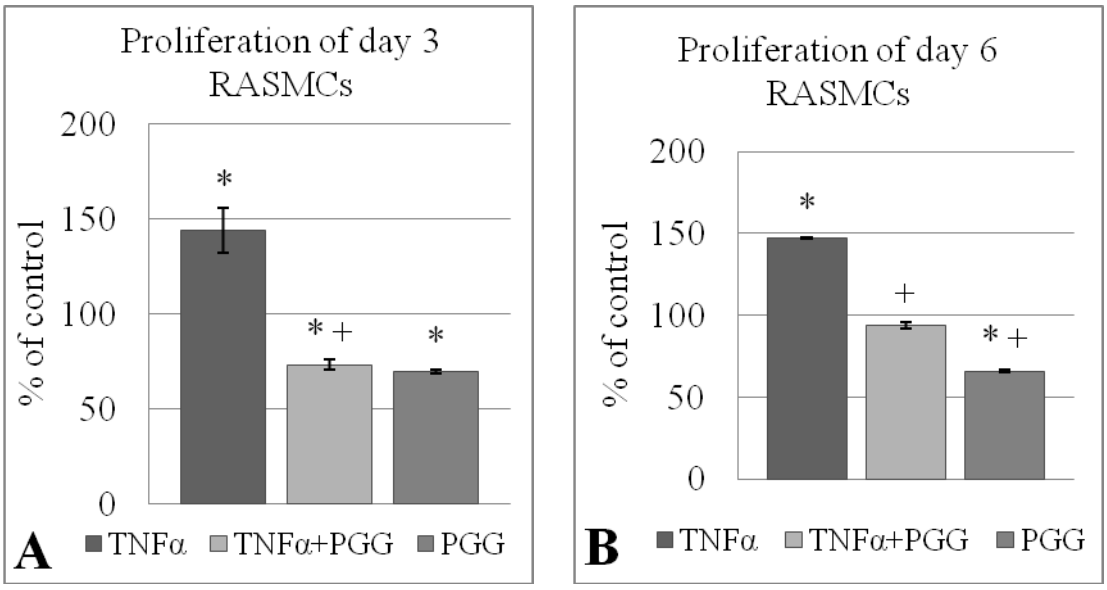

Figure 5.2: Proliferation of RASMCs as assessed by MTT assay. *indicates significantly different from the control group and + indicates significantly different from the TNFα group ($p<0.05$).

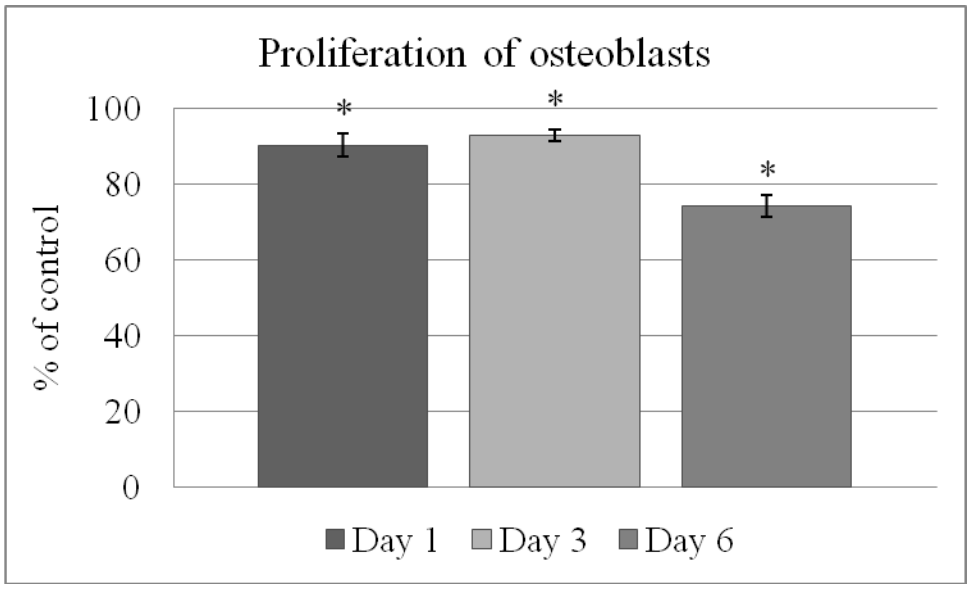

Figure 5.3: Proliferation of osteoblasts measured using MTT assay. * indicates significantly lower than the control group ($p<0.05$).

5.3.c PGG inhibits gene expression of osteogenic markers in RASMCs

To understand if PGG affects the osteogenic markers at transcription level, real-time PCR was conducted. Gene expression at days 3 and 6 indicated that PGG affected the mRNA levels of some osteogenic proteins (Figures 5.4A, 5.4B). Msx-2 (muscle segment homeobox-2) is an important transcription factor in the differentiation of osteoblasts. TNFα increased expression of Msx-2 by 3.3-fold which was reduced by PGG by almost 50% at day 3. At day 3 and 6, gene expression of CBFA-1 (core binding factor alpha-1) was significantly upregulated by TNFα by 2.5 and 5.4 times, respectively. Gene expression of alkaline phosphatase and CBFA-1 (core binding factor alpha-1) were lower at day 6 by PGG, but not significantly. Gene expression of osteocalcin, a marker of late osteogenic differentiation showed no difference between the groups at both time points. Alkaline phosphatase, a late gene marker of osteogenesis, was upregulated by TNFα 3.8-fold at day 6 and was decreased by PGG 2.5 fold.

Gene expression of transcription factors c-Jun and c-Fos, major components of activating protein-1 (AP-1), was measured to study the effect of PGG on cellular proliferation (Figures 5.5A, 5.5B). At day 3 and day 6, c-Fos expression was increased by TNFα by 1.8-fold and 2.2-fold respectively ($p<0.05$). At day 6, this increase in c-Fos gene expression was significantly decreased by PGG to 1.6-fold ($p<0.01$). This data demonstrated that PGG affects cellular proliferation at the transcription level.

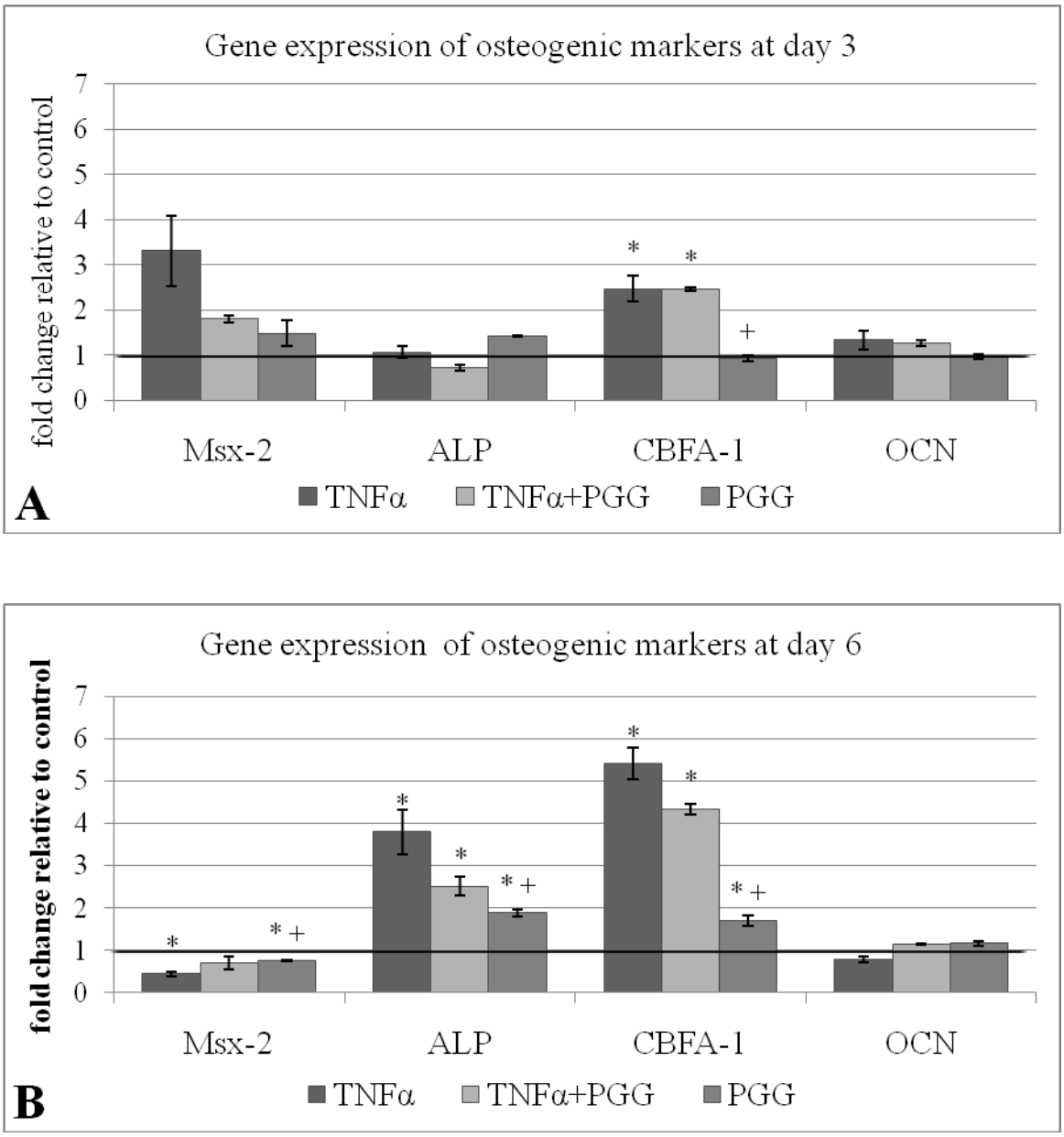

Figure 5.4: Gene expression of osteogenic markers at day 3 (A) and day 6 (B). * indicates significantly different from the control group and + indicates significantly different from the TNFα group ($p<0.05$).

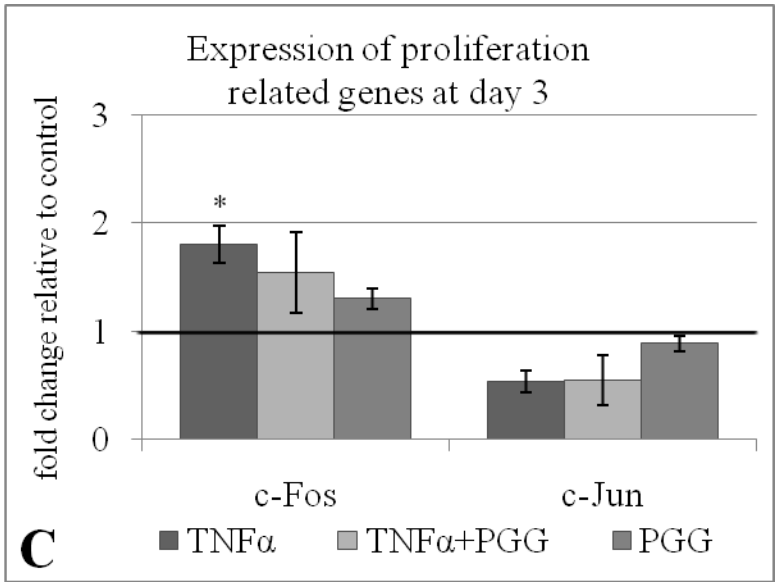

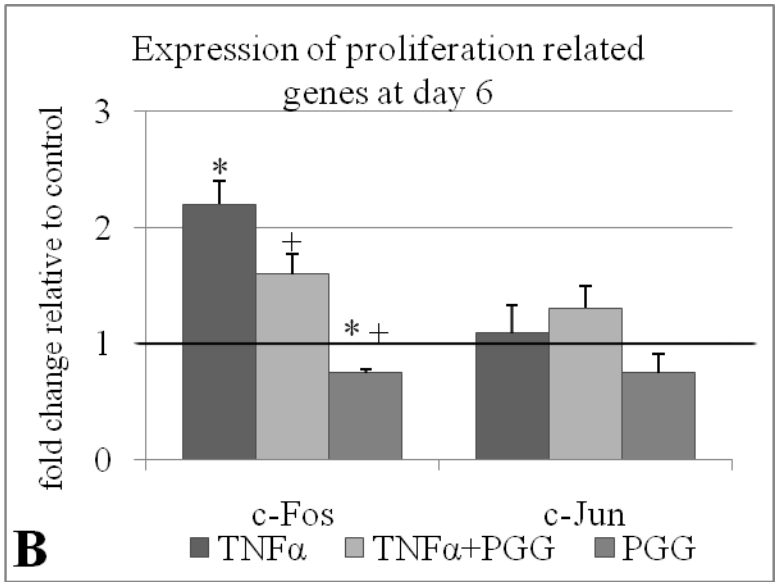

Figure 5.5: Gene expression of transcription factors involved in proliferation at day 3 (A) and day 6 (B). * indicates significantly different from the control group and + indicates significantly different from the TNFα group ($p<0.05$).

5.3.d PGG inhibits and reverses the increase in alkaline phosphatase activity induced by TNFα

Intracellular alkaline phosphatase is an enzyme that is considered to be a characteristic feature of osteoblast-like cells. Observation of alkaline phosphatase activity in aortic smooth muscle cells is indicative of an osteogenic transdifferentiation of the smooth muscle cells. Determination of alkaline phosphatase activity was conducted quantitatively by a colorimetric assay using pNPP phosphate as substrate and qualitatively by using BCIP/NBT substrate.

Alkaline phosphatase activity in cells treated with TNFα was significantly increased compared to control cells at days 1, 3 and 6. At all these time points, PGG inhibited the alkaline phosphatase activity significantly (Fig 5.6). As shown in Figures 5.7 and 5.8, staining for alkaline phosphatase activity also showed similar results as the colorimetric assay results for alkaline phosphatase.

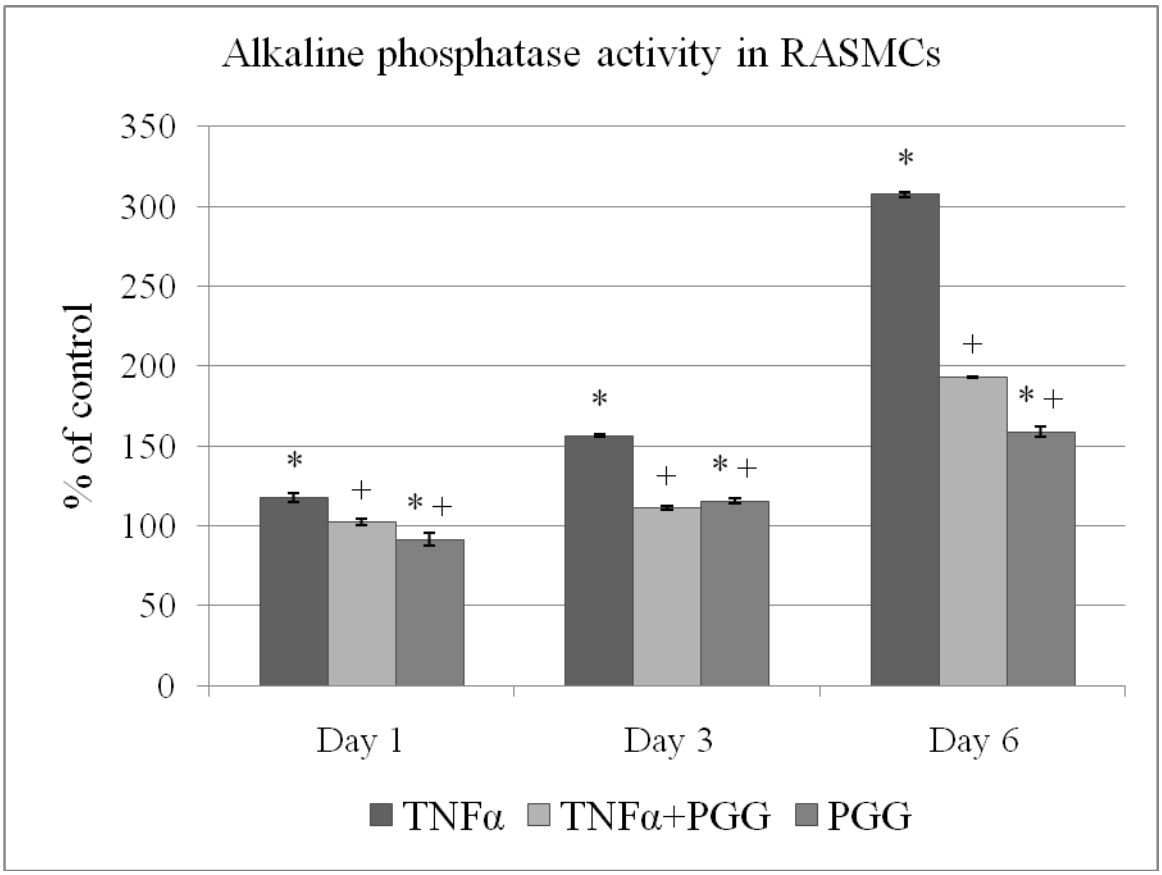

Figure 5.6: Alkaline phosphatase activity in RASMCs. * indicates significantly different from the control group and + indicates significantly different from the TNFα group ($p<0.05$).

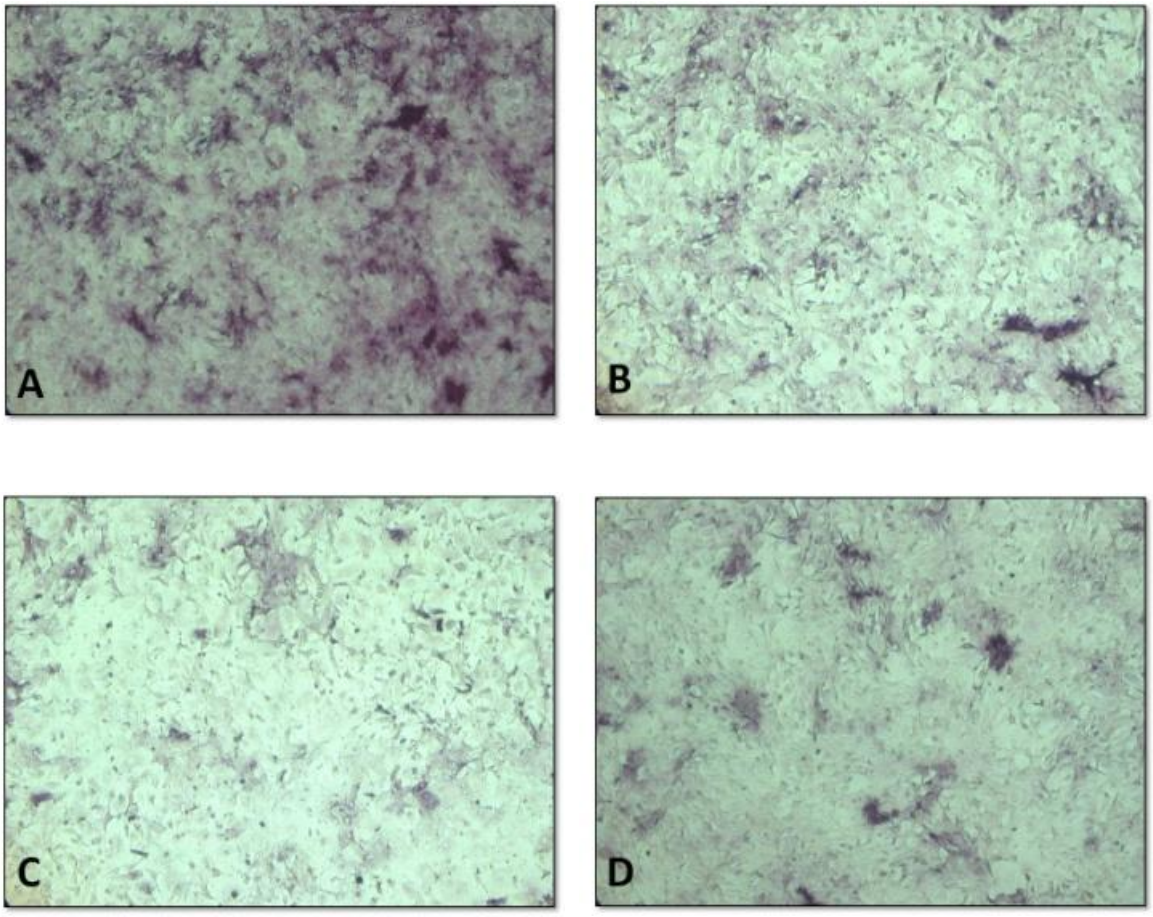

Figure 5.7: Alkaline phosphatase staining for RASMCs at day 3. Alkaline phosphatase activity is denoted by purple staining. Cells were treated with TNFα (A), TNFα+PGG (B), PGG (C) or none (D) and stained for alkaline phosphatase at day 3. (Magnification 200X)

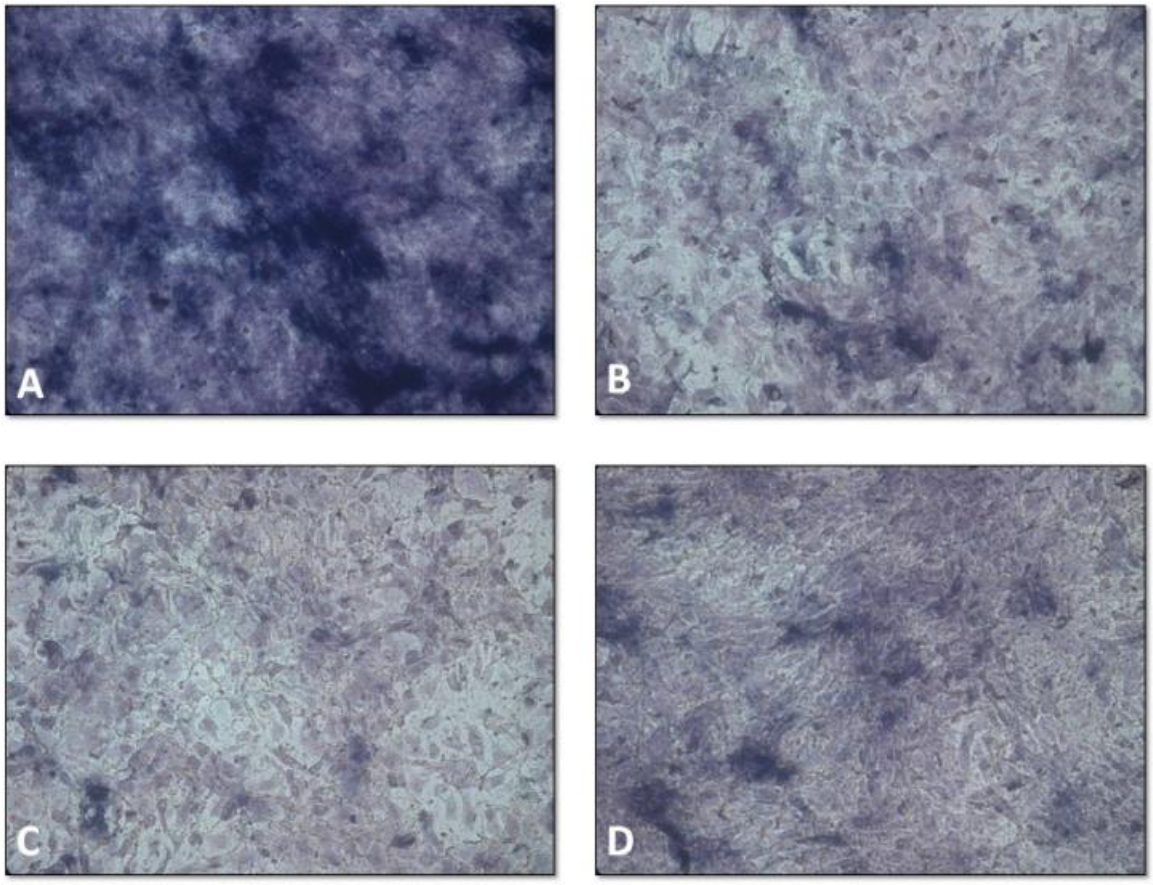

Figure 5.8: Alkaline phosphatase staining for RASMCs at day 6. Alkaline phosphatase activity is denoted by purple staining. Cells were treated with TNFα (A), TNFα+PGG (B), PGG (C) or none (D) and stained for alkaline phosphatase at day 6. Purple staining indicates alkaline phosphatase activity. (Magnification 200X)

In order to determine if PGG has an inhibitory effect on alkaline phosphatase following TNFα treatment, cells were treated with TNFα for 3 days, then incubated for 3 days with PGG (referred to as D6 in Materials and Methods). Alkaline phosphatase activity determined at day 6 is shown in Figure 5.9. Not only PGG inhibited alkaline phosphatase activity when added simultaneously with TNFα (Figure 5.6) but also reversed alkaline phosphatase activity when added 3 days following TNFα treatment. Staining for alkaline phosphatase also confirmed that PGG decreased alkaline phosphatase levels when added 3 days past TNFα treatment.

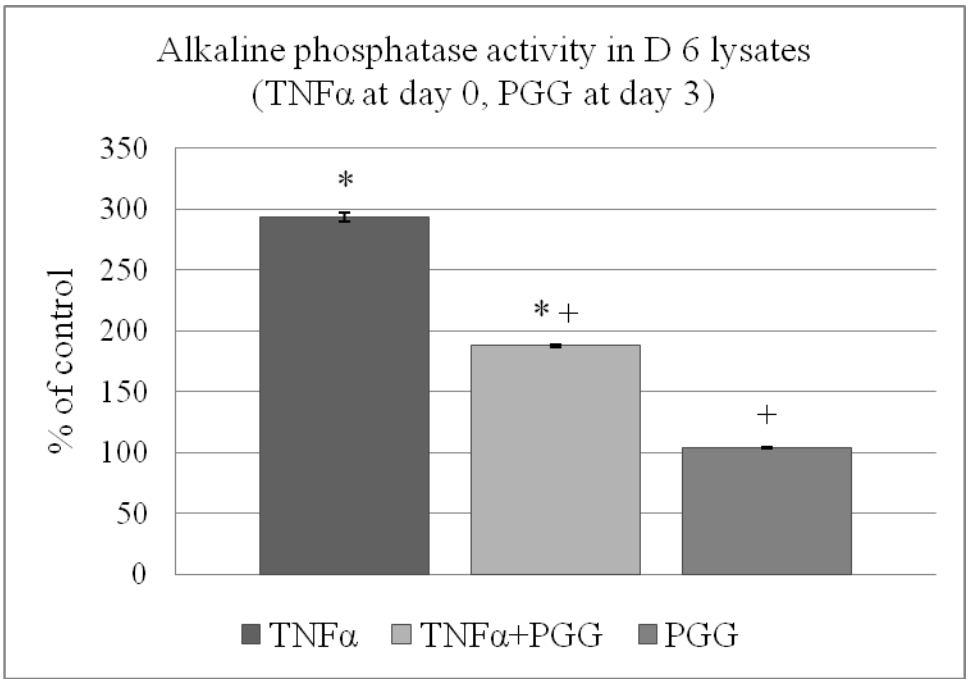

Figure 5.9: Alkaline phosphatase activity at day 6 in cells that were treated with 50ng/ml of TNFα for 3 days followed by 3 days of treatment with both TNFα and PGG. * indicates significantly different from the control group and + indicates significantly different from the TNFα group ($p<0.05$).

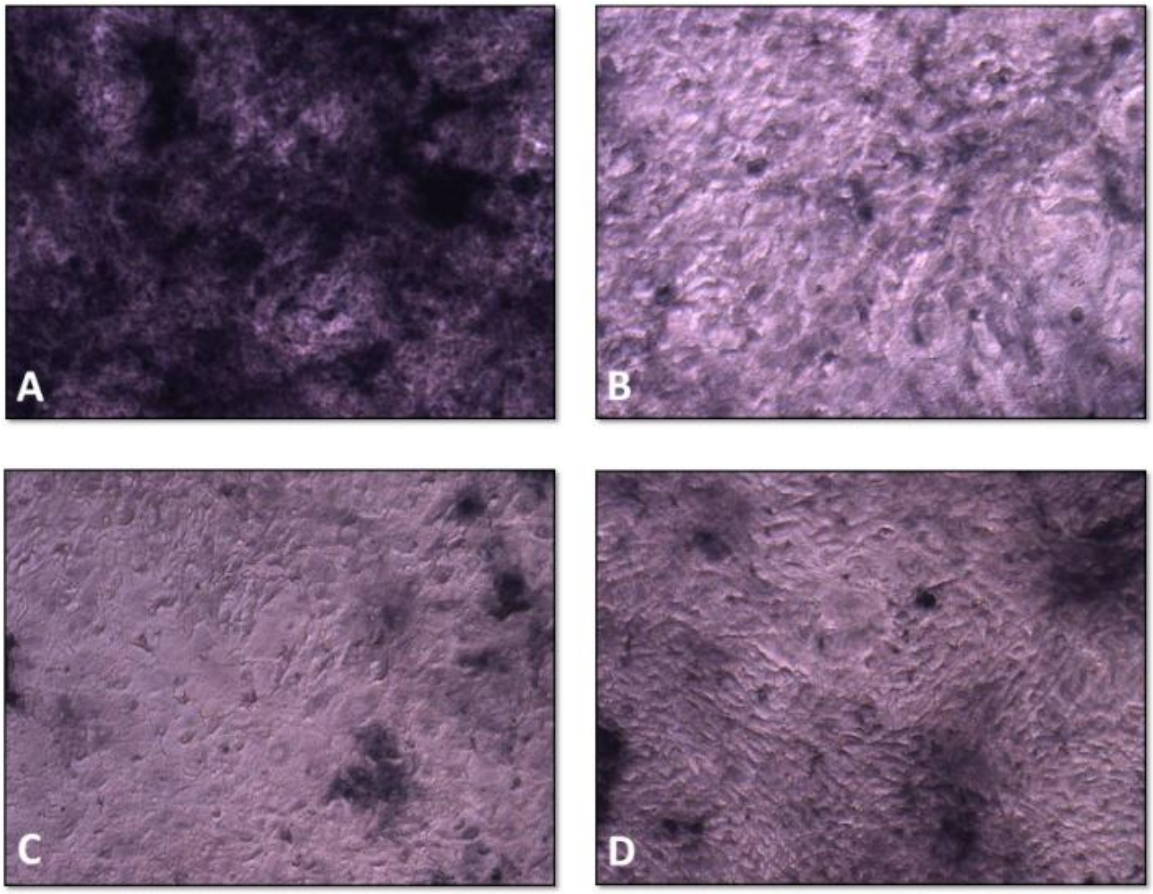

Figure 5.10: Staining for alkaline phosphatase activity in D6 experimental groups. Alkaline phosphatase activity is denoted by purple staining. RASMCs were treated with 50 ng/ml TNFα at day 0 (A), 50 ng/ml TNFα at day 0 followed by 10 µmol/L PGG at day 3 (B), no treatment at day 0 followed by 10 µmol/L PGG at day 3 (C) and no treatment at either day 0 or day 3 (D).

Since alkaline phosphatase is an important enzyme in osteoblast functioning, we decided to investigate the effect of PGG on the activity of this enzyme in osteoblasts. As seen in Fig 5.11, histological staining showed that at day 6, PGG showed increased alkaline phosphatase activity in osteoblasts. PGG increases calcium deposition by osteoblasts at day 14 and day 21 as shown as seen in figures 5.12 and 5.13.

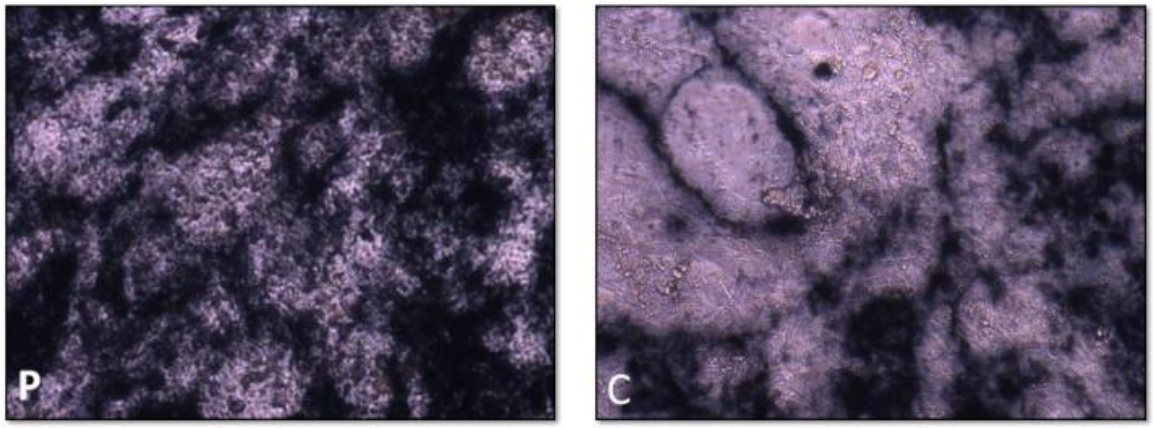

Figure 5.11: Histological staining for alkaline phosphatase in 6 day osteoblasts. Alkaline phosphatase activity is denoted by purple staining. Cells treated with 10 µmol/L PGG (marked P) shows increased alkaline phosphatase activity compared to no treatment control (marked C) cells.

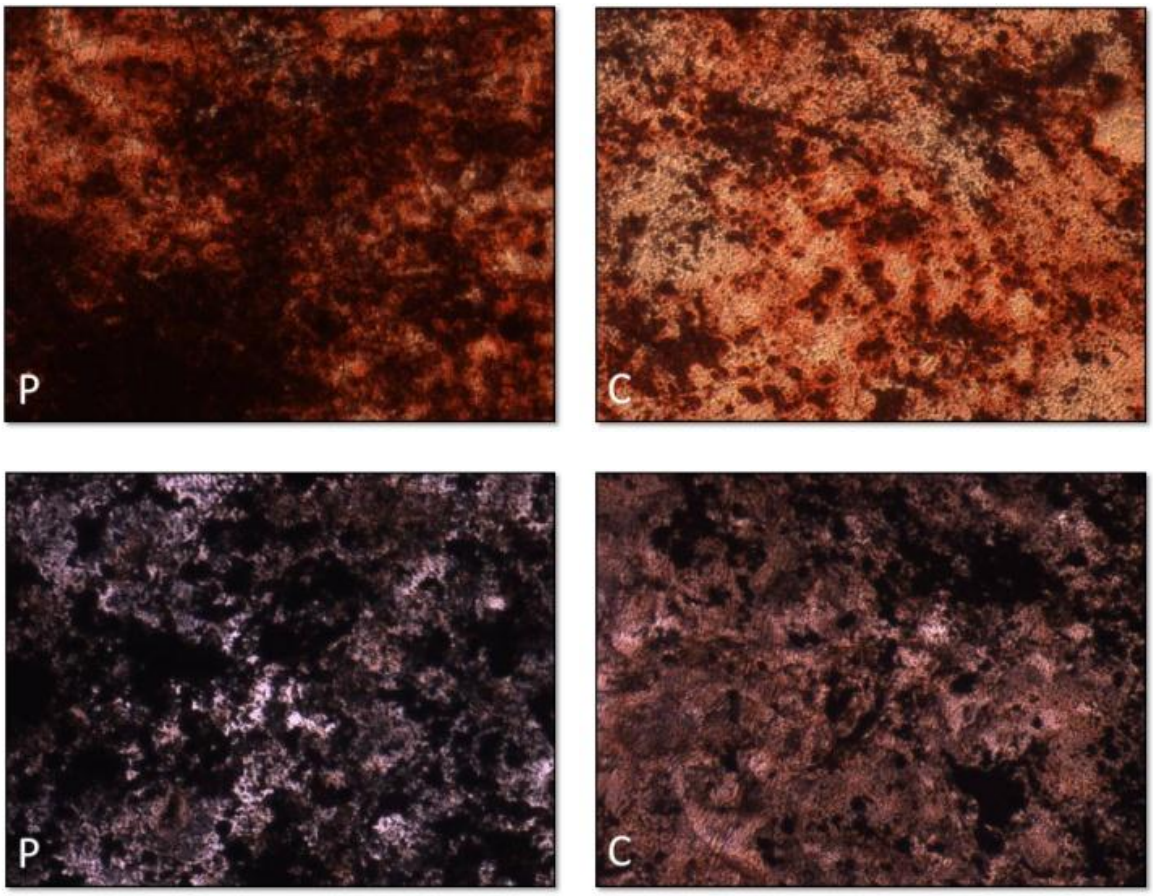

Figure 5.12: Alizarin red staining (top row) and von Kossa staining (bottom row) for 14 day osteoblasts. Alizarin red stains calcium deposits red and von Kossa staining causes in calcium deposits to color black. Cells treated with PGG (marked P) showed increased staining for calcium deposits relative to untreated control (marked C) cells.

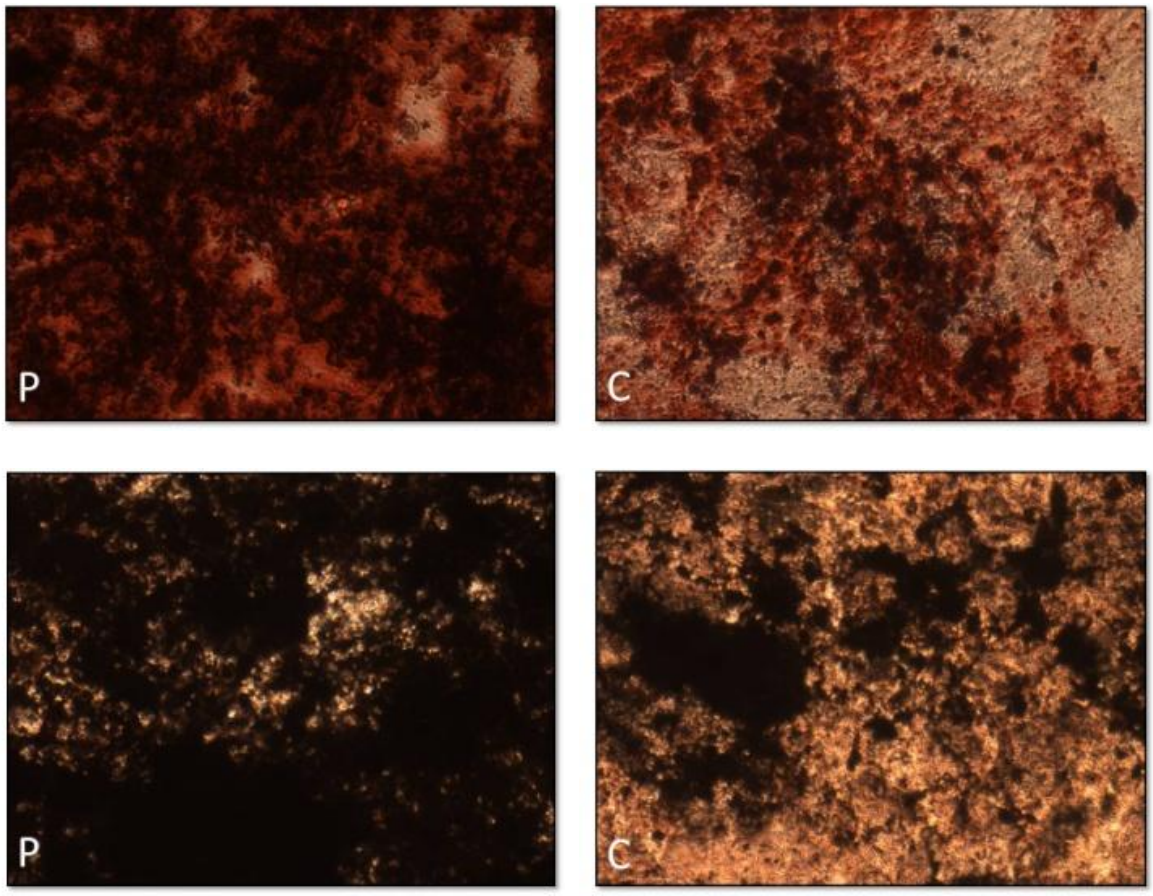

Figure 5.13: Alizarin red staining (top row) and von Kossa staining (bottom row) for 21 day osteoblasts. Alizarin red stains calcium deposits red and von Kossa staining causes in calcium deposits to color black. Cells treated with PGG (marked P) showed increased staining for calcium deposits relative to untreated control (marked C) group.

5.3.e PGG increases calcium deposition by osteoblasts

Calcium deposition as quantified by O'Cresolphthalein method showed that osteoblasts treated with PGG deposited significantly higher amount of calcium than the control groups at the corresponding time points. As shown in Figure 5.14, at both time points, PGG significantly increased mineralization by osteoblasts.

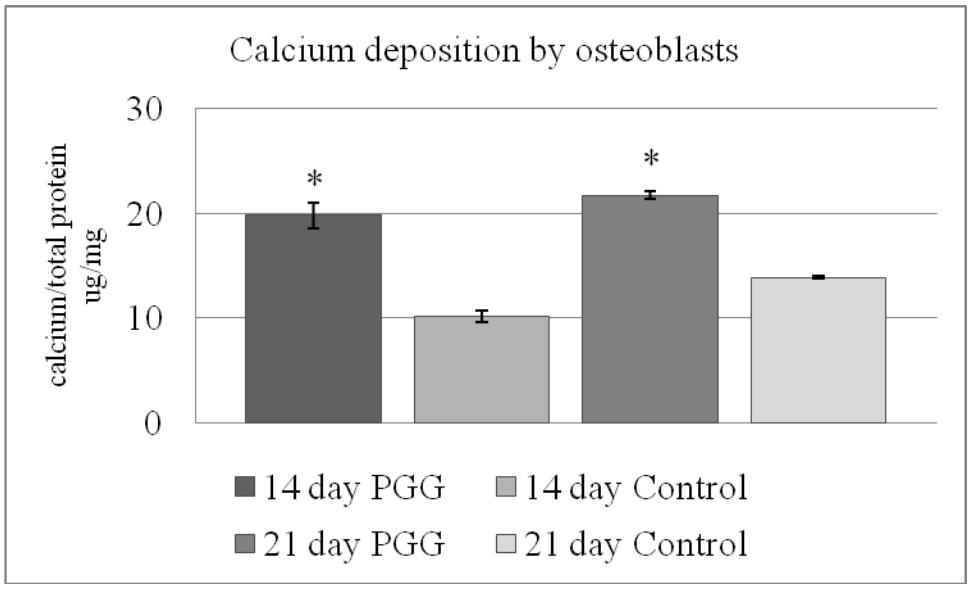

Figure 5.14: Quantification of calcium deposition by osteoblasts at days 14 and 21. * indicates significantly different from the control group ($p<0.05$).

5.4. DISCUSSION

In this study, we show that PGG inhibits many characteristics associated with the transformation of vascular smooth muscle cells into osteoblast-like cells under inflammatory conditions. In addition, we show that PGG also helps to increase osteogenic characteristics such as alkaline phosphatase and mineral deposition by osteoblasts. It has been observed that osteoporosis, loss of mineralization from bones and vascular calcification, ectopic deposition of mineralization in arteries, occur often together.[159,160] Thus, a therapeutic agent developed for vascular calcification should be designed such that it should not adversely affect the ability of bone cells to deposit or resorb hydroxyapatite. Bisphosphonates are a class of drugs that were developed for osteoporosis but are considered to have beneficial effects on atherosclerosis and vascular calcification; however, these benefits have not been proven. [160,169-171]

Studies have shown that arterial mineralization and osteoporosis occur hand in hand with inflammatory conditions. Inflammation triggers phenotypical changes in vascular smooth muscle cells as well as cause increased resorption of bone.[159,172,173] One study compared the effects of oxidative stress on calcifying vascular cells and osteoblasts, and has suggested that oxidative stress may be a common factor between osteoporosis and vascular calcification.[174]

PGG inhibited the expression of multiple genes associated osteogenesis. PGG showed a trend of reduced expression of many genes we studied (Figures 4A, 4B). MSX-2, an early marker of osteoblast differentiation was upregulated at day 3 by TNFα and

then reduced at day 6. Msx-2 is expressed in pre-osteoblasts prior to differentiation into osteoblasts. Msx-2 expression is reduced during the final differentiation of osteoblasts. The increase in expression of Msx-2 at day 3 and its decreased expression at day 6 indicates the transformation of the smooth muscle cells into osteoblast-like cells similar to osteoblast differentiation in bone. PGG inhibited the over-expression of MSX-2 at day 3 so PGG may inhibit the early markers of osteoblast differentiation in smooth muscle cells.

In rat aortic smooth muscle cells, PGG significantly decreased the activity of alkaline phosphatase, an enzyme considered to be important in the osteoblast mediated deposition of calcium phosphate (Figures 5.6-5.10). In contrast, alkaline phosphatase activity and mineralization were increased by PGG in osteoblasts as shown in Figures 5.11-5.13.

PGG exerted similar effects on the proliferation of both vascular smooth muscle cells and osteoblasts. This could be an important factor in explaining the contrasting effects of PGG on the two types of cells we studied. We hypothesize that PGG inhibits cells from multiplying and causes the cells to remain in a differentiated state. It has been shown that aortic smooth muscle cells do not exist in a finally differentiated state and are more flexible to proliferate and deposit extracellular matrix in case of injury or inflammation.[105,175] PGG may therefore prevent the dedifferentiation of vascular smooth muscle cells into osteoblastic lineage and allow the cells to function as smooth muscle cells. In the case of osteoblasts, PGG may allow the cells to remain in their differentiated state and promote their function of depositing calcium apatite. The transcription factors c-

Fos and c-Jun are members of the AP-1 family. AP-1 is the product of dimerization between c-Fos and c-Jun or between c-Jun and c-Jun. AP-1 binds to the enhancer region of target genes and regulates the transcription of genes associated with proliferation. Correlation between the expressions of c-Fos and c-Jun is an important factor in regulating the pathways of proliferation and growth.[176-179] Other studies have shown that some polyphenolic compounds including epigallocatechin and curcumin inhibit the cell cycle progression and AP-1 activity in vascular cells.[180-182] Therefore, we investigated the gene expression of c-Fos and c-Jun in our experiments. Our results show that c-Jun gene expression was unaffected in all the groups at both days 3 and 6, compared to the control (Figures 5.5A, 5.5B). However, TNFα increased the expression of c-Fos significantly at days 3 & 6. PGG decreased the expression of c-Fos at both day 3 ($p>0.05$) and day 6 ($p<0.05$) when combined with TNFα. PGG alone also showed significantly decreased expression compared to control at day 6. These results could indicate that PGG could influence the cell cycle and affect the pathways of growth and DNA replication.

The exact mechanism by which PGG causes the above mentioned effects is not understood. Further studies to assess the expression of transcription factors involved in cell cycle progression and dedifferentiation of vascular smooth muscle cells such as GATA-6 could reveal more specifics of the actions of PGG. We believe that this is the first study that shows the reversal of osteogenic properties (alkaline phosphatase activity) in smooth muscle cells. More studies need to be conducted to better understand the effects and possible side effects of PGG.

CHAPTER 6

TO PREPARE AND CHARACTERIZE POLY(LACTIC-CO-GLYCOLIC) ACID NANOPARTICLES ENCAPSULATING PENTAGALLOYLGLUCOSE TO BE POTENTIALLY USED FOR *IN* VIVO DELIVERY OF PENTAGALLOYLGLUCOSE

6.1. INTRODUCTION

From the studies discussed above, we conclude that PGG could be a valuable therapeutic agent due to its various beneficial effects in vascular diseases. As shown in the preceding results, PGG inhibits proliferation due to inflammatory conditions, effectively controls the activity of proteolytic enzymes, and down regulates osteogenic signaling in rat aortic smooth muscle cells. In parallel, PGG demonstrated positive effects on osteoblast function. Thus, PGG can have positive effects in cardiovascular pathologies and bone mineralization if delivered locally. In this study, we studied PGG encapsulated nanoparticles as a potential mode of PGG *in vivo*.

Nanoparticles with a size range of 10-1000 nm are frequently used for drug delivery applications. Drugs or DNA can be entrapped, dissolved, encapsulated or attached to nanoparticles. The advantages of nanoparticles include high surface area to volume ratio, controlled degradation time, and storage stability. Disadvantages of nanoparticles include particle aggregation, limited drug loading and optimized drug release.[183] We wanted to test the possibility of preparing PGG loaded nanoparticles and

studied the release profile of these nanoparticles. Poly-(lactic-co-glycolic) acid (PLGA) nanoparticles encapsulating pentagalloylglucose (PGG) were prepared as 'proof of concept'.

6.2. MATERIALS AND METHODS

6.2.a PLGA nanoparticle synthesis

Two hundred milligrams of PLGA was dissolved in 12 ml of dichloromethane. Ten ml of aqueous PGG solution (500 µg/ml) was sonicated with the PLGA (1^{st} sonication) to obtain a water-in-oil (W/O) emulsion. This emulsion was diluted in 50 ml of 1.5% polyvinyl alcohol (PVA) and further sonicated (2^{nd} sonication) to obtain a water-in-oil-in-water (W/O/W) emulsion. Various sonication times were used as shown in Tables6.1 and 6.4. The resultant W/O/W emulsion was stirred under a fume hood overnight to obtain PGG encapsulated nanoparticles. The nanoparticles were centrifuged at 30,000g. The resultant pellet was washed twice with distilled water, and centrifuged at 30,000g between washes. The pellet was frozen at -80 ^{o}C and lyophilized.

6.2.b Measurement of nanoparticles size

The lyophilized nanoparticles (1 mg) was resuspended in water and analyzed with particle analyzer. Lyophilized particles were imaged with scanning electron microscope (Hitachi S4800).

6.2.c Encapsulation efficiency

The lyophilized nanoparticles (5 mg) were sonicated on ice for 1 hour and analyzed for encapsulation efficiency by measuring the absorbance of PGG at 245nm against a PGG standard curve.

6.2.d *In vitro* release profile

Release profile of the nanoparticles was conducted *in vitro* to test the amount of PGG released over time. Ten mg of nanoparticles were added to 5 ml of PBS (pH 7.4) and shaken at 37 ˚C for 48 hours. Samples were collected at indicated time points after centrifugation. PGG released was measure by UV absorbance at 245 nm with blank nanoparticle release used as blank readings.

6.3. RESULTS

We were able to successfully prepare PLGA nanoparticles encapsulating PGG. Measurement of nanoparticles size using particle analyzer (Table 6.2) and scanning electron microscope (Figure 6.1) showed that the nanoparticle diameters were within the range of 250-300 nm. The polydispersity increased when the W/O/W sonication time was increased. However, W/O/W sonication of more than 3 minutes decreased the polydispersity as displayed in Table 6.2. Increase in sonication times lead to decreased encapsulation efficiency of PGG as shown 6.3.

Release profile of the nanoparticles prepared as shown in Table 6.4 showed a linear release profile and released about 97% of encapsulated PGG over 48 hours as shown in Figure 6.2.

Sample #	W/O sonication time	W/O/W sonication time
1	2 min	1 min
2	3 min	2 min
3	3 min	3 min
4	3 min	5 min

Table 6.1: Nanoparticles were synthesized using different combinations of sonication times

Sample #	Diameter	Polydispersity
1	295	0.133
2	396	0.162
3	236	0.174
4	267	0.129

Table 6.2: Diameter and polydispersity of nanoparticles measured with a particle analyzer. Nanoparticles were prepared with sonication times shown in Table 6.1

Sample #	PGG (µg) in 5mg nanoparticles	PGG (µg) in 5mg nanoparticles	Average % loading of PGG
1	610	423	12.2%
2	473	396	9.46%
3	366	402	7.32%
4	238	248	4.76%

Table 6.3: Encapsulation efficiency of PGG-PLGA nanoparticles prepared with sonication times shown in Table 6.1

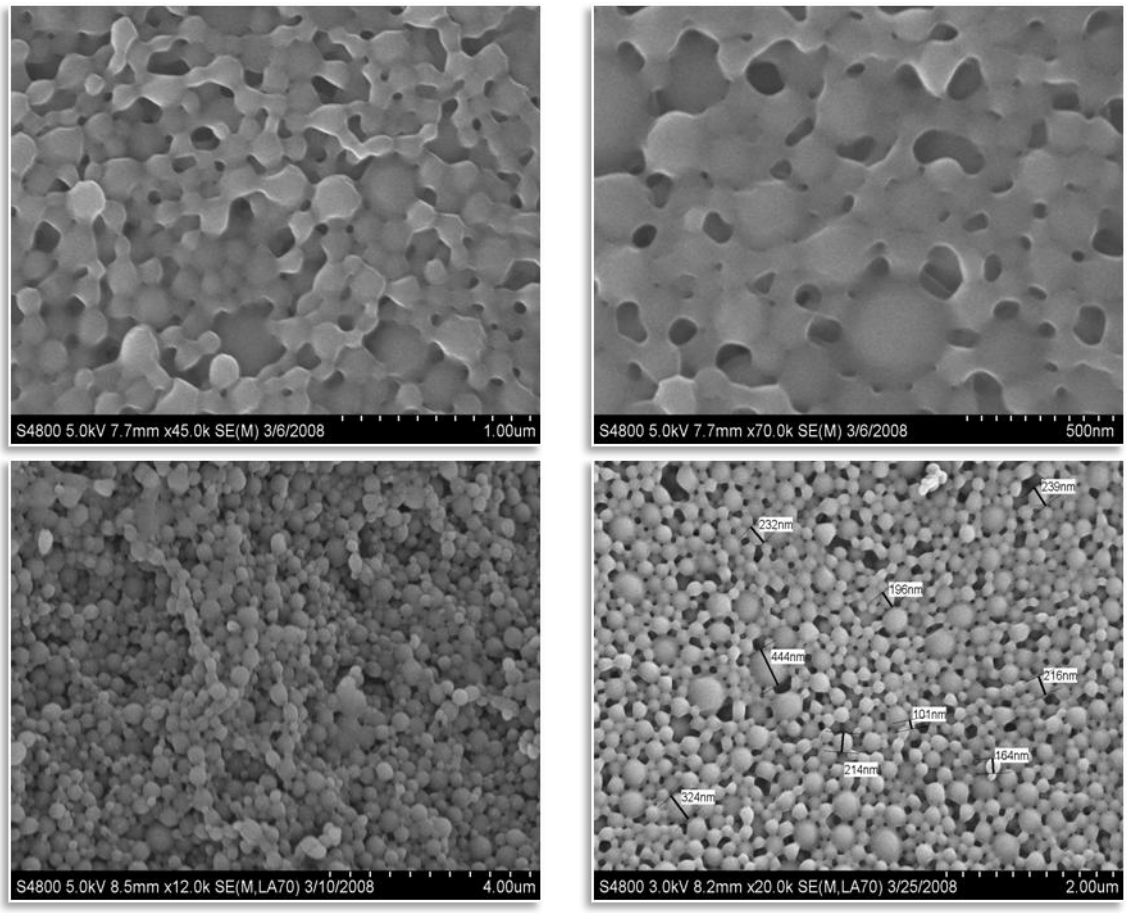

Figure 6.1: Scanning electron microscope images of PGG encapsulated PLGA nanoparticles prepared with sonication times shown in Table 6.1

Sample #	W/O sonication time	W/O/W sonication time
A	45 sec	30 sec
B	30 sec	30 sec

Table 6.4: Nanoparticles were synthesized again with indicated sonication times for W/O and W/O/W emulsions

Sample #	Initial weight of nanoparticles (mg)	µg of PGG	% loading of PGG
A	4.32	510	11.81%
B	4.21	498	11.83%

Table 6.5: Percentage loading of nanoparticles prepared with sonication times shown in Table 6.4

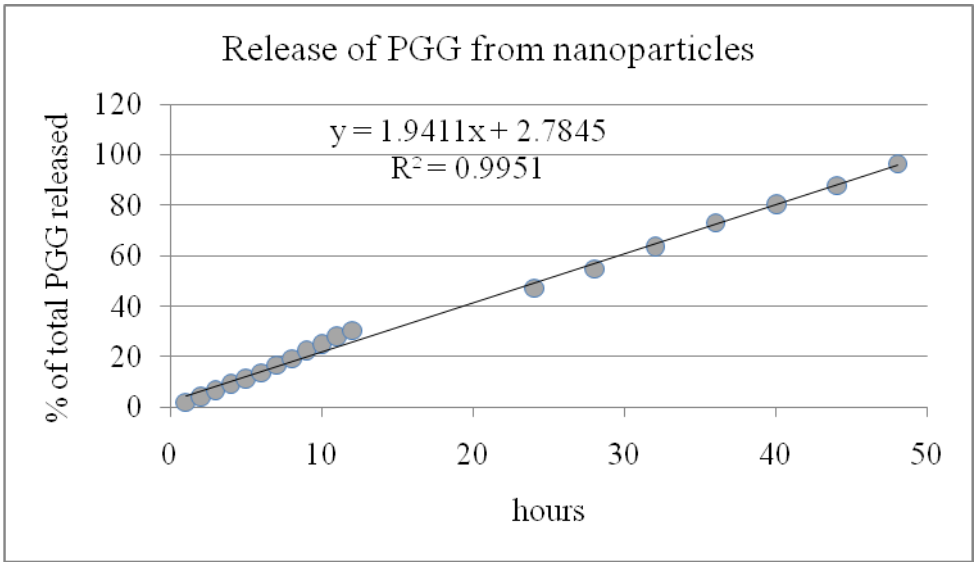

Figure 6.2: Release profile of PGG from nanoparticles prepared with sonication times shown in Table 6.4

6.4. DISCUSSION

We have demonstrated that PGG can indeed be encapsulated into PLGA nanoparticles. Variation in sonication times during W/O and W/O/W emulsions can affect the size and loading of the nanoparticles as seen in Tables 6.2 and 6.3. *In* vitro release profile of nanoparticles prepared as shown in Table 6.4 released almost 97% of PGG within 48 hours. Further optimization of loading and sonication times is needed to prepare PGG nanoparticles that have longer release times.

Release of PGG from nanoparticles may differ significantly *in vivo* from *in vitro* release. The *in vivo* therapeutic effects of PGG could be affected due to acidification of the local area (of delivery) caused by the release of lactic acid, a product of PLGA degradation. Studies need to be conducted in order to verify that the change in pH will not adversely affect the beneficial effects of PGG. Further optimization is necessary to design nanoparticles with the required size, encapsulation efficiency and release profile for *in vivo* delivery.

CHAPTER 7

IMPLEMENTATION AND PRELIMINARY CHARACTERIZATION OF A NEW *IN VITRO* MODEL OF MEDIAL VASCULAR CALCIFICATION USING CRYO-SECTIONED ARTERIAL SCAFFOLDS

7.1. INTRODUCTION

Cell-matrix interactions are an important aspect of cell behavior and function. Some proteins such as collagen and laminin can be easily coated on the bottom of well plates. Interactions between cells and collagen or laminin can be studied by growing cells on these substrates. Commercially available well plates with their proteins coated on them are easily available. Coating proteins such as collagen and laminin is a fairly straightforward procedure involving solubilizing the protein, coating the bottom of the well plate uniformly with the solubilized protein, letting it dry and hydrating it before seeding cells.

Medial vascular calcification involves mineralization of elastic fibers and transformation of vascular smooth muscle cells into osteoblast-like cells. Interactions between vascular smooth muscle cells and their native environment are important to understand so that we can better comprehend the factors involved in vascular calcification. However, currently there are no established methods to simulate the interactions between elastic fibers and smooth muscle cells *in vitro* mainly because elastic fibers cannot be solubilized and coated on culture plates.

The following method describes a procedure by which arterial cryo-sections can be prepared so that interactions between the medial extracellular matrix proteins and cells can be studied *in vitro*. The arterial sections can also be processed to remove specific proteins and create a controlled extracellular matrix substrate.

7.2. MATERIALS AND METHODS

7.2.a Preparation of scaffolds

Fresh porcine thoracic aortae (obtained from a local slaughterhouse) were rinsed with distilled water and cut along the longitudinal axis to obtain a rectangular piece of aorta. These were cut into smaller rectangles so that the tissue section covered the bottom of a well in a 24-well plate. These smaller rectangles were then embedded with OCT (optimal cutting temperature compound) with the luminal side down and frozen at -20 ^{o}C until sectioned. The embedded aortae were then sectioned to obtain flat sections (perpendicular to the normal cross sections) of 20 microns thickness. These were placed on the bottom of 24 well plates.

7.2.b Decellularization

The scaffolds were washed with distilled de-ionized water for 15 minutes to remove the water soluble OCT compound followed by decellularization. Decellularization was performed by incubation in 0.1% sodium dodecyl sulfate (SDS) in PBS for 20 minutes, followed by rinsing with sterile PBS thrice.

7.2.c Scaffold characterization

Cleaned and decellularized scaffolds were fixed with 4% formalin/PBS solution for 10 minutes and stained with routine Hematoxylin and Eosin (H&E) staining to detect the presence of cells or cell debris.

7.2.d Seeding cells

Once decellularized and rinsed thoroughly, the scaffolds were incubated in 70% ethanol for 15 minutes to sterilize them. The scaffolds were then rinsed thrice with sterile PBS thrice and incubated with DMEM containing 10% FBS and 1% penicillin streptomycin for 15 minutes before seeding cells.

7.2.e Cell culture experiments

Primary RASMCs were seeded onto these scaffolds and onto untreated tissue culture well plates without scaffolds (referred to as tissue culture polystyrene or TCPS). The cells were allowed to attach for 24 hours before treatment. The treatments were TNFα (10 ng/ml), Pi (2 mmol/L) + Ca (4 mmol/L), TNFα (10 ng/ml) + Pi (2 mmol/L) + Ca (4 mmol/L), untreated (control). Media was changed at day 3 along with corresponding treatments. At the end of day 7, cells were rinsed with PBS and fixed with 4% formalin/PBS for 10 minutes and stained for calcium using silver nitrate (Von Kossa method). Samples for calcium quantification were collected with 0.5 mol/L hydrochloric acid and calcium deposition quantified using O-cresolphthalein-complexone method.

7.3. RESULTS

7.3.a Decellularization

Decellularization efficiency was assessed by H&E staining which stains nuclei blue. Scaffold decellularization using 0.1% SDS-PBS showed incomplete removal of cellular material from scaffolds. However, using sodium hydroxide resulted in complete decellularization and removal of collagen, leaving behind pure elastin scaffolds (Fig 8-1). Ideally, the 20µm thick sections should be incubated in 0.1mol/L sodium hydroxide for at least 5 hours to achieve complete decellularization and removal of collagen (Fig 8-2).

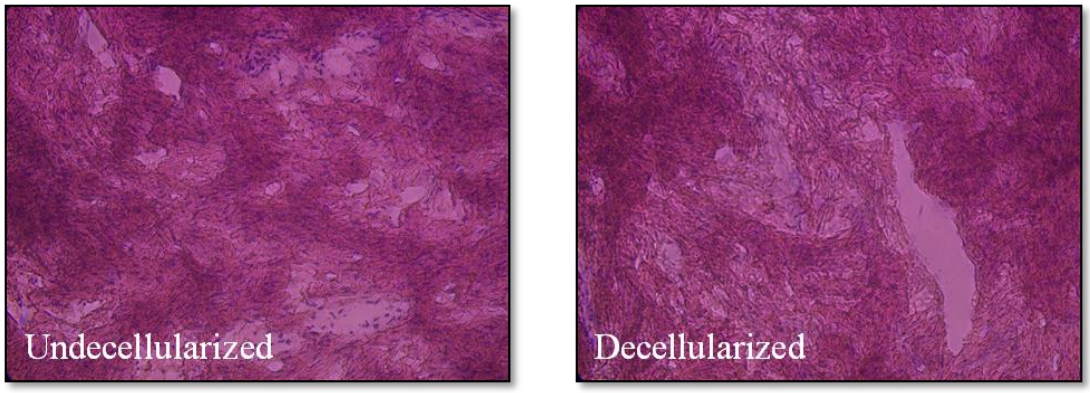

Figure 7.1: Decellularization of scaffolds using 0.1% SDS-PBS solution

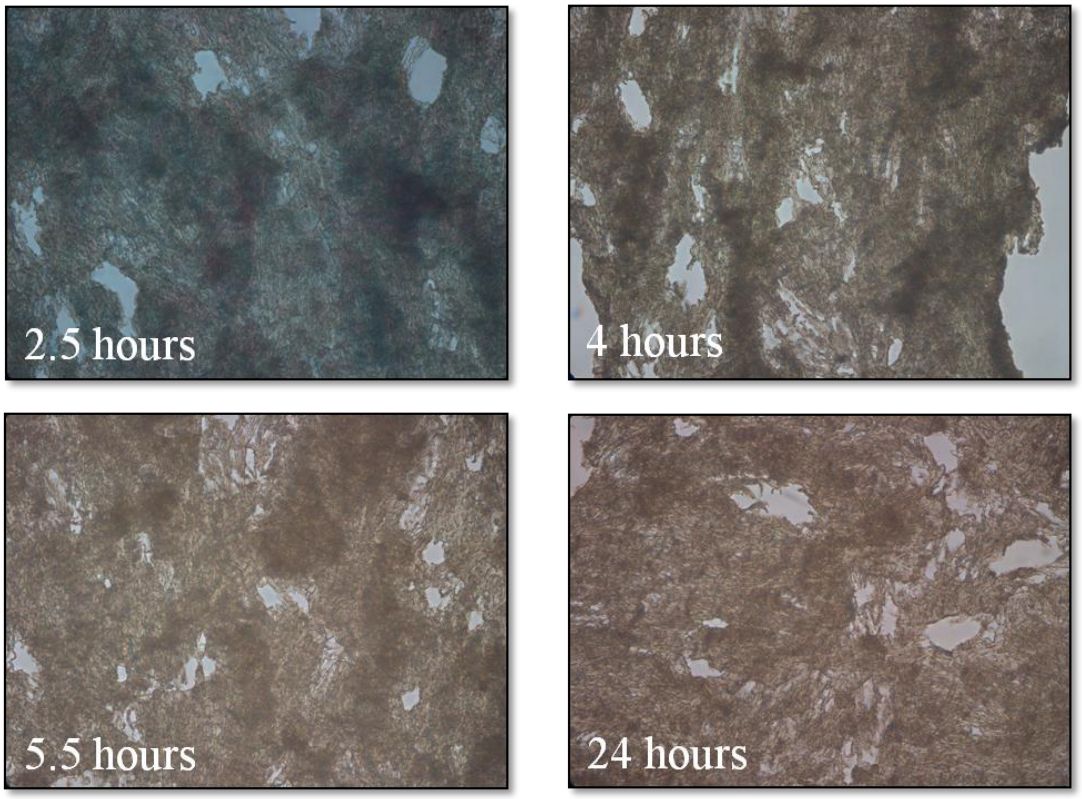

Figure 7.2: Decellularization and removal of all extracellular matrix proteins except elastin form the scaffolds using 0.1 mol/L sodium hydroxide

7.3.b Calcium deposition was higher in cells grown on arterial scaffolds

When RASMCs were grown on TCPS or arterial scaffolds for 7 days with treatment groups as described above, it was observed that cells seeded on scaffolds deposited increased calcium than the TCPS counterpart (Figure 7.3). This difference was statistically significant between the cells treated with TNFα+Pi+Ca on arterial scaffold and cells treated with TNFα+Pi+Ca on untreated tissue culture well plates (Fig 7.4).

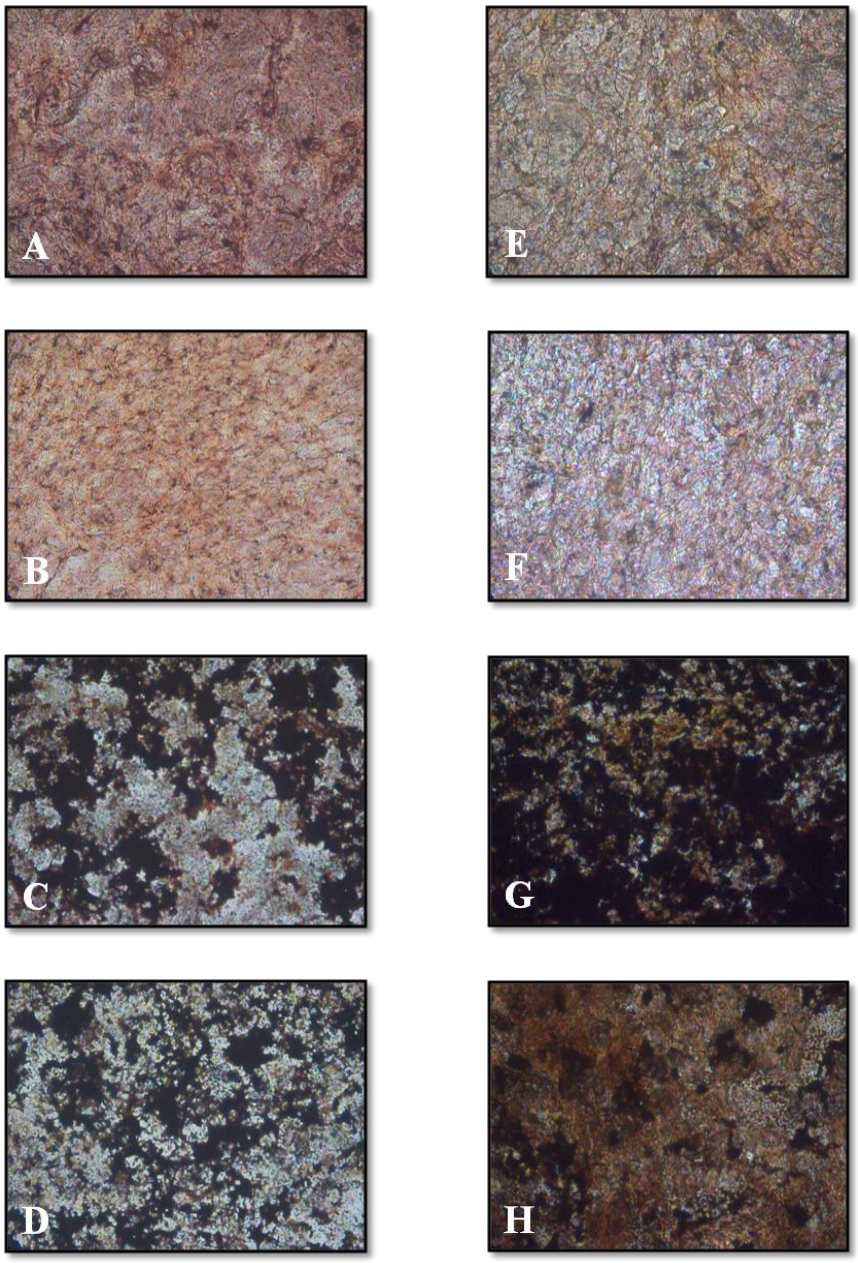

Figure 7.3: von Kossa staining for RASMCs seeded on arterial scaffolds (A-D) or untreated tissue culture well plates (E-H). A and E - Control (no treatment), B and F – 10 ng/ml TNFα, C and G – 10 ng/ml TNFα + 2 mmol/L Pi + 4 mmol/L Ca.

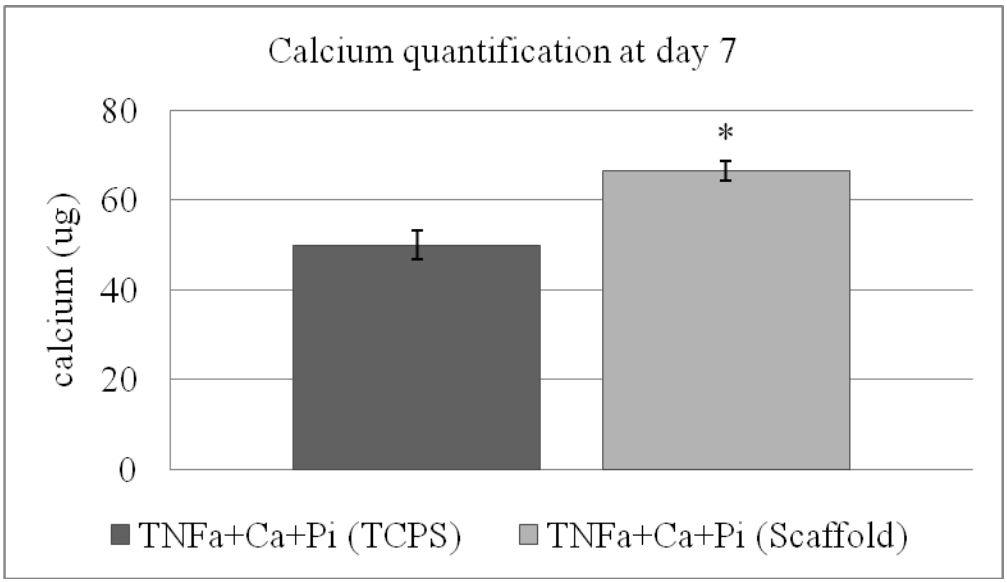

Figure 7.4: Influence of arterial scaffolds on RASMC calcification

7.3.c Gelatin zymography

Cells grown on arterial scaffold had increased MMP-2 and MMP-9 activities compared to their corresponding TCPS groups (Figure 7.5). Interestingly, MMP-2 activity in the conditioned media of cells treated with increased calcium and phosphate showed lower activity than the control (untreated) group. However, this was a pilot study and the experiment needs to be repeated with more samples in order to obtain statistically relevant results.

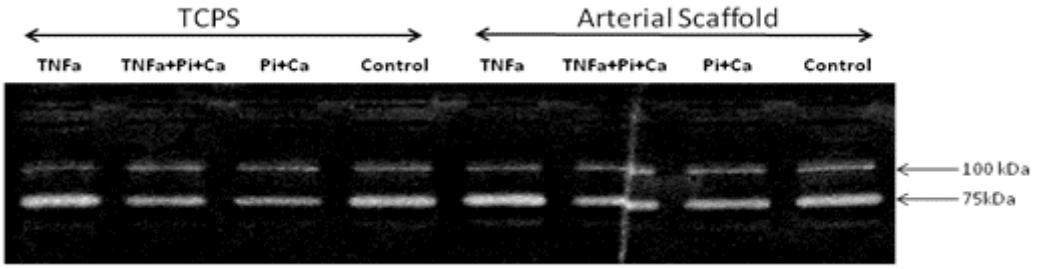

Figure 7.5: Gelatin zymography to detect MMPs in day 7 conditioned media

7.4. DISCUSSION

Studying the influence of elastic fibers on the behavior of aortic smooth muscle cells is important to understand many factors involved in arterial calcification and aneurysms. The model described here provides a simple, inexpensive and effective way to simulate the medial layer of arteries *in vitro*. Vascular medial calcification involves accumulation of calcium phosphate in the elastic fibers and this model helps to simulate this condition *in vitro*. This model can be used in conjunction with existing models of pathological conditions such as addition of cytokines to gain a deeper understanding of the smooth muscle cell responses.

CHAPTER 8

CONCLUSIONS AND RECOMMENDATIONS

8.1. CONCLUSIONS

Atherosclerosis, vascular calcification and aneurysms share some common pathological conditions such as excess proteolytic activity, increased proliferation and migration of aortic smooth muscle cells. Arterial calcification also involves the morphological transformation of aortic smooth muscle cells into osteoblast-like cells. Reversing these pathological conditions can help to control or even reverse these vascular diseases. However, current treatments for vascular diseases are very limited. We investigated pentagalloylglucose (PGG) as a therapeutic agent that inhibits many characteristics of vascular diseases using an *in vitro* model. We were able to arrive at the following conclusions:

(1) PGG inhibits the release of excess proteolytic enzymes specifically MMP-2, cathepsins K, L and S

(2) PGG inhibits the differentiation of rat aortic smooth muscle cells into osteoblast-like cells

(3) PGG increases the release of tropoelastin and deposition of insoluble elastin by primary rat aortic smooth muscle cells

(4) PLGA nanoparticles encapsulating PGG can be prepared and potentially used to deliver PGG *in vivo*

8.2. RECOMMENDATIONS

Based on our experimental results, the following studies are recommended for future work:

A) Examine the effects of PGG on *in vivo* models of vascular diseases. Studies should be conducted to optimize the dosage of PGG to be delivered systemically or orally. Hypercholesterolemic and ApoE knockout mice could be used as a model for atherosclerosis. Warfarin and vitamin K treated mice can simulate chronic kidney disease associated vascular calcification. Aneurysmal model can be simulated by using the elastase perfusion method. Optimized PGG doses can be delivered to study if PGG can have beneficial effects *in vivo*.

B) Use PGG treated primary rat aortic smooth muscle cells to deposit insoluble elastin in tissue engineered scaffolds to use as vascular grafts. From our results, PGG has shown promise in the *in vitro* generation of insoluble elastin. Electron microscopy and immunostaining should be conducted to further characterize the insoluble elastin produced by RASMCs *in vitro*. Creating tissue engineered grafts that contain elastin could be beneficial in many ways including better mechanical and structural properties. Synthetic polymeric scaffolds or naturally derived, decellularized vein scaffolds could be used. Mechanical testing and elastase degradation could be used to test these grafts *in vitro*.

C) Use cryo-sectioned arterial scaffolds to study medial calcification *in vitro*. Aortic smooth muscle cells seeded on the arterial scaffolds described in chapter 8 can be induced to calcify using existing *in vitro* models of vascular calcification. The scaffold could provide a simulation of medial arterial layer and provide the extracellular matrix to simulate a more physiologically relevant condition.

CHAPTER 9

REFERENCES

1. Lloyd-Jones D, Adams RJ, Brown TM, Carnethon M, Dai S, De Simone G, Ferguson TB, Ford E, Furie K, Gillespie C, Go A, Greenlund K, Haase N, Hailpern S, Ho PM, Howard V, Kissela B, Kittner S, Lackland D, Lisabeth L, Marelli A, McDermott MM, Meigs J, Mozaffarian D, Mussolino M, Nichol G, Roger V, Rosamond W, Sacco R, Sorlie P, Stafford R, Thom T, Wasserthiel-Smoller S, Wong ND, Wylie-Rosett J, on behalf of the American Heart Association Statistics Committee and Stroke Statistics Subcommittee. Heart disease and stroke statistics--2010 update. A report from the american heart association. *Circulation.* 2009.

2. Kinosian B, Glick H, Garland G. Cholesterol and coronary heart disease: Predicting risks by levels and ratios. *Ann Intern Med*. 1994;121:641-7.

3. Lorkowski S CP. Atherosclerosis: Pathogenesis, clinical features and treatment. *ENCYCLOPEDIA OF LIFE SCIENCES*. 2007; www.els.net doi: 10.1002/9780470015902.a0004228.

4. Ross & Romrell, ed. *Histology – A Text and Atlas.* 2nd ed.

5. Cullen P, Rauterberg J,Lorkowski S. The pathogenesis of arteriosclerosis. *Handbook of Experimental Pharmacology* . 2005;170:3–70.

6. IW F. Emerging relations between infectious diseases and coronary artery disease and atherosclerosis. *Canadian Medical Association Journal*. 2000;163:49–56.

7. Raggi P, Callister TQ, Cooil B, He ZX, Lippolis NJ, Russo DJ, Zelinger A, Mahmarian JJ. Identification of patients at increased risk of first unheralded acute myocardial infarction by electron-beam computed tomography. *Circulation*. 2000;101:850-855.

8. Raggi P, Cooil B, Callister TQ. Use of electron beam tomography data to develop models for prediction of hard coronary events. *Am Heart J*. 2001;141:375-382.

9. Detrano RC, Wong ND, Doherty TM, Shavelle R. Prognostic significance of coronary calcific deposits in asymptomatic high-risk subjects. *Am J Med*. 1997;102:344-349.

10. Vattikuti R, Towler DA. Osteogenic regulation of vascular calcification: An early perspective. *Am J Physiol Endocrinol Metab*. 2004;286:E686-96.

11. Parhami F, Bostrom K, Watson K, Demer LL. Role of molecular regulation in vascular calcification. *J Atheroscler Thromb*. 1996;3:90-4.

12. Lusis AJ. Atherosclerosis. *Nature*. 2000;407:233-241.

13. Detrano RC, Doherty TM, Davies MJ, Stary HC. Predicting coronary events with coronary calcium: Pathophysiologic and clinical problems. *Curr Probl Cardiol*. 2000;25:374-402.

14. Doherty TM, Asotra K, Fitzpatrick LA, Qiao JH, Wilkin DJ, Detrano RC, Dunstan CR, Shah PK, Rajavashisth TB. Calcification in atherosclerosis: Bone biology and chronic inflammation at the arterial crossroads. *Proc Natl Acad Sci U S A*. 2003;100:11201-11206.

15. Doherty TM, Detrano RC, Mautner SL, Mautner GC, Shavelle RM. Coronary calcium: The good, the bad, and the uncertain. *Am Heart J*. 1999;137:806-814.

16. Doherty TM, Detrano RC. Coronary arterial calcification as an active process: A new perspective on an old problem. *Calcif Tissue Int*. 1994;54:224-230.

17. *Primer on Metabolic Bone Diseases and Disorders of Mineral Metabolism.* 5th ed. ASMBR.

18. Komori T, Yagi H, Nomura S, Yamaguchi A, Sasaki K, Deguchi K, Shimizu Y, Bronson RT, Gao YH, Inada M, Sato M, Okamoto R, Kitamura Y, Yoshiki S, Kishimoto T. Targeted disruption of Cbfa1 results in a complete lack of bone formation owing to maturational arrest of osteoblasts. *Cell*. 1997;89:755-764.

19. Ducy P, Zhang R, Geoffroy V, Ridall AL, Karsenty G. Osf2/Cbfa1: A transcriptional activator of osteoblast differentiation. *Cell*. 1997;89:747-54.

20. Doherty TM, Fitzpatrick LA, Inoue D, Qiao JH, Fishbein MC, Detrano RC, Shah PK, Rajavashisth TB. Molecular, endocrine, and genetic mechanisms of arterial calcification. *Endocr Rev*. 2004;25:629-672.

21. Giuliani N, Colla S, Morandi F, Lazzaretti M, Sala R, Bonomini S, Grano M, Colucci S, Svaldi M, Rizzoli V. Myeloma cells block RUNX2/CBFA1 activity in human bone marrow osteoblast progenitors and inhibit osteoblast formation and differentiation. *Blood*. 2005;106:2472-2483.

22. Pinto JP, Conceicao NM, Viegas CS, Leite RB, Hurst LD, Kelsh RN, Cancela ML. Identification of a new pebp2alphaA2 isoform from zebrafish runx2 capable of inducing osteocalcin gene expression in vitro. *J Bone Miner Res*. 2005;20:1440-1453.

23. Cheng SL, Shao JS, Charlton-Kachigian N, Loewy AP, Towler DA. MSX2 promotes osteogenesis and suppresses adipogenic differentiation of multipotent mesenchymal progenitors. *J Biol Chem*. 2003;278:45969-45977.

24. Urry DW, Krivacic JR, Haider J. Calcium ion effects a notable change in elastin conformation by interacting at neutral sites. *Biochem Biophys Res Commun*. 1971;43:6-11.

25. Jahnen-Dechent W, Schafer C, Heiss A, Grotzinger J. Systemic inhibition of spontaneous calcification by the serum protein alpha 2-HS glycoprotein/fetuin. *Z Kardiol*. 2001;90 Suppl 3:47-56.

26. Blumenthal NC. Mechanisms of inhibition of calcification. *Clin Orthop Relat Res*. 1989;(247):279-289.

27. Glimcher MJ. Recent studies of the mineral phase in bone and its possible linkage to the organic matrix by protein-bound phosphate bonds. *Philos Trans R Soc Lond B Biol Sci*. 1984;304:479-508.

28. Anderson HC. Matrix vesicles and calcification. *Curr Rheumatol Rep*. 2003;5:222-6.

29. Hsu HH, Camacho NP, Sun F, Tawfik O, Aono H. Isolation of calcifiable vesicles from aortas of rabbits fed with high cholesterol diets. *Atherosclerosis*. 2000;153:337-348.

30. Hsu HH, Camacho NP. Isolation of calcifiable vesicles from human atherosclerotic aortas. *Atherosclerosis*. 1999;143:353-362.

31. Wuthier RE. Mechanism of de novo mineral formation by matrix vesicles. *Connect Tissue Res*. 1989;22:27-33; discussion 53-61.

32. Eanes ED. Biophysical aspects of lipid interaction with mineral: Liposome model studies. *Anat Rec*. 1989;224:220-225.

33. Zebboudj AF, Shin V, Bostrom K. Matrix GLA protein and BMP-2 regulate osteoinduction in calcifying vascular cells. *J Cell Biochem*. 2003;90:756-765.

34. Balica M, Bostrom K, Shin V, Tillisch K, Demer LL. Calcifying subpopulation of bovine aortic smooth muscle cells is responsive to 17 beta-estradiol. *Circulation*. 1997;95:1954-1960.

35. Steitz SA, Speer MY, Curinga G, Yang HY, Haynes P, Aebersold R, Schinke T, Karsenty G, Giachelli CM. Smooth muscle cell phenotypic transition associated with calcification: Upregulation of Cbfa1 and downregulation of smooth muscle lineage markers. *Circ Res*. 2001;89:1147-54.

36. Shioi A, Katagi M, Okuno Y, Mori K, Jono S, Koyama H, Nishizawa Y. Induction of bone-type alkaline phosphatase in human vascular smooth muscle cells: Roles of tumor necrosis factor-alpha and oncostatin M derived from macrophages. *Circ Res*. 2002;91:9-16.

37. Shanahan CM, Proudfoot D, Tyson KL, Cary NR, Edmonds M, Weissberg PL. Expression of mineralisation-regulating proteins in association with human vascular calcification. *Z Kardiol*. 2000;89 Suppl 2:63-68.

38. Engelse MA, Neele JM, Bronckers AL, Pannekoek H, de Vries CJ. Vascular calcification: Expression patterns of the osteoblast-specific gene core binding factor alpha-1 and the protective factor matrix gla protein in human atherogenesis. *Cardiovasc Res*. 2001;52:281-289.

39. Hunt JL, Fairman R, Mitchell ME, Carpenter JP, Golden M, Khalapyan T, Wolfe M, Neschis D, Milner R, Scoll B, Cusack A, Mohler ER,3rd. Bone formation in carotid plaques: A clinicopathological study. *Stroke*. 2002;33:1214-9.

40. Virchow R. Cellular pathology: As based upon physiological and pathological histology. . 1863:404-408.

41. Jeziorska M, McCollum C, Wooley DE. Observations on bone formation and remodelling in advanced atherosclerotic lesions of human carotid arteries. *Virchows Arch*. 1998;433:559-65.

42. Doherty TM, Uzui H, Fitzpatrick LA, Tripathi PV, Dunstan CR, Asotra K, Rajavashisth TB. Rationale for the role of osteoclast-like cells in arterial calcification. *Faseb J*. 2002;16:577-82.

43. Bostrom K, Watson KE, Horn S, Wortham C, Herman IM, Demer LL. Bone morphogenetic protein expression in human atherosclerotic lesions. *J Clin Invest*. 1993;91:1800-9.

44. Schulz E, Arfai K, Liu X, Sayre J, Gilsanz V. Aortic calcification and the risk of osteoporosis and fractures. *J Clin Endocrinol Metab*. 2004;89:4246-4253.

45. Hofbauer LC, Brueck CC, Shanahan CM, Schoppet M, Dobnig H. Vascular calcification and osteoporosis--from clinical observation towards molecular understanding. *Osteoporos Int*. 2007;18:251-259.

46. Hak AE, Pols HA, van Hemert AM, Hofman A, Witteman JC. Progression of aortic calcification is associated with metacarpal bone loss during menopause: A population-based longitudinal study. *Arterioscler Thromb Vasc Biol*. 2000;20:1926-1931.

47. Price PA, June HH, Buckley JR, Williamson MK. Osteoprotegerin inhibits artery calcification induced by warfarin and by vitamin D. *Arterioscler Thromb Vasc Biol*. 2001;21:1610-6.

48. Price PA, Faus SA, Williamson MK. Bisphosphonates alendronate and ibandronate inhibit artery calcification at doses comparable to those that inhibit bone resorption. *Arterioscler Thromb Vasc Biol*. 2001;21:817-24.

49. Khosla S. Minireview: The OPG/RANKL/RANK system. *Endocrinology*. 2001;142:5050-5055.

50. Lederle FA, Johnson GR, Wilson SE, Gordon IL, Chute EP, Littooy FN, Krupski WC, Bandyk D, Barone GW, Graham LM, Hye RJ, Reinke DB. Relationship of age, gender, race, and body size to infrarenal aortic diameter. the aneurysm detection and management (ADAM) veterans affairs cooperative study investigators. *J Vasc Surg*. 1997;26:595-601.

51. Wassef M, Baxter BT, Chisholm RL, Dalman RL, Fillinger MF, Heinecke J, Humphrey JD, Kuivaniemi H, Parks WC, Pearce WH, Platsoucas CD, Sukhova GK, Thompson RW, Tilson MD, Zarins CK. Pathogenesis of abdominal aortic aneurysms: A multidisciplinary research program supported by the national heart, lung, and blood institute. *Journal of Vascular Surgery*. 2001;34:730-738.

52. Ra HJ, Parks WC. Control of matrix metalloproteinase catalytic activity. *Matrix Biol*. 2007;26:587-596.

53. VanSaun MN, Matrisian LM. Matrix metalloproteinases and cellular motility in development and disease. *Birth Defects Res C Embryo Today*. 2006;78:69-79.

54. Galis ZS, Sukhova GK, Lark MW, Libby P. Increased expression of matrix metalloproteinases and matrix degrading activity in vulnerable regions of human atherosclerotic plaques. *J Clin Invest*. 1994;94:2493-503.

55. Libby P, Ridker PM, Maseri A. Inflammation and atherosclerosis. *Circulation*. 2002;105:1135-43.

56. Vyavahare N, Ogle M, Schoen FJ, Levy RJ. Elastin calcification and its prevention with aluminum chloride pretreatment. *Am J Pathol*. 1999;155:973-82.

57. Bailey M, Xiao H, Ogle M, Vyavahare N. Aluminum chloride pretreatment of elastin inhibits elastolysis by matrix metalloproteinases and leads to inhibition of elastin-oriented calcification. *Am J Pathol*. 2001;159:1981-6.

58. McGrath ME. The lysosomal cysteine proteases. *Annu Rev Biophys Biomol Struct*. 1999;28:181-204.

59. Turk B, Turk D, Turk V. Lysosomal cysteine proteases: More than scavengers. *Biochim Biophys Acta*. 2000;1477:98-111.

60. Littlewood-Evans AJ, Bilbe G, Bowler WB, Farley D, Wlodarski B, Kokubo T, Inaoka T, Sloane J, Evans DB, Gallagher JA. The osteoclast-associated protease cathepsin K is expressed in human breast carcinoma. *Cancer Res*. 1997;57:5386-5390.

61. Drake FH, Dodds RA, James IE, Connor JR, Debouck C, Richardson S, Lee-Rykaczewski E, Coleman L, Rieman D, Barthlow R, Hastings G, Gowen M. Cathepsin K, but not cathepsins B, L, or S, is abundantly expressed in human osteoclasts. *J Biol Chem*. 1996;271:12511-12516.

62. Bromme D, Okamoto K, Wang BB, Biroc S. Human cathepsin O2, a matrix protein-degrading cysteine protease expressed in osteoclasts. functional expression of human cathepsin O2 in spodoptera frugiperda and characterization of the enzyme. *J Biol Chem*. 1996;271:2126-2132.

63. Bromme D, Okamoto K. Human cathepsin O2, a novel cysteine protease highly expressed in osteoclastomas and ovary molecular cloning, sequencing and tissue distribution. *Biol Chem Hoppe Seyler*. 1995;376:379-384.

64. Tezuka K, Tezuka Y, Maejima A, Sato T, Nemoto K, Kamioka H, Hakeda Y, Kumegawa M. Molecular cloning of a possible cysteine proteinase predominantly expressed in osteoclasts. *J Biol Chem*. 1994;269:1106-1109.

65. Yagel S, Warner AH, Nellans HN, Lala PK, Waghorne C, Denhardt DT. Suppression by cathepsin L inhibitors of the invasion of amnion membranes by murine cancer cells. *Cancer Res*. 1989;49:3553-3557.

66. Kakegawa H, Nikawa T, Tagami K, Kamioka H, Sumitani K, Kawata T, Drobnic-Kosorok M, Lenarcic B, Turk V, Katunuma N. Participation of cathepsin L on bone resorption. *FEBS Lett*. 1993;321:247-250.

67. Esser RE, Angelo RA, Murphey MD, Watts LM, Thornburg LP, Palmer JT, Talhouk JW, Smith RE. Cysteine proteinase inhibitors decrease articular cartilage and bone destruction in chronic inflammatory arthritis. *Arthritis Rheum*. 1994;37:236-247.

68. Zheng T, Kang MJ, Crothers K, Zhu Z, Liu W, Lee CG, Rabach LA, Chapman HA, Homer RJ, Aldous D, De Sanctis GT, Underwood S, Graupe M, Flavell RA, Schmidt JA, Elias JA. Role of cathepsin S-dependent epithelial cell apoptosis in IFN-gamma-induced alveolar remodeling and pulmonary emphysema. *J Immunol*. 2005;174:8106-8115.

69. Riese RJ, Wolf PR, Bromme D, Natkin LR, Villadangos JA, Ploegh HL, Chapman HA. Essential role for cathepsin S in MHC class II-associated invariant chain processing and peptide loading. *Immunity*. 1996;4:357-366.

70. Petanceska S, Burke S, Watson SJ, Devi L. Differential distribution of messenger RNAs for cathepsins B, L and S in adult rat brain: An in situ hybridization study. *Neuroscience*. 1994;59:729-738.

71. Tousoulis D, Koniari K, Antoniades C, Papageorgiou N, Miliou A, Noutsou M, Nikolopoulou A, Marinou K, Stefanadi E, Siasos G, Charakida M, Kamboli AM, Stefanadis C. Combined effects of atorvastatin and metformin on glucose-induced variations of inflammatory process in patients with diabetes mellitus. *Int J Cardiol*. 2009.

72. Koleganova N, Piecha G, Ritz E, Schirmacher P, Muller A, Meyer HP, Gross ML. Arterial calcification in patients with chronic kidney disease. *Nephrol Dial Transplant*. 2009;24:2488-2496.

73. Al-Aly Z. Arterial calcification: A tumor necrosis factor-alpha mediated vascular wnt-opathy. *Transl Res*. 2008;151:233-239.

74. Al-Aly Z, Shao JS, Lai CF, Huang E, Cai J, Behrmann A, Cheng SL, Towler DA. Aortic Msx2-wnt calcification cascade is regulated by TNF-alpha-dependent signals in diabetic ldlr-/- mice. *Arterioscler Thromb Vasc Biol*. 2007;27:2589-2596.

75. Lee HL, Woo KM, Ryoo HM, Baek JH. Tumor necrosis factor-alpha increases alkaline phosphatase expression in vascular smooth muscle cells via MSX2 induction. *Biochem Biophys Res Commun*. 2009.

76. Xiong W, MacTaggart J, Knispel R, Worth J, Persidsky Y, Baxter BT. Blocking TNF-alpha attenuates aneurysm formation in a murine model. *J Immunol*. 2009;183:2741-2746.

77. Tintut Y, Patel J, Parhami F, Demer LL. Tumor necrosis factor-alpha promotes in vitro calcification of vascular cells via the cAMP pathway. *Circulation*. 2000;102:2636-2642.

78. Libinaki R, Tesanovic S, Heal A, Nikolovski B, Vinh A, Widdop RE, Gaspari TA, Devaraj S, Ogru E. The effect of tocopheryl phosphate on key biomarkers of

inflammation: Implication in the reduction of atherosclerosis progression in a hypercholesterolemic rabbit model. *Clin Exp Pharmacol Physiol*. 2010.

79. Angel K, Provan SA, Gulseth HL, Mowinckel P, Kvien TK, Atar D. Tumor necrosis factor-alpha antagonists improve aortic stiffness in patients with inflammatory arthropathies: A controlled study. *Hypertension*. 2010;55:333-338.

80. Manach C, Scalbert A, Morand C, Remesy C, Jimenez L. Polyphenols: Food sources and bioavailability. *Am J Clin Nutr*. 2004;79:727-747.

81. Giovannini C, Scazzocchio B, Vari R, Santangelo C, D'Archivio M, Masella R. Apoptosis in cancer and atherosclerosis: Polyphenol activities. *Ann Ist Super Sanita*. 2007;43:406-416.

82. Dragsted LO. Antioxidant actions of polyphenols in humans. *Int J Vitam Nutr Res*. 2003;73:112-119.

83. Weisburger JH. Lifestyle, health and disease prevention: The underlying mechanisms. *Eur J Cancer Prev*. 2002;11 Suppl 2:S1-7.

84. Urquiaga I, Leighton F. Plant polyphenol antioxidants and oxidative stress. *Biol Res*. 2000;33:55-64.

85. Biesalski HK. Polyphenols and inflammation: Basic interactions. *Curr Opin Clin Nutr Metab Care*. 2007;10:724-728.

86. Biswas S, Rahman I. Modulation of steroid activity in chronic inflammation: A novel anti-inflammatory role for curcumin. *Mol Nutr Food Res*. 2008;52:987-994.

87. Santangelo C, Vari R, Scazzocchio B, Di Benedetto R, Filesi C, Masella R. Polyphenols, intracellular signalling and inflammation. *Ann Ist Super Sanita*. 2007;43:394-405.

88. Frei B, Higdon JV. Antioxidant activity of tea polyphenols in vivo: Evidence from animal studies. *J Nutr*. 2003;133:3275S-84S.

89. Lee AS, Jung YJ, Kim DH, Lee TH, Kang KP, Lee S, Lee NH, Sung MJ, Kwon DY, Park SK, Kim W. Epigallocatechin-3-O-gallate decreases tumor necrosis factor-alpha-induced fractalkine expression in endothelial cells by suppressing NF-kappaB. *Cell Physiol Biochem*. 2009;24:503-510.

90. Dong Z. Effects of food factors on signal transduction pathways. *Biofactors*. 2000;12:17-28.

91. Ono K, Sawada T, Murata Y, Saito E, Iwasaki A, Arakawa Y, Kurokawa K, Hashimoto Y. Pentagalloylglucose, an antisecretory component of paeoniae radix, inhibits gastric H+, K(+)-ATPase. *Clin Chim Acta*. 2000;290:159-167.

92. Abdelwahed A, Bouhlel I, Skandrani I, Valenti K, Kadri M, Guiraud P, Steiman R, Mariotte AM, Ghedira K, Laporte F, Dijoux-Franca MG, Chekir-Ghedira L. Study of antimutagenic and antioxidant activities of gallic acid and 1,2,3,4,6-

pentagalloylglucose from pistacia lentiscus. confirmation by microarray expression profiling. *Chem Biol Interact*. 2007;165:1-13.

93. Hu H, Chai Y, Wang L, Zhang J, Lee HJ, Kim SH, Lu J. Pentagalloylglucose induces autophagy and caspase-independent programmed deaths in human PC-3 and mouse TRAMP-C2 prostate cancer cells. *Mol Cancer Ther*. 2009;8:2833-2843.

94. Hua KT, Way TD, Lin JK. Pentagalloylglucose inhibits estrogen receptor alpha by lysosome-dependent depletion and modulates ErbB/PI3K/Akt pathway in human breast cancer MCF-7 cells. *Mol Carcinog*. 2006;45:551-560.

95. Chen WJ, Lin JK. Induction of G1 arrest and apoptosis in human jurkat T cells by pentagalloylglucose through inhibiting proteasome activity and elevating p27Kip1, p21Cip1/WAF1, and bax proteins. *J Biol Chem*. 2004;279:13496-13505.

96. Abdul-Hussien H, Soekhoe RG, Weber E, von der Thusen JH, Kleemann R, Mulder A, van Bockel JH, Hanemaaijer R, Lindeman JH. Collagen degradation in the abdominal aneurysm: A conspiracy of matrix metalloproteinase and cysteine collagenases. *Am J Pathol*. 2007;170:809-817.

97. Beaudeux JL, Giral P, Bruckert E, Foglietti MJ, Chapman MJ. Matrix metalloproteinases, inflammation and atherosclerosis: Therapeutic perspectives. *Clin Chem Lab Med*. 2004;42:121-131.

98. Allaire E, Forough R, Clowes M, Starcher B, Clowes AW. Local overexpression of TIMP-1 prevents aortic aneurysm degeneration and rupture in a rat model. *J Clin Invest*. 1998;102:1413-20.

99. Bendeck MP, Irvin C, Reidy MA. Inhibition of matrix metalloproteinase activity inhibits smooth muscle cell migration but not neointimal thickening after arterial injury. *Circ Res*. 1996;78:38-43.

100. Basalyga DM, Simionescu DT, Xiong W, Baxter BT, Starcher BC, Vyavahare NR. Elastin degradation and calcification in an abdominal aorta injury model: Role of matrix metalloproteinases. *Circulation*. 2004;110:3480-7.

101. Cheng XW, Kuzuya M, Sasaki T, Arakawa K, Kanda S, Sumi D, Koike T, Maeda K, Tamaya-Mori N, Shi GP, Saito N, Iguchi A. Increased expression of elastolytic cysteine proteases, cathepsins S and K, in the neointima of balloon-injured rat carotid arteries. *Am J Pathol*. 2004;164:243-251.

102. Burns-Kurtis CL, Olzinski AR, Needle S, Fox JH, Capper EA, Kelly FM, McQueney MS, Romanic AM. Cathepsin S expression is up-regulated following balloon angioplasty in the hypercholesterolemic rabbit. *Cardiovasc Res*. 2004;62:610-620.

103. Kitamoto S, Sukhova GK, Sun J, Yang M, Libby P, Love V, Duramad P, Sun C, Zhang Y, Yang X, Peters C, Shi GP. Cathepsin L deficiency reduces diet-induced atherosclerosis in low-density lipoprotein receptor-knockout mice. *Circulation*. 2007;115:2065-2075.

104. Colyer WR,Jr, Cooper CJ. Cardiovascular morbidity and mortality and renal artery stenosis. *Prog Cardiovasc Dis*. 2009;52:238-242.

105. Hao H, Gabbiani G, Bochaton-Piallat ML. Arterial smooth muscle cell heterogeneity: Implications for atherosclerosis and restenosis development. *Arterioscler Thromb Vasc Biol*. 2003;23:1510-1520.

106. Annabi B, Lachambre MP, Bousquet-Gagnon N, Page M, Gingras D, Beliveau R. Green tea polyphenol (-)-epigallocatechin 3-gallate inhibits MMP-2 secretion and MT1-MMP-driven migration in glioblastoma cells. *Biochim Biophys Acta*. 2002;1542:209-220.

107. Katiyar SK. Matrix metalloproteinases in cancer metastasis: Molecular targets for prostate cancer prevention by green tea polyphenols and grape seed proanthocyanidins. *Endocr Metab Immune Disord Drug Targets*. 2006;6:17-24.

108. Chuang TH, Stabler C, Simionescu A, Simionescu DT. Polyphenol-stabilized tubular elastin scaffolds for tissue engineered vascular grafts. *Tissue Eng Part A*. 2009;15:2837-2851.

109. Isenburg JC, Simionescu DT, Starcher BC, Vyavahare NR. Elastin stabilization for treatment of abdominal aortic aneurysms. *Circulation*. 2007;115:1729-37.

110. Isenburg JC, Karamchandani NV, Simionescu DT, Vyavahare NR. Structural requirements for stabilization of vascular elastin by polyphenolic tannins. *Biomaterials*. 2006;27:3645-3651.

111. Livak KJ, Schmittgen TD. Analysis of relative gene expression data using real-time quantitative PCR and the 2(-delta delta C(T)) method. *Methods*. 2001;25:402-408.

112. Abramoff, M.D., Magelhaes, P.J., Ram, S.J. Image processing with ImageJ. *Biophot Intl*. 2004;11:36-42.

113. Liang CC, Park AY, Guan JL. In vitro scratch assay: A convenient and inexpensive method for analysis of cell migration in vitro. *Nat Protoc*. 2007;2:329-333.

114. Liu J, Sukhova GK, Sun JS, Xu WH, Libby P, Shi GP. Lysosomal cysteine proteases in atherosclerosis. *Arterioscler Thromb Vasc Biol*. 2004;24:1359-1366.

115. Fuster JJ, Fernandez P, Gonzalez-Navarro H, Silvestre C, Nabah YN, Andres V. Control of cell proliferation in atherosclerosis: Insights from animal models and human studies. *Cardiovasc Res*. 2010;86:254-264.

116. Karas SP, Santoian EC, Gravanis MB. Restenosis following coronary angioplasty. *Clin Cardiol*. 1991;14:791-801.

117. Libby P. Inflammation in atherosclerosis. *Nature*. 2002;420:868-874.

118. Weissberg PL, Bennett MR. Atherosclerosis--an inflammatory disease. *N Engl J Med*. 1999;340:1928-9.

119. Lusis AJ. Atherosclerosis. *Nature*. 2000;407:233-41.

120. Jovinge S, Hultgardh-Nilsson A, Regnstrom J, Nilsson J. Tumor necrosis factor-alpha activates smooth muscle cell migration in culture and is expressed in the balloon-injured rat aorta. *Arterioscler Thromb Vasc Biol*. 1997;17:490-497.

121. Garcia-Touchard A, Henry TD, Sangiorgi G, Spagnoli LG, Mauriello A, Conover C, Schwartz RS. Extracellular proteases in atherosclerosis and restenosis. *Arterioscler Thromb Vasc Biol*. 2005;25:1119-1127.

122. Lijnen HR. Extracellular proteolysis in the development and progression of atherosclerosis. *Biochem Soc Trans*. 2002;30:163-7.

123. Robert L, Robert AM, Jacotot B. Elastin-elastase-atherosclerosis revisited. *Atherosclerosis*. 1998;140:281-295.

124. Simionescu A, Philips K, Vyavahare N. Elastin-derived peptides and TGF-beta1 induce osteogenic responses in smooth muscle cells. *Biochem Biophys Res Commun*. 2005;334:524-32.

125. Robinet A, Fahem A, Cauchard JH, Huet E, Vincent L, Lorimier S, Antonicelli F, Soria C, Crepin M, Hornebeck W, Bellon G. Elastin-derived peptides

enhance angiogenesis by promoting endothelial cell migration and tubulogenesis through upregulation of MT1-MMP. *J Cell Sci*. 2005;118:343-56.

126. T. F,Jr, Larbi A, Fortun A, Robert L, Khalil A. Elastin peptides induced oxidation of LDL by phagocytic cells. *Pathol Biol (Paris)*. 2005;53:416-23.

127. Fulop T,Jr, Jacob MP, Khalil A, Wallach J, Robert L. Biological effects of elastin peptides. *Pathol Biol (Paris)*. 1998;46:497-506.

128. Rizas KD, Ippagunta N, Tilson MD,3rd. Immune cells and molecular mediators in the pathogenesis of the abdominal aortic aneurysm. *Cardiol Rev*. 2009;17:201-210.

129. Abdul-Hussien H, Soekhoe RG, Weber E, von der Thusen JH, Kleemann R, Mulder A, van Bockel JH, Hanemaaijer R, Lindeman JH. Collagen degradation in the abdominal aneurysm: A conspiracy of matrix metalloproteinase and cysteine collagenases. *Am J Pathol*. 2007;170:809-817.

130. Chung AW, Au Yeung K, Sandor GG, Judge DP, Dietz HC, van Breemen C. Loss of elastic fiber integrity and reduction of vascular smooth muscle contraction resulting from the upregulated activities of matrix metalloproteinase-2 and -9 in the thoracic aortic aneurysm in marfan syndrome. *Circ Res*. 2007;101:512-522.

131. Jin D, Sheng J, Yang X, Gao B. Matrix metalloproteinases and tissue inhibitors of metalloproteinases expression in human cerebral ruptured and unruptured aneurysm. *Surg Neurol*. 2007;68 Suppl 2:S11-6; discussion S16.

132. Dell'Agli M, Canavesi M, Galli G, Bellosta S. Dietary polyphenols and regulation of gelatinase expression and activity. *Thromb Haemost*. 2005;93:751-760.

133. Aikawa E, Aikawa M, Libby P, Figueiredo JL, Rusanescu G, Iwamoto Y, Fukuda D, Kohler RH, Shi GP, Jaffer FA, Weissleder R. Arterial and aortic valve calcification abolished by elastolytic cathepsin S deficiency in chronic renal disease. *Circulation*. 2009;119:1785-1794.

134. Kitamoto S, Sukhova GK, Sun J, Yang M, Libby P, Love V, Duramad P, Sun C, Zhang Y, Yang X, Peters C, Shi GP. Cathepsin L deficiency reduces diet-induced atherosclerosis in low-density lipoprotein receptor-knockout mice. *Circulation*. 2007;115:2065-2075.

135. Liu J, Sukhova GK, Yang JT, Sun J, Ma L, Ren A, Xu WH, Fu H, Dolganov GM, Hu C, Libby P, Shi GP. Cathepsin L expression and regulation in human abdominal aortic aneurysm, atherosclerosis, and vascular cells. *Atherosclerosis*. 2006;184:302-311.

136. Lutgens E, Lutgens SP, Faber BC, Heeneman S, Gijbels MM, de Winther MP, Frederik P, van der Made I, Daugherty A, Sijbers AM, Fisher A, Long CJ, Saftig P, Black D, Daemen MJ, Cleutjens KB. Disruption of the cathepsin K gene reduces

atherosclerosis progression and induces plaque fibrosis but accelerates macrophage foam cell formation. *Circulation*. 2006;113:98-107.

137. Saren P, Welgus HG, Kovanen PT. TNF-alpha and IL-1beta selectively induce expression of 92-kDa gelatinase by human macrophages. *J Immunol*. 1996;157:4159-4165.

138. Watari M, Watari H, Nachamkin I, Strauss JF. Lipopolysaccharide induces expression of genes encoding pro-inflammatory cytokines and the elastin-degrading enzyme, cathepsin S, in human cervical smooth-muscle cells. *J Soc Gynecol Investig*. 2000;7:190-198.

139. Watari M, Watari H, DiSanto ME, Chacko S, Shi G, Strauss JF,III. Pro-inflammatory cytokines induce expression of matrix-metabolizing enzymes in human cervical smooth muscle cells. *Am J Pathol*. 1999;154:1755-1762.

140. Branen L, Hovgaard L, Nitulescu M, Bengtsson E, Nilsson J, Jovinge S. Inhibition of tumor necrosis factor-alpha reduces atherosclerosis in apolipoprotein E knockout mice. *Arterioscler Thromb Vasc Biol*. 2004;24:2137-2142.

141. Tedder ME, Liao J, Weed B, Stabler C, Zhang H, Simionescu A, Simionescu DT. Stabilized collagen scaffolds for heart valve tissue engineering. *Tissue Eng Part A*. 2009;15:1257-1268.

142. Lee CW, Lin CC, Lin WN, Liang KC, Luo SF, Wu CB, Wang SW, Yang CM. TNF-alpha induces MMP-9 expression via activation of Src/EGFR, PDGFR/PI3K/Akt cascade and promotion of NF-kappaB/p300 binding in human tracheal smooth muscle cells. *Am J Physiol Lung Cell Mol Physiol*. 2007;292:L799-812.

143. Lee SO, Jeong YJ, Yu MH, Lee JW, Hwangbo MH, Kim CH, Lee IS. Wogonin suppresses TNF-alpha-induced MMP-9 expression by blocking the NF-kappaB activation via MAPK signaling pathways in human aortic smooth muscle cells. *Biochem Biophys Res Commun*. 2006;351:118-125.

144. Cohen M, Meisser A, Haenggeli L, Bischof P. Involvement of MAPK pathway in TNF-alpha-induced MMP-9 expression in human trophoblastic cells. *Mol Hum Reprod*. 2006;12:225-232.

145. Pasterkamp G, de Kleijn DP, Borst C. Arterial remodeling in atherosclerosis, restenosis and after alteration of blood flow: Potential mechanisms and clinical implications. *Cardiovasc Res*. 2000;45:843-852.

146. Schoene NW, Kelly MA, Polansky MM, Anderson RA. Water-soluble polymeric polyphenols from cinnamon inhibit proliferation and alter cell cycle distribution patterns of hematologic tumor cell lines. *Cancer Lett*. 2005;230:134-140.

147. Pianetti S, Guo S, Kavanagh KT, Sonenshein GE. Green tea polyphenol epigallocatechin-3 gallate inhibits her-2/neu signaling, proliferation, and transformed phenotype of breast cancer cells. *Cancer Res*. 2002;62:652-655.

148. Iijima K, Yoshizumi M, Hashimoto M, Kim S, Eto M, Ako J, Liang YQ, Sudoh N, Hosoda K, Nakahara K, Toba K, Ouchi Y. Red wine polyphenols inhibit proliferation of vascular smooth muscle cells and downregulate expression of cyclin A gene. *Circulation*. 2000;101:805-811.

149. Liang YC, Chen YC, Lin YL, Lin-Shiau SY, Ho CT, Lin JK. Suppression of extracellular signals and cell proliferation by the black tea polyphenol, theaflavin-3,3'-digallate. *Carcinogenesis*. 1999;20:733-736.

150. Ketteler M, Giachelli C. Novel insights into vascular calcification. *Kidney Int Suppl*. 2006;(105):S5-9.

151. Johnson RC, Leopold JA, Loscalzo J. Vascular calcification: Pathobiological mechanisms and clinical implications. *Circ Res*. 2006;99:1044-1059.

152. Trion A, van der Laarse A. Vascular smooth muscle cells and calcification in atherosclerosis. *Am Heart J*. 2004;147:808-814.

153. Towler DA, Shao JS, Cheng SL, Pingsterhaus JM, Loewy AP. Osteogenic regulation of vascular calcification. *Ann N Y Acad Sci*. 2006;1068:327-333.

154. Park SJ, Kim YH. Percutaneous coronary intervention for unprotected left main coronary artery stenosis. *Cardiol Clin*. 2010;28:81-95.

155. Trivedi RA, Weerakkody RA, Turner C, Kirkpatrick PJ. Carotid artery stenosis-an evidence-based review of surgical and non-surgical treatments. *Br J Neurosurg*. 2009;23:387-392.

156. Iyemere VP, Proudfoot D, Weissberg PL, Shanahan CM. Vascular smooth muscle cell phenotypic plasticity and the regulation of vascular calcification. *J Intern Med*. 2006;260:192-210.

157. Hruska KA, Mathew S, Saab G. Bone morphogenetic proteins in vascular calcification. *Circ Res*. 2005;97:105-114.

158. Mody N, Tintut Y, Radcliff K, Demer LL. Vascular calcification and its relation to bone calcification: Possible underlying mechanisms. *J Nucl Cardiol*. 2003;10:177-183.

159. Persy V, D'Haese P. Vascular calcification and bone disease: The calcification paradox. *Trends Mol Med*. 2009;15:405-416.

160. Choi SH, An JH, Lim S, Koo BK, Park SE, Chang HJ, Choi SI, Park YJ, Park KS, Jang HC, Shin CS. Lower bone mineral density is associated with higher coronary calcification and coronary plaque burdens by multidetector row coronary computed tomography in pre- and postmenopausal women. *Clin Endocrinol (Oxf)*. 2009;71:644-651.

161. Danilevicius CF, Lopes JB, Pereira RM. Bone metabolism and vascular calcification. *Braz J Med Biol Res*. 2007;40:435-442.

162. Towler DA. Inorganic pyrophosphate: A paracrine regulator of vascular calcification and smooth muscle phenotype. *Arterioscler Thromb Vasc Biol*. 2005;25:651-654.

163. Steitz SA, Speer MY, Curinga G, Yang HY, Haynes P, Aebersold R, Schinke T, Karsenty G, Giachelli CM. Smooth muscle cell phenotypic transition associated with calcification: Upregulation of Cbfa1 and downregulation of smooth muscle lineage markers. *Circ Res*. 2001;89:1147-1154.

164. Bear M, Butcher M, Shaughnessy SG. Oxidized low-density lipoprotein acts synergistically with beta-glycerophosphate to induce osteoblast differentiation in primary cultures of vascular smooth muscle cells. *J Cell Biochem*. 2008.

165. Yang H, Curinga G, Giachelli CM. Elevated extracellular calcium levels induce smooth muscle cell matrix mineralization in vitro. *Kidney Int*. 2004;66:2293-2299.

166. Simionescu A, Philips K, Vyavahare N. Elastin-derived peptides and TGF-beta1 induce osteogenic responses in smooth muscle cells. *Biochem Biophys Res Commun*. 2005;334:524-532.

167. Li X, Yang HY, Giachelli CM. BMP-2 promotes phosphate uptake, phenotypic modulation, and calcification of human vascular smooth muscle cells. *Atherosclerosis*. 2008;199:271-277.

168. Villa-Bellosta R, Levi M, Sorribas V. Vascular smooth muscle cell calcification and SLC20 inorganic phosphate transporters: Effects of PDGF, TNF-alpha, and pi. *Pflugers Arch.* 2009;458:1151-1161.

169. Fiore CE, Pennisi P, Pulvirenti I, Francucci CM. Bisphosphonates and atherosclerosis. *J Endocrinol Invest*. 2009;32:38-43.

170. Bevilacqua M, Dominguez LJ, Rosini S, Barbagallo M. Bisphosphonates and atherosclerosis: Why? *Lupus*. 2005;14:773-779.

171. Toussaint ND, Elder GJ, Kerr PG. Bisphosphonates in chronic kidney disease; balancing potential benefits and adverse effects on bone and soft tissue. *Clin J Am Soc Nephrol*. 2009;4:221-233.

172. Demer LL. Vascular calcification and osteoporosis: Inflammatory responses to oxidized lipids. *Int J Epidemiol*. 2002;31:737-741.

173. Rubin MR, Silverberg SJ. Vascular calcification and osteoporosis--the nature of the nexus. *J Clin Endocrinol Metab*. 2004;89:4243-4245.

174. Mody N, Parhami F, Sarafian TA, Demer LL. Oxidative stress modulates osteoblastic differentiation of vascular and bone cells. *Free Radic Biol Med*. 2001;31:509-519.

175. Nikolovski J, Kim BS, Mooney DJ. Cyclic strain inhibits switching of smooth muscle cells to an osteoblast-like phenotype. *FASEB J*. 2003;17:455-457.

176. Angel P, Karin M. The role of jun, fos and the AP-1 complex in cell-proliferation and transformation. *Biochim Biophys Acta*. 1991;1072:129-157.

177. Ransone LJ, Verma IM. Nuclear proto-oncogenes fos and jun. *Annu Rev Cell Biol*. 1990;6:539-557.

178. Nakabeppu Y, Ryder K, Nathans D. DNA binding activities of three murine jun proteins: Stimulation by fos. *Cell*. 1988;55:907-915.

179. Rauscher FJ,3rd, Voulalas PJ, Franza BR,Jr, Curran T. Fos and jun bind cooperatively to the AP-1 site: Reconstitution in vitro. *Genes Dev*. 1988;2:1687-1699.

180. Stangl V, Dreger H, Stangl K, Lorenz M. Molecular targets of tea polyphenols in the cardiovascular system. *Cardiovasc Res*. 2007;73:348-358.

181. Pendurthi UR, Williams JT, Rao LV. Resveratrol, a polyphenolic compound found in wine, inhibits tissue factor expression in vascular cells : A possible mechanism for the cardiovascular benefits associated with moderate consumption of wine. *Arterioscler Thromb Vasc Biol*. 1999;19:419-426.

182. Chen HW, Huang HC. Effect of curcumin on cell cycle progression and apoptosis in vascular smooth muscle cells. *Br J Pharmacol*. 1998;124:1029-1040.

183. VJ Mohanraj and Y Chen. Nanoparticles - A review. *Tropical Journal of Pharmaceutical Research*. 2006;5:561-573.